

**Biodegradable Paclitaxel-loaded  
Nanoparticles and Stent Coatings  
as Local Delivery Systems  
for the Prevention of Restenosis**

**Dissertation**

zur

Erlangung des Doktorgrades

der Naturwissenschaften

(Dr. rer. nat.)

dem Fachbereich Pharmazie der

Philipps-Universität Marburg

vorgelegt von

Ulrich Westedt

aus Brome / Niedersachsen

Marburg/Lahn 2004

Vom Fachbereich Pharmazie der Philipps-Universität Marburg als Dissertation am  
13.01.2004 angenommen.

Erstgutachter:

Prof. Dr. T. Kissel

Zweitgutachter:

Prof. Dr. U. Bakowsky

Tag der mündlich Prüfung

13. Januar 2004

**Biodegradable Paclitaxel-loaded  
Nanoparticles and Stent Coatings  
as Local Delivery Systems  
for the Prevention of Restenosis**

von

Ulrich Westedt

Die vorliegende Arbeit  
entstand auf Anregung und unter der Leitung von

*Herrn Prof. Dr. Thomas Kissel*

am Institut für Pharmazeutische Technologie und Biopharmazie  
der Philipps-Universität Marburg

# TABLE OF CONTENTS

<b>1. INTRODUCTION</b> .....	<b>1</b>
INTRODUCTION .....	2
RESTENOSIS: INCIDENCE AND PATHOPHYSIOLOGY .....	2
RATIONALE FOR LOCAL DRUG DELIVERY .....	4
DRUG ELUTING STENTS .....	5
POROUS BALLOON CATHETER-BASED DRUG DELIVERY .....	8
PACLITAXEL FOR PREVENTION OF RESTENOSIS .....	10
OBJECTIVES OF THIS WORK .....	11
REFERENCES .....	13
<b>2. DEPOSITION OF NANOPARTICLES IN THE ARTERIAL VESSEL BY POROUS BALLOON CATHETERS: LOCALIZATION BY CONFOCAL LASER SCANNING MICROSCOPY AND TRANSMISSION ELECTRON MICROSCOPY</b> .....	<b>25</b>
SUMMARY.....	26
INTRODUCTION .....	27
MATERIALS AND METHODS .....	28
RESULTS AND DISCUSSION .....	31
CONCLUSIONS .....	37
REFERENCES .....	38

<b>3. EFFECTS OF DIFFERENT APPLICATION PARAMETERS ON PENETRATION CHARACTERISTICS AND ARTERIAL VESSEL WALL INTEGRITY AFTER LOCAL NANOPARTICLE DELIVERY USING A POROUS BALLOON CATHETER .....</b>	<b>42</b>
SUMMARY.....	43
INTRODUCTION .....	44
MATERIALS AND METHODS .....	45
RESULTS AND DISCUSSION .....	49
CONCLUSIONS .....	55
REFERENCES .....	56
<b>4. PACLITAXEL LOADED NANOPARTICLES FROM BIODEGRADABLE POLY(VINYL ALCOHOL)-GRAFT-POLY(LACTIDE-CO-GLYCOLIDE) FOR CATHETER BASED LOCAL TREATMENT OF RESTENOSIS.....</b>	<b>61</b>
SUMMARY.....	62
INTRODUCTION .....	63
MATERIALS AND METHODS .....	64
RESULTS AND DISCUSSION .....	70
CONCLUSIONS .....	79
REFERENCES .....	79

<b>5. PACLITAXEL RELEASING STENTS FOR THE TREATMENT OF RESTENOSIS: BIODEGRADABLE COATINGS CONSISTING OF POLY(VINYL ALCOHOL)-GRAFT-POLY(LACTIDE-CO-GLYCOLIDE) .....</b>	<b>85</b>
SUMMERY .....	86
INTRODUCTION .....	87
MATERIALS AND METHODS .....	88
RESULTS AND DISCUSSION .....	94
CONCLUSIONS .....	104
REFERENCES .....	104
<b>6. SUMMARY AND OUTLOOK FOR FURTHER STUDIES .....</b>	<b>109</b>
SUMMARY.....	110
OUTLOOK FOR FURTHER STUDIES.....	114
ZUSAMMENFASSUNG .....	116
AUSBLICK.....	121
REFERENCES / LITERATURSTELLEN.....	123
<b>7. APPENDICES.....</b>	<b>126</b>
LIST OF PUBLICATIONS.....	127
CURRICULUM VITAE.....	129

## **CHAPTER 1**

---

### **INTRODUCTION**

---

## **INTRODUCTION**

In this work, nanoparticles and films consisting of biodegradable comb polyesters, poly(vinyl alcohol)-graft-poly(lactide-co-glycolide) (PVA-g-PLGA) [1,2], have been investigated as delivery systems for paclitaxel to prevent the pathogenesis of postangioplastic restenosis. A more detailed introduction dealing with the specific objectives of each research topic is provided in the following chapters. This chapter serves as a general introduction explaining the basic problems that arise from percutaneous revascularization interventions and local drug delivery strategies to reduce restenosis. At the end of the chapter the objectives of this work are outlined.

## **RESTENOSIS: INCIDENCE AND PATHOPHYSIOLOGY**

Percutaneous transluminal (coronary) angioplasty, PT(C)A is a very useful technique for the treatment of vascular occlusions. Unfortunately, its success is often limited by the development of a secondary arterial obstruction, also known as restenosis. According to both clinical and angiographic definitions, 25 – 35 % of successfully treated atherosclerotic lesions re occlude within 3 – 6 months [3], generating increased costs for additional revascularization procedures, atherectomy or bypass surgery [4]. Restenosis is primarily attributed to neointimal hyperplasia. Balloon angioplasty denudes the endothelial layer which normally prevents of blood components from interaction with tissue factors and subendothelial parts of the injured vessel wall. When such interactions occur, platelet aggregation and the activation of the coagulation cascade leads to thrombus formation [5]. This, in turn, stimulates the release of cytokines and growth factors, such as platelet-derived growth factor (PDGF), basic fibroblast growth factor (bFGF), transforming growth factor b (TGFb), thrombin, and angiotensinII [6-10]. Consequently,

mononuclear leukocytes enter the arterial wall followed by a transformation to macrophages.

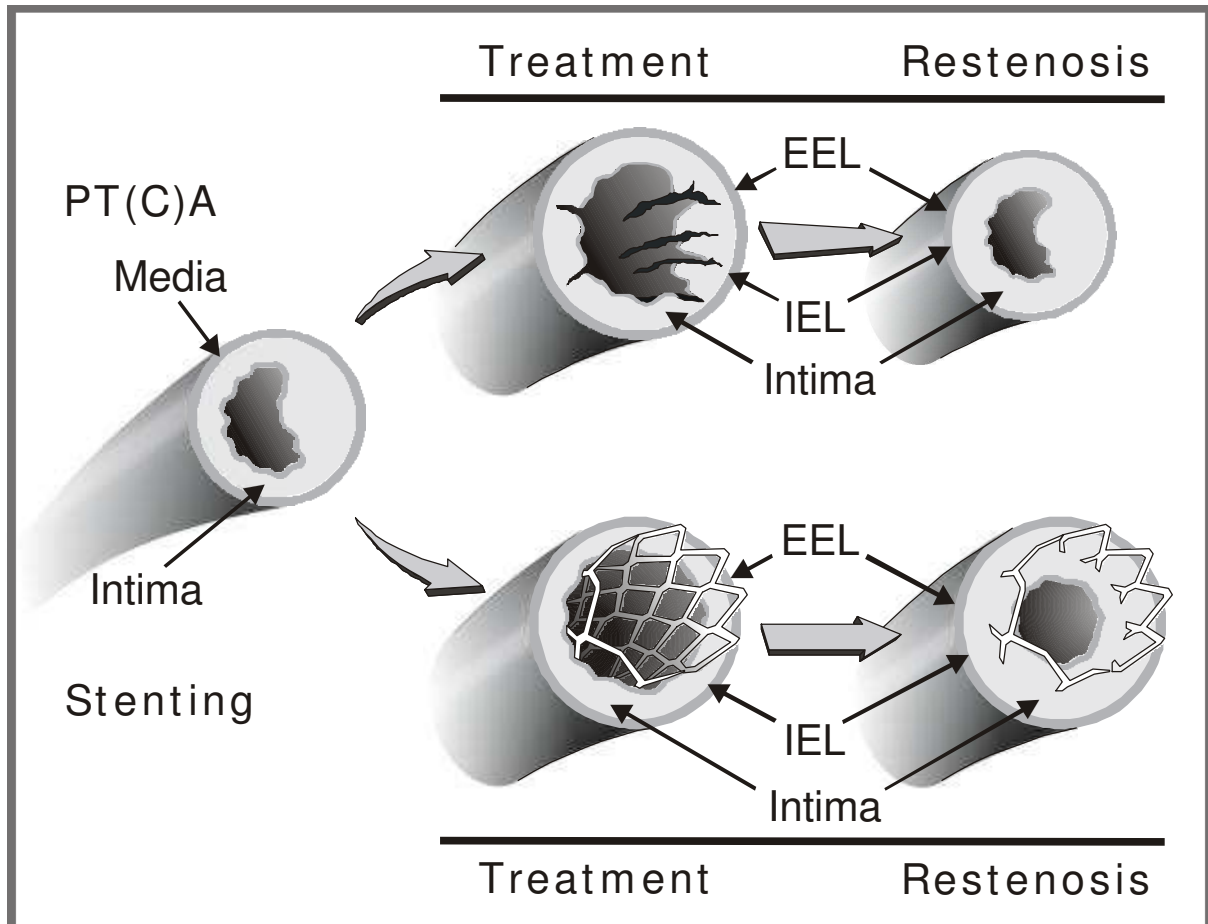


**Fig. 1:** Possible mechanisms of restenosis after PT(C)A and stenting. PTA leads to plaque disruptions, and dissections penetrating the media through the internal elastic lamina (IEL). Restenosis, caused by arterial remodelling, is characterized by shrinkage of the area circumscribed by the external elastic lamina (EEL), and intimal hyperplasia. Stenting also enlarges the cross-sectional area of the vessel wall. Stents prevent vessel shrinkage, however intimal hyperplasia can be excessive (adapted from [11]).

These macrophages produce additional vascular smooth muscle cell (VSMC) activation elements. Vascular trauma by angioplasty catheter and stents application induces necrosis and the activation of VSMC in the media and myofibroblasts in the adventitia. Subsequently, cells migrate into the intima, where they proliferate and secrete extracellular matrix. VSMC proliferation is

due to upregulation and expression of cell division regulating genes such as c-myc [12,13]. This neointimal tissue then spreads into the lumen [14,15]. Collagen deposition and scarring, two processes associated with elastic recoil of the vessel wall, dramatically decrease the lumen diameter [16,17].

To prevent early elastic vessel recoil and late remodelling of artery rigid metallic scaffolds are introduced into the treated segment. Unfortunately, this method of intervention can also cause intimal hyperplasia. However, in comparison to the angioplasty-induced restenosis, the stent-induced restenosis originates from a local tissue reaction to non-biocompatible materials [18-24]. Fig. 1 schematically summarizes the morphological consequences of PTA and vascular stenting.

## **RATIONALE FOR LOCAL DRUG DELIVERY**

Despite pharmacologic agents, including antithrombotic, antiplatelet, anti proliferative, anti-inflammatory drugs, as well as vasodilators and lipid-lowering substances, showed efficient antirestenotic effects in vitro and in animal studies, several clinical trial in humans failed [25-30]. The limited efficiency in decreasing intimal hyperplasia is often coupled with serious systemic side effects, due to inadequate local and high systemic drug concentrations. Therefore, interest has focused on the local administration of potentially antirestenotic drugs directly to the site of arterial injury following angioplastic interventions. This approach has several advantages:

- High local drug concentrations,
- Decrease of general drug burden,
- Decrease of systemic side effects, and
- Sustained local pharmacodynamic effects by physical or chemical binding of the drug to a carrier system.

---

To achieve local drug delivery, different devices have been developed combining the technical possibility of delivering the drug with a method of angioplasty intervention. These strategies may be classified in balloon catheter delivery systems, polymeric or coated stents [30-37], and devices for facilitated diffusion. Such devices must meet the following demands:

- Efficient, homogeny site-specific drug concentrations
- Little to no additional vascular trauma (proliferative response is proportional to the extent of initial arterial injury [38,39])
- Simple handling
- Lesion dilatation
- Maintains distal vascular perfusion if prolonged delivery times are required.

## **DRUG ELUTING STENTS**

A very promising approach to prevent vascular renarrowing after a PTA is the implantation of intraluminal stents. Stents are small wire-mesh metal tubes which provide a scaffolding to support the damaged arterial wall, thus reducing the chance of vessel collapse caused by elastic recoil and vascular remodelling. Unfortunately, stent implantation causes intimal hyperplasia. The degree of neointima formation is influenced by stent design [40-42], degree of vascular injury [38], and stent and coating material [43]. A number of polymers and polymer combinations were investigated as potential drug delivery vehicles to reduce the incidence of restenosis. These include poly(vinyl pyrrolidone)/cellulose esters, poly(vinyl pyrrolidone)/polyurethane, poly(methylidene maloleate), polylactide/polyglycolide copolymers, poly(ethylene glycol) copolymers, poly(vinyl alcohol) and poly(dimethylsiloxane)-based systems [44]. Among the most commonly used methods of coating stents with polymers are spray coating (spraying the drug-polymer solution onto the stent)

and dip coating (dipping the device in the coating solution and drying upon withdrawal) [45]. To minimize platelet activation and reduce thrombus formation it is essential that a smooth and defect-free stent coating is achieved.

Approach	Drug release	Benefits	Problems
Polymeric, non-biodegradable stents	Diffusion from matrix	Load and release of drugs	Poor stent stability, inflammation
Polymeric, biodegradable stents	Degradation of matrix	Controlled delivery	Inflammation from degradation products
Metallic stents, drug coated on surface	Drug dissolution	No issues with coatings	No controlled or sustained release
Chemically attached drug onto stent surface	Cleavage of drug-substrate bond	Controlled release	Side effects of pro-drug
Sponge like coatings, drugs are absorbed	Diffusion from the matrix	Load and release of drugs	Inflammatory reactions
Biodegradable stent coatings	Degradation of the matrix	Controlled delivery	Inflammation from degradation products

**Tab. 1:** *Stent-based methods for local drug delivery (adapted from [46]).*

Despite excellent mechanical properties, several polymers exhibit a poor biocompatibility characterized by inflammatory and proliferative responses after stent implantation [47-49]. To prevent this reactions inhibiting intimal hyperplasia and (sub)acute stent thrombosis the drug should be delivered in the local area of the stent. Antirestenotic drugs that inhibit thrombus formation (e.g. heparin), inflammation (e.g. dexamethasone), and cellular proliferation (e.g. sirolimus, paclitaxel), can be incorporated into and released from a polymer matrix, or alternatively, can be surrounded by and released through the polymer membrane that coats (strut adherent) or spans (strut-spanning) the stent struts. In other formulations, the substance is bound directly to the sent surface and can be removed by chemical or biological reactions, which cleave drug-substrate bond

[46,50]. Other researches have developed stents composed of biodegradable polymers in to which the drug is embedded [62,63] to promote optimal healing and further reduction of restenotic processes.

Tab. 1 describes a section of potential ways in which a drug can be delivered to the arterial vessel wall. As a result of these intense research efforts, several drug eluting stent systems have been developed and are already under investigation in clinical trials, as displayed in Tab. 2.

<b>Polymer</b>	<b>Drug</b>	<b>Trial name</b>	<b>Results</b>	<b>Ref.</b>
Poly(ethyl methacrylate)/ n-butyl metacrylate	sirolimus	FIM	safety	[51]
Poly(ethyl methacrylate)/ n-butyl metacrylate	sirolimus	RAVEL	reduction of restenosis	[52]
Poly(ethyl methacrylate)/ n-butyl metacrylate	sirolimus	SIRIUS	ongoing; reduction of restenosis	[53,54]
Phosphorylcholine	dexamethasone	STRIDE	ongoing	[55]
No coating	paclitaxel	ASPECT	reduction of restenosis	[56]
No coating	paclitaxel	ELUTES	reduction of restenosis	[57]
Not specified	paclitaxel	TAXUS I	reduction of restenosis	[58]
Polyacrylate	7-hexanoltaxol	SCORE	stopped	[59]
No coating	heparin	COST	no reduction	[60]
Phoshorylcholine	batimastat	BRILLANT	stopped	[61]

**Tab. 2:** Selected clinical studies with polymer coated drug eluting stents (adapted from [50]).

## POROUS BALLOON CATHETER-BASED DRUG DELIVERY

The rapid washout of infused drug from the target site after administration of drug solutions using drug delivery catheters [64] is the main problem of intraluminal delivery [34,65,66]. Consequently, researchers have attempted to delay drug loss from the vessel wall by incorporating the drug into biocompatible and biodegradable polymers formulated as micro- and nanoparticles. When infused locally (Fig. 2), the particles may penetrate the vessel wall and form a depot, which provide a local, and sustained release of the drug in the arterial wall [67-71]. Some researches described a close connection between particle size and the penetration into and cellular uptake of particles in the vessel wall [70,72].

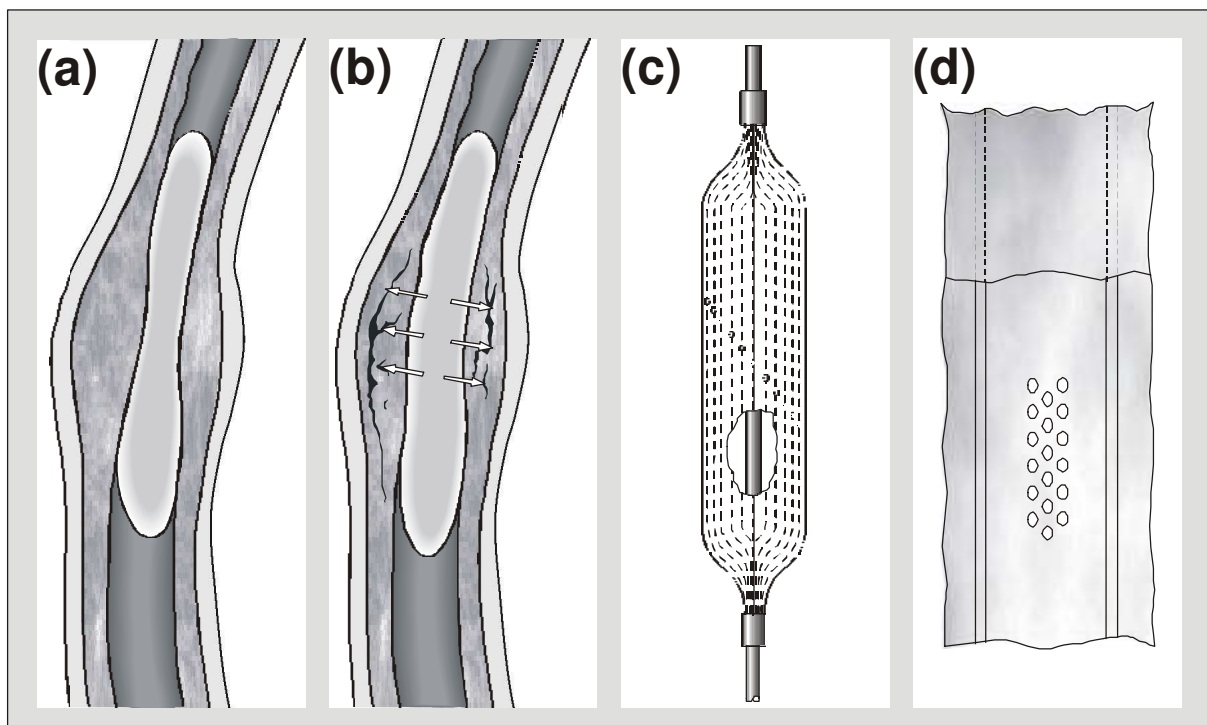


**Fig. 2:** Schematic presentation of the balloon angioplasty combined with intraluminal nanoparticle application using porous delivery catheters. (a) Catheter is positioned in the artery narrowing. (b) When the balloon is inflated, the nanoparticle suspension leak through the micropores and is infused into the vessel wall. (c) and (d) show a channelled balloon catheter (SCIMED REMEDY™), described in detail by Hong (1993) [86] and Ropiak (1999) [87].

<b>Polymer</b>	<b>Size</b>	<b>Drug</b>	<b>Technique</b>	<b>Ref.</b>
PLGA	6–8 $\mu\text{m}$	colchicine	not specified	[68]
PLGA	90-250 nm	dexamethasone	emulsion evaporation	[76]
PLGA	5–10 $\mu\text{m}$	hydrocortisone	emulsion evaporation	[71]
PLA	600-700 nm	dexamethasone colchicine	emulsion evaporation/precipitation	[75]
PLGA	110–160 nm	2-aminochromone	emulsion evaporation	[77]
PLGA	60-200 nm	dexamethasone 2-aminochromone	emulsion evaporation	[78]
PLGA	60-140 nm	2-aminochromone	emulsion evaporation	[74,79]
PLGA	200 nm	probucol	emulsion evaporation	[80]
PLA	90-160 nm	AG-1295 PTK inhibitor	spontaneous emulsification/solvent displacement	[81,82]
Albumin	not specified	paclitaxel	high-pressure homogenisation	[83]
Per- fluorcarbon	250 nm	doxorubicin paclitaxel	high-pressure homogenisation	[84]
PLGA	300 nm	PDGF $\beta$ R-AS	emulsion evaporation	[85]

**Tab. 3:** Summary of drug loaded micro – and nanoparticles and applied polymeric materials for the prevention of restenosis.

---

Additionally, particle size may even determine the biological response of the tissue to the foreign particle material [73,74]. For instance, inflammatory reactions with subsequent fibrosis of vascular tissue have been observed when applying particles of 5 to 10  $\mu\text{m}$  [68,75].

Other crucial aspects for a gentle and efficient intraluminal application are the infusion pressure and the volume of the infusate, both factors which may cause further vascular trauma. Nevertheless, recent studies have reported that the particle administration does not aggravate vessel damages caused by vascular intervention [71,76]. An overview of colloidal drug delivery vehicles for restenosis therapy is provided in Tab. 3.

## **PACLITAXEL FOR PREVENTION OF RESTENOSIS**

A suitable drug for the treatment of restenosis should be able to inhibit several components of the complex process of intimal hyperplasia. Excessive neointima formation shows parallels to tumor cell growth making the use of anti proliferative agents a reasonable therapeutic approach. Paclitaxel, originally isolated from the bark of *Taxus brevifolia* and commonly used to treat breast and ovarian cancer, has been shown to inhibit intimal hyperplasia in vivo [88,89]. By binding on the  $\beta$ -subunits of tubulin, paclitaxel promotes the formation of numerous decentralized, unorganized, and extremely stable microtubule bundles, which ultimately leads to inhibition of cell cycle process in late  $G_2$  and M phase [90,91]. Furthermore, paclitaxel induces long-lasting effects in the cell, due to structural alterations of the cytoskeleton.

---

## OBJECTIVES OF THIS WORK

The current work outlines the preparation and characterization of nanoparticles (NP) and stent coatings, consisting of the biodegradable comb polyester, poly(vinyl alcohol)-graft-poly(lactide-co-glycolide) (PVA-g-PLGA). These delivery systems, when loaded with paclitaxel, may be used for the prevention of a myointimal response after percutaneous transluminal angioplasty, (PTA) which is, as mentioned previously, a factor contributing to the development of restenosis.

The delivery efficiency of free or encapsulated marker substances from balloon catheters has already been assessed in several studies. While liquid agents showed a very short intramural residence time, the local delivery of colloidal drug carriers may help to achieve a sustained and regional release. It is known that particle size plays an important role in the penetration and uptake of particles into the vessel wall, however, the role of nanoparticle migration and deposition has not yet been clearly established. For this reason, the size dependent penetration of fluorescently-labelled polystyrene nanoparticles into the aorta abdominalis of New Zealand white rabbits was investigated using confocal laser scanning microscopy and transmission electron imaging, as described in **Chapter 2**.

Because high delivery pressures and large volumes of infusate may cause severe vascular damage, a further set of experiments (**Chapter 3**), provided more information about the influence of infusion parameters, as well as particle concentration with regard to the intramural nanoparticle distribution pattern and delivery efficiency. As already described in Chapter 2, model nanoparticles consisting of fluorescently-labelled polystyrene, were infused into the aorta abdominalis of rabbits. The aim of the study was to define how to modulate the infusion parameters for an optimal NP delivery without severe intramural dissections.

---

After optimization of the delivery conditions for polystyrene NP, investigations were carried out to prepare and characterize NP consisting of PVA-g-PLGA comb polyesters in vitro (**Chapter 4**). These polymers may be suitable systems to guarantee a controlled, sustained release of paclitaxel, a highly lipophilic, anti proliferative substance. PVA-g-PLGA NP were prepared by a modified solvent displacement technique [92]. Paclitaxel release, the cellular uptake and, in vitro cytotoxicity of the paclitaxel loaded particles were evaluated using rabbit vascular smooth muscle cells (RbVSMC).

**Chapter 5** focuses on paclitaxel loaded films prepared from PVA-g-PLGA, which, when coated onto a metallic stent, serve as drug release matrices. The drug release, degradation, and erosion properties were monitored. Additionally, the dispersion state of paclitaxel within the polymer matrices was investigated using differential scanning calorimetry (DSC) and wide angle X-ray diffraction (WAXD). The Integrity of PVA-g-PLGA coatings after stent expansion was visualized using scanning electron microscopy (SEM). A summary and prospects for future studies based on the results of this work are outlined in the last chapter.

---

**REFERENCES**

- [1] A. Breitenbach, Y.X. Li and T. Kissel, Branched biodegradable polyesters for parenteral drug delivery systems, *J Controlled Release* 64(1-3) (2000) 167-178.
- [2] A. Breitenbach and T. Kissel, Biodegradable comb polyesters: Part 1 - Synthesis, characterisation and structural analysis of PLA and PLGA grafted onto water-soluble PVA as backbone, *Polymers* 39(14) (1998) 3261-3271.
- [3] M. Nobuyoshi, T. Kimura, H. Ohishi et al., Restenosis after percutaneous transluminal coronary angioplasty: pathologic observations in 20 patients, *J Am Coll Cardiol* 17(2) (1991) 433-439.
- [4] M. Chorny, I. Fishbein and G. Golomb, Drug Delivery Systems for Treatment of Restenosis, *Crit Rev Ther Drug Carrier Syst* 17(3) (2000) 249-284.
- [5] H.R. Baumgartner and C. Haudenschild, Adhesion of platelets to subendothelium, *Ann N Y Acad Sci* 201 (1972) 22-36.
- [6] J.M. Breuss, M. Cejna, H. Bergmeister et al., Activation of nuclear factor-kappa B significantly contributes to lumen loss in a rabbit iliac artery balloon angioplasty model, *Circulation* 105(5) (2002) 633-638.
- [7] P. Cirillo, P. Golino, M. Ragni et al., Activated platelets and leucocytes cooperatively stimulate smooth muscle cell proliferation and proto-oncogene expression via release of soluble growth factors, *Cardiovasc Res* 43(1) (1999) 210-218.

- 
- [8] J.E. Rectenwald, L.L. Moldawer, T.S. Huber, J.M. Seeger and C.K. Ozaki, Direct evidence for cytokine involvement in neointimal hyperplasia, *Circulation* 102(14) (2000) 1697-1702.
- [9] Y. Furukawa, A. Matsumori, N. Ohashi et al., Anti-monocyte chemoattractant protein-1/monocyte chemoattractant and activating factor antibody inhibits neointimal hyperplasia in injured rat carotid arteries, *Circ Res* 84(3) (1999) 306-314.
- [10] M.G. Sirois, M. Simons, D.J. Kuter, R.D. Rosenberg and E.R. Edelman, Rat arterial wall retains myointimal hyperplastic potential long after arterial injury, *Circulation* 96(4) (1997) 1291-1298.
- [11] J.A. Bittl, Advances in coronary angioplasty, *N Engl J Med* 335(17) (1996) 1290-1302.
- [12] N.N. Kipshidze, H.S. Kim, P. Iversen et al., Intramural coronary delivery of advanced antisense oligonucleotides reduces neointimal formation in the porcine stent restenosis model, *J Am Coll Cardiol* 39(10) (2002) 1686-1691.
- [13] C. Bauters, P. De Groote, M. Adamantidis et al., Proto-oncogene expression in rabbit aorta after wall injury. First marker of the cellular process leading to restenosis after angioplasty?, *Eur Heart J* 13(4) (1992) 556-559.
- [14] S.M. Schwartz, D. Deblois and E.R. O'brien, The intima. Soil for atherosclerosis and restenosis, *Circ Res* 77(3) (1995) 445-465.
- [15] C. Bauters and J.M. Isner, The biology of restenosis, *Prog Cardiovasc Dis* 40(2) (1997) 107-116.

- 
- [16] D.P. Faxon, W. Coats and J. Currier, Remodeling of the coronary artery after vascular injury, *Prog Cardiovasc Dis* 40(2) (1997) 129-140.
- [17] Y. Shi, M. Pieniek, A. Fard et al., Adventitial Remodeling After Coronary Arterial Injury, *Circulation* 93(2) (1996) 340-348.
- [18] R. Hoffmann, G.S. Mintz, G.R. Dussaillant et al., Patterns and mechanisms of in-stent restenosis. A serial intravascular ultrasound study, *Circulation* 94(6) (1996) 1247-1254.
- [19] A. Farb, G. Sangiorgi, A.J. Carter et al., Pathology of acute and chronic coronary stenting in humans, *Circulation* 99(1) (1999) 44-52.
- [20] A. Farb, D.K. Weber, F.D. Kolodgie, A.P. Burke and R. Virmani, Morphological predictors of restenosis after coronary stenting in humans, *Circulation* 105(25) (2002) 2974-2980.
- [21] G.S. Mintz, J.J. Popma, M.K. Hong et al., Intravascular ultrasound to discern device-specific effects and mechanisms of restenosis, *Am J Cardiol* 78(3A) (1996) 18-22.
- [22] R. Virmani and A. Farb, Pathology of in-stent restenosis, *Curr Opin Lipidol* 10(6) (1999) 499-506.
- [23] R. Kornowski, M.K. Hong, F.O. Tio et al., In-stent restenosis: contributions of inflammatory responses and arterial injury to neointimal hyperplasia, *J Am Coll Cardiol* 31(1) (1998) 224-230.
- [24] R. Komatsu, M. Ueda, T. Naruko, A. Kojima and A.E. Becker, Neointimal tissue response at sites of coronary stenting in humans: macroscopic, histological, and immunohistochemical analyses, *Circulation* 98(3) (1998) 224-233.

- 
- [25] A. Kastrati, H. Schuhlen, J. Hausleiter et al., Restenosis after coronary stent placement and randomization to a 4-week combined antiplatelet or anticoagulant therapy: six-month angiographic follow-up of the Intracoronary Stenting and Antithrombotic Regimen (ISAR) Trial, *Circulation* 96(2) (1997) 462-467.
- [26] C.W. Lee, J.K. Chae, H.Y. Lim et al., Prospective randomized trial of corticosteroids for the prevention of restenosis after intracoronary stent implantation, *Am Heart J* 138(1 Pt 1) (1999) 60-63.
- [27] T. Meurice, C. Bauters, X. Hermant et al., Effect of ACE inhibitors on angiographic restenosis after coronary stenting (PARIS): a randomised, double-blind, placebo-controlled trial, *Lancet* 357(9265) (2001) 1321-1324.
- [28] P.W. Serruys, D.P. Foley, G. Jackson et al., A randomized placebo-controlled trial of fluvastatin for prevention of restenosis after successful coronary balloon angioplasty; final results of the fluvastatin angiographic restenosis (FLARE) trial, *Eur Heart J* 20(1) (1999) 58-69.
- [29] P.W. Serruys, D.P. Foley, M. Pieper, J.A. Kleijne and P.J. De Feyter, The TRAPIST Study. A multicentre randomized placebo controlled clinical trial of trapidil for prevention of restenosis after coronary stenting, measured by 3-D intravascular ultrasound, *Eur Heart J* 22(20) (2001) 1938-1947.
- [30] S.G. Ellis, Acute platelet inhibition with abciximab does not reduce in-stent restenosis (ERASER study). The ERASER Investigators, *Circulation* 100(8) (1999) 799-806.

- 
- [31] R.K. Aggarwal, D.C. Ireland, M.A. Azrin et al., Antithrombotic potential of polymer-coated stents eluting platelet glycoprotein IIb/IIIa receptor antibody, *Circulation* 94(12) (1996) 3311-3317.
- [32] A.M. Lincoff, J.G. Furst, S.G. Ellis, R.J. Tuch and E.J. Topol, Sustained local delivery of dexamethasone by a novel intravascular eluting stent to prevent restenosis in the porcine coronary injury model, *J Am Coll Cardiol* 29(4) (1997) 808-816.
- [33] E.J. Topol and P.W. Serruys, *Frontiers in interventional cardiology*, *Circulation* 98(17) (1998) 1802-1820.
- [34] T.L. Lambert, V. Dev, E. Rechavia et al., Localized arterial wall drug delivery from a polymer-coated removable metallic stent. Kinetics, distribution, and bioactivity of forskolin, *Circulation* 90(2) (1994) 1003-1011.
- [35] V. Dev, N. Eigler, S. Sheth et al., Kinetics of drug delivery to the arterial wall via polyurethane-coated removable nitinol stent: comparative study of two drugs, *Cathet Cardiovasc Diagn* 34(3) (1995) 272-278.
- [36] Y. Nakayama, K. Ji-Youn, S. Nishi, H. Ueno and T. Matsuda, Development of high-performance stent: gelatinous photogel-coated stent that permits drug delivery and gene transfer, *J Biomed Mater Res* 57(4) (2001) 559-566.
- [37] Y.W. Ye, C. Landau, J.E. Willard et al., Bioresorbable microporous stents deliver recombinant adenovirus gene transfer vectors to the arterial wall, *Ann Biomed Eng* 26(3) (1998) 398-408.
- [38] R.S. Schwartz, K.C. Huber, J.G. Murphy et al., Restenosis and the proportional neointimal response to coronary artery injury: results in a porcine model, *J Am Coll Cardiol* 19(2) (1992) 267-274.

- 
- [39] R.E. Kuntz, C.M. Gibson, M. Nobuyoshi and D.S. Baim, Generalized model of restenosis after conventional balloon angioplasty, stenting and directional atherectomy, *J Am Coll Cardiol* 21(1) (1993) 15-25.
- [40] S.V. Lossef, R.J. Lutz, J. Mundorf and K.H. Barth, Comparison of mechanical deformation properties of metallic stents with use of stress-strain analysis, *J Vasc Interv Radiol* 5(2) (1994) 341-349.
- [41] C. Rogers and E.R. Edelman, Endovascular stent design dictates experimental restenosis and thrombosis, *Circulation* 91(12) (1995) 2995-3001.
- [42] R. Hoffmann, G.S. Mintz, P.K. Haager et al., Relation of stent design and stent surface material to subsequent in-stent intimal hyperplasia in coronary arteries determined by intravascular ultrasound, *Am J Cardiol* 89(12) (2002) 1360-1364.
- [43] E.R. Edelman, P. Seifert, A. Groothuis et al., Gold-coated NIR stents in porcine coronary arteries, *Circulation* 103(3) (2001) 429-434.
- [44] J. Gunn and D. Cumberland, Stent coatings and local drug delivery; state of the art, *Eur Heart J* 20(23) (1999) 1693-1700.
- [45] K. Al-Lamee and D. Cook, Polymer coating techniques for drug-eluting stents, *Med Device Technol* 14(1) (2003) 12-14.
- [46] A. Lewis and T. Vick, Site-specific drug delivery from coronary stents, *Drug Delivery Systems and Science* 1 (2002) 65-71.
- [47] J. Van Der Giessen, A.M. Lincoff, R.S. Schwartz et al., Marked Inflammatory Sequelae to Implantation of Biodegradable and Nonbiodegradable Polymers in Porcine Coronary Arteries, *Circulation* 94(7) (1996) 1690-1697.

- 
- [48] T. Peng, P. Gibula, K.D. Yao and M.F. Goosen, Role of polymers in improving the results of stenting in coronary arteries, *Biomaterials* 17(7) (1996) 685-694.
- [49] O.F. Bertrand, R. Sipehia, R. Mongrain et al., Biocompatibility aspects of new stent technology, *J Am Coll Cardiol* 32(3) (1998) 562-571.
- [50] H. Wieneke, T. Sawitowski, S. Wnendt et al., Stent coating: a new approach in interventional cardiology, *Herz* 27(6) (2002) 518-526.
- [51] J.E. Sousa, M.A. Costa, A. Abizaid et al., Lack of Neointimal Proliferation After Implantation of Sirolimus-Coated Stents in Human Coronary Arteries : A Quantitative Coronary Angiography and Three-Dimensional Intravascular Ultrasound Study, *Circulation* 103(2) (2001) 192-195.
- [52] M.-C. Morice, P.W. Serruys, J.E. Sousa et al., A Randomized Comparison of a Sirolimus-Eluting Stent with a Standard Stent for Coronary Revascularization, *N Engl J Med* 346(23) (2002) 1773-1780.
- [53] J. Schofer, M. Schluter, A.H. Gershlick et al., Sirolimus-eluting stents for treatment of patients with long atherosclerotic lesions in small coronary arteries: double-blind, randomised controlled trial (E-SIRIUS), *Lancet* 362(9390) (2003) 1093-1099.
- [54] J.W. Moses, M.B. Leon, J.J. Popma et al., Sirolimus-eluting stents versus standard stents in patients with stenosis in a native coronary artery, *N Engl J Med* 349(14) (2003) 1315-1323.
- [55] X. Liu, Y. Huang, C. Hanet et al., Study of antirestenosis with the BiodivYsio dexamethasone-eluting stent (STRIDE): A first-in-human multicenter pilot trial, *Catheter Cardiovasc Interv* 60(2) (2003) 172-178.

- 
- [56] S.J. Park, W.H. Shim, D.S. Ho et al., A paclitaxel-eluting stent for the prevention of coronary restenosis, *N Engl J Med* 348(16) (2003) 1537-1545.
- [57] E. Grube and L. Bullesfeld, Initial experience with paclitaxel-coated stents, *J Interv Cardiol* 15(6) (2002) 471-475.
- [58] E. Grube, S. Silber, K.E. Hauptmann et al., TAXUS I: six- and twelve-month results from a randomized, double-blind trial on a slow-release paclitaxel-eluting stent for de novo coronary lesions, *Circulation* 107(1) (2003) 38-42.
- [59] F. Liistro, G. Stankovic, C. Di Mario et al., First Clinical Experience With a Paclitaxel Derivate-Eluting Polymer Stent System Implantation for In-Stent Restenosis: Immediate and Long-Term Clinical and Angiographic Outcome, *Circulation* 105(16) (2002) 1883-1886.
- [60] M. Haude, T.F. Konorza, U. Kalnins et al., Heparin-coated stent placement for the treatment of stenoses in small coronary arteries of symptomatic patients, *Circulation* 107(9) (2003) 1265-1270.
- [61] I. De Scheerder, K. Wang, K. Wilczek et al., Experimental study of thrombogenicity and foreign body reaction induced by heparin-coated coronary stents, *Circulation* 95(6) (1997) 1549-1553.
- [62] H. Tamai, K. Igaki, E. Kyo et al., Initial and 6-month results of biodegradable poly-l-lactic acid coronary stents in humans, *Circulation* 102(4) (2000) 399-404.
- [63] T. Tsuji, H. Tamai, K. Igaki et al., Biodegradable stents as a platform to drug loading, *Int J Cardiovasc Intervent* 5(1) (2003) 13-16.

- 
- [64] D.S. Eccleston and A.M. Lincoff, Catheter-based drug delivery for restenosis, *Adv Drug Del Rev* 24 (1997)
- [65] J.F. Mitchel, D.B. Fram, D.F. Palme, 2nd et al., Enhanced intracoronary thrombolysis with urokinase using a novel, local drug delivery system. In vitro, in vivo, and clinical studies, *Circulation* 91(3) (1995) 785-793.
- [66] D.W. Muller, E.J. Topol, G.D. Abrams, K.P. Gallagher and S.G. Ellis, Intramural methotrexate therapy for the prevention of neointimal thickening after balloon angioplasty, *J Am Coll Cardiol* 20(2) (1992) 460-466.
- [67] R.L. Wilensky, K.L. March and D.R. Hathaway, Direct intraarterial wall injection of microparticles via a catheter: a potential drug delivery strategy following angioplasty, *Am Heart J* 122(4 Pt 1) (1991) 1136-1140.
- [68] I. Gradus-Pizlo, R.L. Wilensky, K.L. March et al., Local delivery of biodegradable microparticles containing colchicine or a colchicine analogue: effects on restenosis and implications for catheter-based drug delivery, *J Am Coll Cardiol* 26(6) (1995) 1549-1557.
- [69] R.L. Wilensky, K.L. March, I. Gradus-Pizlo et al., Regional and arterial localization of radioactive microparticles after local delivery by unsupported or supported porous balloon catheters, *Am Heart J* 129(5) (1995) 852-859.
- [70] T.K. Nasser, R.L. Wilensky, K. Mehdi and K.L. March, Microparticle deposition in periarterial microvasculature and intramural dissections after porous balloon delivery into atherosclerotic vessels: quantitation and localization by confocal scanning laser microscopy, *Am Heart J* 131(5) (1996) 892-898.

- 
- [71] F. Valero, M. Hamon, C. Fournier et al., Intramural injection of biodegradable microspheres as a local drug- delivery system to inhibit neointimal thickening in a rabbit model of balloon angioplasty, *J Cardiovasc Pharmacol* 31(4) (1997) 513-519.
- [72] J. Rome, V. Shayani, M. Flugelman et al., Anatomic barriers influence the distribution of in vivo gene transfer into the arterial wall. Modeling with microscopic tracer particles and verification with a recombinant adenoviral vector, *Arteriosclerosis and Thrombosis* 14(1) (1994) 148-161.
- [73] J.M. Anderson, Biodegradation and biocompatibility of PLA and PLGA microparticles, *Adv Drug Del Rev* 28 (1997) 5-24.
- [74] V. Labhasetwar, C. Song, W. Humphrey, R. Shebuski and J. Levy, Arterial Uptake of Biodegradable Nanoparticles: Effect of Surface Modifications, *J Pharm Sci* 87(10) (1998) 1229-1234.
- [75] V. Dev, N. Eigler, M.C. Fishbein et al., Sustained local drug delivery to the arterial wall via biodegradable microspheres, *Cathet Cardiovasc Diagn* 41(3) (1997) 324-332.
- [76] L.A. Guzman, V. Labhasetwar, C. Song et al., Local Intraluminal Infusion of Biodegradable Polymeric Nanoparticles. A novel Approach for Prolonged Drug Delivery After Balloon Angioplasty, *Circulation* 94 (1996) 1441-1448.
- [77] W. Humphrey, L.A. Erickson, C.A. Simmons et al., The effect of intramural delivery of polymeric nanoparticles loaded with the anti proliferative 2-aminochromone U-86983 on neointimal hyperplasia development in ballon-injured porcine coronary arteries, *Adv Drug Del Rev* 24 (1997) 87-108.

- 
- [78] C. Song, V. Labhasetwar, H. Murphy et al., Formulation and characterization of biodegradable nanoparticles for intravascular local drug delivery, *J Controlled Release* 43 (1997) 197-212.
- [79] C. Song, V. Labhasetwar, X. Cui, T. Underwood and R.J. Levy, Arterial uptake of biodegradable nanoparticles for intravascular local drug delivery: results with an acute dog model, *J Controlled Release* 54(2) (1998) 201-211.
- [80] B.D. Klugherz, N. Meneveau, W. Chen et al., Sustained Intramural Retention and Regional Redistribution Following Local Vascular Delivery of Polylactic-Coglycolic Acid and Liposomal Nanoparticulate Formulations Containing Probucol, *J Cardiovasc Pharmacol Ther* 4(3) (1999) 167-174.
- [81] I. Fishbein, M. Chorny, L. Rabinovich et al., Nanoparticulate delivery system of a tyrphostin for the treatment of restenosis, *J Controlled Release* 65(1-2) (2000) 221-229.
- [82] I. Fishbein, M. Chorny, S. Banai et al., Formulation and delivery mode affect disposition and activity of tyrphostin-loaded nanoparticles in the rat carotid model, *Arterioscler Thromb Vasc Biol* 21(9) (2001) 1434-1439.
- [83] F.D. Kolodgie, M. John, C. Khurana et al., Sustained Reduction of In-Stent Neointimal Growth With the Use of a Novel Systemic Nanoparticle Paclitaxel, *Circulation* 106(10) (2002) 1195-1198.
- [84] G.M. Lanza, X. Yu, P.M. Winter et al., Targeted Anti proliferative Drug Delivery to Vascular Smooth Muscle Cells With a Magnetic Resonance Imaging Nanoparticle Contrast Agent: Implications for Rational Therapy of Restenosis, *Circulation* 106(22) (2002) 2842-2847.

- 
- [85] H. Cohen-Sacks, Y. Najajreh, V. Tchaikovski et al., Novel PDGFbetaR antisense encapsulated in polymeric nanospheres for the treatment of restenosis, *Gene Ther* 9(23) (2002) 1607-1616.
- [86] M.K. Hong, S.C. Wong, A. Farb et al., Feasibility and drug delivery efficiency of a new balloon angioplasty catheter capable of performing simultaneous local drug delivery, *Coron Artery Dis* 4(11) (1993) 1023-1027.
- [87] S.M. Ropiak, Multiple hole drug delivery balloon, US 5,860,954, September 29, 1997.
- [88] D.I. Axel, W. Kunert, C. Goggelmann et al., Paclitaxel inhibits arterial smooth muscle cell proliferation and migration in vitro and in vivo using local drug delivery, *Circulation* 96(2) (1997) 636-645.
- [89] C. Herdeg, M. Oberhoff, A. Baumbach et al., Local paclitaxel delivery for the prevention of restenosis: biological effects and efficacy in vivo, *J Am Coll Cardiol* 35(7) (2000) 1969-1976.
- [90] S.B. Horwitz, Mechanism of action of taxol, *Trends Pharmacol Sci* 13(4) (1992) 134-136.
- [91] E.K. Rowinsky and R.C. Donehower, Paclitaxel (taxol), *N Engl J Med* 332(15) (1995) 1004-1014.
- [92] T. Jung, A. Breitenbach and T. Kissel, Sulfobutylated poly(vinyl alcohol)-graft-poly(lactide-co-glycolide)s facilitate the preparation of small negatively charged biodegradable nanospheres, *J Controlled Release* 67(2-3) (2000) 157-169.

## **CHAPTER 2**

---

# **DEPOSITION OF NANOPARTICLES IN THE ARTERIAL VESSEL BY POROUS BALLOON CATHETERS: LOCALIZATION BY CONFOCAL LASER SCANNING MICROSCOPY AND TRANSMISSION ELECTRON MICROSCOPY**

---

## SUMMARY

Restenosis remains the major limitation of percutaneous transluminal angioplasty (PTA) and stenting in the treatment of patients with atherosclerotic disease. Catheter-based local delivery of pharmacologic agents offers a potential therapeutic approach to reducing restenosis and minimizing undesirable systemic side effects. However, the intramural retention of liquid agents is low. Therefore, to achieve a sustained and regional release of the therapeutic agent it must be encapsulated in nanoparticle carrier systems. The purpose of this study was to investigate the size dependence of the penetration of nanoparticles after local delivery into the vessel wall of the aorta abdominalis of New Zealand white rabbits. Two milliliters of a 0.025% fluorescence-labelled polystyrene nanoparticle suspension with diameters ranging from 110 to 514 nm were infused at 2 atm and at constant PTA pressure of 8 atm into the aorta abdominalis. After the infused segments were removed, the location of nanoparticles was visualized using confocal laser scanning microscopy and transmission electron microscopy. The study demonstrates a size-dependent nanoparticle penetration into the intact vessel wall. While nanoparticles of about 100 and 200 nm were deposited in the inner regions of the vessel wall, 514-nm nanoparticles accumulated primarily at the luminal surface of the aorta. The observations confirm that size plays a critical role in the distribution of particles in the arterial vessel wall. It is additionally influenced by the formation of pressure-induced infusion channels, as well as by the existence of anatomic barriers, such as plaques, at the luminal surface of the aorta or the connective elastic tissue.

---

## INTRODUCTION

Restenosis is defined as a reobstruction of an artery following arterial interventions, such as balloon angioplasty, atherectomy, or stenting of an atherosclerotic plaque, and is characterized by intimal hyperplasia and vessel remodeling [1-4]. Intimal growth results from vascular smooth muscle cell (VSMC) migration and proliferation into the media [5] followed by the formation of extracellular matrix [6]. Currently, different routes of drug administration in restenosis therapy are under investigation. The proliferation of VSMC, the cause of restenosis development, could be inhibited by the application of radioactive [7] and drug eluting stents [8,9]. Another method to reduce VSMC growth and neointimal formation is the local administration of a drug solution using drug delivery catheters [10]; however, the delivery efficiency and intramural retention time of infused agents remains rather low [11,12]. Therefore, researchers have developed colloidal drug carrier systems from biodegradable polymers that may provide a local release and sustained retention of the drug in the arterial wall [13-17].

Recent studies have indicated that particle size plays an important role in the penetration and cellular uptake of particles into the vessel wall [16,18]. Furthermore, particle size may even determine the biological response of the tissue to the foreign particle material [19,20]. For instance, inflammatory reactions with subsequent fibrosis of vascular tissue have been found when applying particles with a size of 5 to 10  $\mu\text{m}$  [13,21].

Guzman et al [22] observed that fluorescent-labelled particles of 165 nm that were first deposited in the luminal, medial, and adventitial layers of the artery were found afterward in only the adventitia. They concluded that the adventitial layer acts as a reservoir for particles and eluted drugs, which then subsequently diffuse in the direction of the media. A discontinuous particle distribution has been also found by Rome et al [18]. They showed that different

---

types of particles, ranging between 90 to 500 nm in size, tended to accumulate in the outer wall layers but not in the media. These authors suggested that the particles reach the adventitia via the vasa vasorum, but not directly by penetrating the wall. Song et al [23,24] explained the fluorescence activity of rhodamine B-loaded poly(D,L-lactide-co-glycolide (PLG) nanoparticles in the media of a dog carotid artery by the possibility of inward migration of nanoparticles from the adsorption site at the intraluminal surface. On the one hand, these findings suggest that particles smaller than 300 nm are well suited as an effective intraluminal drug delivery system. On the other hand, the migration and deposition behavior of nanoparticles in the tissue is not yet clearly established.

The present study concentrates on the size-dependent penetration of nanoparticles into the aorta abdominalis of New Zealand white rabbits. In contrast to other authors, we used fluorescence-labelled instead of fluorescence-loaded particles to avoid any unintentional dye release that would prevent the exact determination of the particle distribution by confocal laser scanning microscopy (CLSM). Our investigations have shown that the particle migration through the wall tissue is in fact size dependent and, furthermore, is strongly influenced by the existence of atherosclerotic plaques at the luminal surface of the aorta, as well as by the formation of channel-like diffusion paths induced by pressurized infusion.

## **MATERIALS AND METHODS**

### **Local nanoparticle delivery**

All animal experiments followed the “Principles of Laboratory Animal Care” (National Institutes of Health publication #85-23, revised 1985) and were approved by an external review committee for laboratory animal care. Male New Zealand white rabbits (3.5-4 kg) were sacrificed using a mixture of

embutramide, mebenzonium iodide, and tetracaine hydrochloride. The aorta abdominalis was exposed in-situ (averaging 20-30 mm in length). For angioplasty and local delivery, a channelled balloon catheter (SCIMED REMEDY, Boston Scientific, Natick, MA) was placed in the aorta abdominalis. The delivery device has been described in detail by Hong et al [25]. Briefly, it is a 3-lumen over-the-wire catheter with separate ports for balloon dilation and local drug delivery. The balloon carries 18 channels, with 1 group of 30- $\mu$ m diameter pores per channel. The catheter shaft is 3.4 French. During this study, we used a balloon length of 20 mm and a diameter of 2.5 mm.

Yellow-green labelled polystyrene nanoparticles of 110, 217, and 514 nm in diameter (Fluoresbrite plain microspheres YG, Polyscience Inc, Warrington, PA) were suspended in water. Two milliliters of each suspension (0.025% (wt/vol) in water) were infused at a constant pressure of 2 atm and at a constant balloon pressure of 8 atm. A control experiment was performed by infusion of 0.9% sodium chloride solution. After the infusion experiments, arterial segments were removed and fixed in formalin solution (4% vol/vol) for CLSM or glutaraldehyde (2.7% vol/vol) in phosphate buffered saline (PBS) 0.1M, pH 7 for transmission electron microscopy.

### **Confocal laser scanning microscopy**

Arterial segments were frozen in isopentane on ice and embedded in Tissue Freezing Medium (Jung, Germany). Cross-sections of 20- $\mu$ m thickness were cut using a Frigocut 2700 cryo microtome (Reichert-Jung, Germany) and mounted on SuperFrost plus (Menzel-Glaeser, Germany) glass slides. They were counterstained with 4'-diamidino-2-phenylindole (DAPI) (1  $\mu$ g/mL) (Molecular Probes, Leiden, The Netherlands) solution in PBS for 30 minutes under light exclusion and embedded in PBS/glycerol (2:1 vol/vol). Localization of fluorescence-labelled nanoparticles was performed using a CLSM (Axiovert, Zeiss CLSM 501, Jena, Germany) equipped with a Zeiss Neofluor 40\*/1.3

objective. Excitation wavelengths were 364 nm (long-pass filter [LP] 385 nm) for DAPI and 488 nm (LP 505 nm) for the yellow-green labelled nanoparticles. All confocal images were acquired with the same settings with respect to laser intensity, filter block, and detector gain.

### **Transmission electron microscopy**

The fixed blood vessels were rinsed 3 times with 0.15M PBS, pH 7 for 1 hour each and postfixed for 75 minutes in 2% osmium tetroxide. Dehydration was accomplished in a series of mixtures of water with component A (a water-soluble aliphatic polyepoxide) of the Durcupan ACM water-soluble embedding medium (Fluka, Germany) as follows:

- 50% component A with 50% water for 30 minutes
- 70% component A with 30% water for 45 minutes
- 90% component A with 10% water for 45 minutes
- 100% component A for 90 minutes

The dehydrated tissue was then placed in a polymerization mixture of the components A through D (components B and C are hardeners; component D is the plasticizer) according to the manufacturer's protocol and left overnight in a refrigerator for final mixing and embedding. Polymerization was performed in a freshly prepared mixture of the above composition for 4 days at 42°C.

Ultrathin sections, about 50-nm thick, were obtained using a Leica Ultracut UCT ultramicrotome and a diamond knife (Leica Microsystems, Bensheim, Germany). The sections were collected on copper grids covered by a thin layer of colodium and carbon. Final staining of the sections included treatment with uranylacetate for 15 minutes and with lead citrate for 9 minutes. Microscopic examinations were carried out with a JEM 3010 transmission electron microscope (Jeol Electron Microscope, Japan) operated at 300 kV,

---

equipped with a MegaScan CCD (charge-coupled device) camera (2048 x 2048 pixel).

## RESULTS AND DISCUSSION

Cross-sections from the infusion experiments without fluorescent probes exhibited no or negligible green autofluorescence at standard confocal settings (Fig. 1A). Green autofluorescent emissions of arterial elastin and collagen structures can be well distinguished from the blue stained nuclei of smooth muscle, endothelial, and adventitial cells, as well as from the nanoparticles. The observed cross-sections of the arterial segments subjected to intramural nanoparticle infusion using a perforated balloon catheter did not show any severe disruptions of the vessel wall.

Confocal laser scanning analyses revealed a size-dependent penetration depth of the nanoparticles in the non-atherosclerotic arterial wall at constant infusion pressure. As displayed in Fig. 1B, the 514-nm nanoparticles were observed to accumulate preferentially at the luminal surface of the aorta. Only a negligible number of particles was detected in the inner parts of the vessel wall. With decreasing diameter, the penetration capability of the particles increased, as shown in the case of 217-nm particles in Fig. 1C and 1D, and 110-nm particles in Fig. 2A. High fluorescent activity in deeper cell layers of the vessel wall, especially in the latter case, indicates that nanoparticles of 110 nm easily penetrate through the arterial wall. Sometimes a tendency toward cluster formations was observed on the luminal surface. Furthermore, it seems quite obvious that the particle distribution between the luminal site and the adventitial layer is not continuous. This is documented by systematic observations and is not based on sectioning artefacts. On the other hand, discontinuous particle concentrations crossing the artery wall may be caused by differences in the

accessibility, the transmission properties, and the holding behavior of the different vessel wall layers.

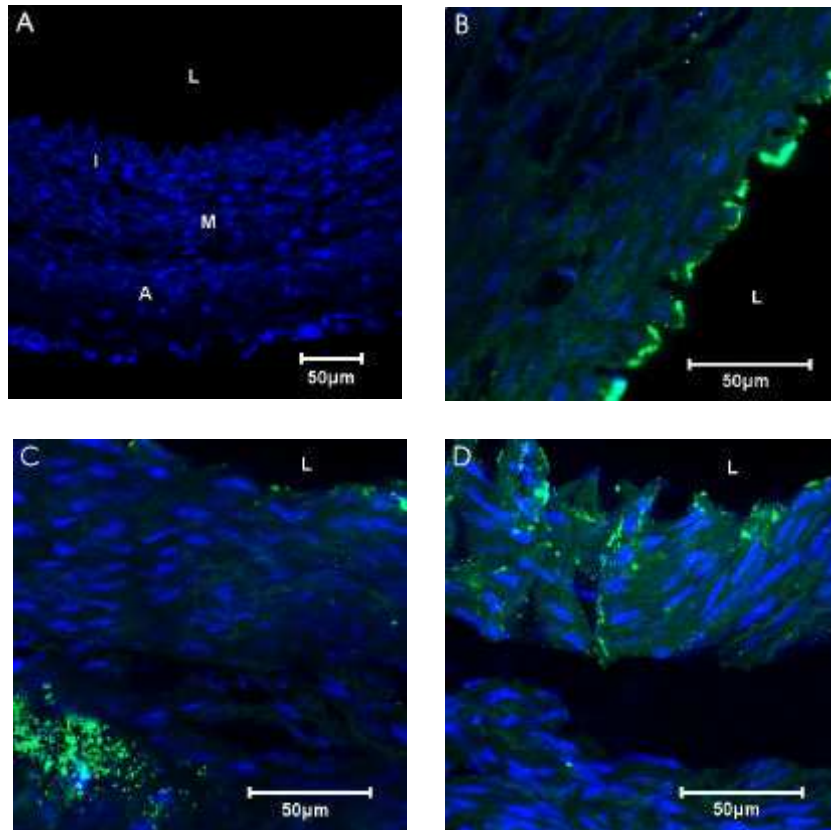


**Fig. 1:** CLSM analysis of the nanoparticle distribution in the vessel wall of the aorta abdominalis of New Zealand white rabbits: nuclei (blue) stained with DAPI, catheter-delivered yellow-green labelled polystyrene nanoparticles (green). P, L, M, and A indicate the atherosclerotic plaque, lumen, media, and adventitia. (A) Balloon-dilated segment of aorta abdominalis: control experiment without nanoparticle infusion. (B) Confocal image: accumulation of 514-nm particles on the luminal surface of the aorta. (C and D) Confocal images: distribution of 217-nm particles in the aorta abdominalis; optical sections were taken from the inner medial (C) and the adventitial part (D) of the vessel wall layers (2.87  $\mu\text{m}$  each layer).

While the CLSM images provide an overview of the delivery characteristics of the nanoparticles across the blood vessel, the precise localization of the particles within a particular tissue layer needs a higher resolution achieved by using transmission electron microscopy. Fig. 3A to 3F

are transmission electron micrographs of stained ultra-thin sections from the endothelial region (Fig. 3A-3C) and the media (Fig. 3D-3F) for the 3 particle sizes used: 514, 217, and 110 nm. In the inner region the endothelial cells show mechanical distortion due to the catheter intervention. In the medial layer typical views of the glycogen strands are revealed. The size dependency of particle deposition is proved by Fig. 3A to 3F, with only the small-sized particles reaching the inner wall regions in considerable amounts.

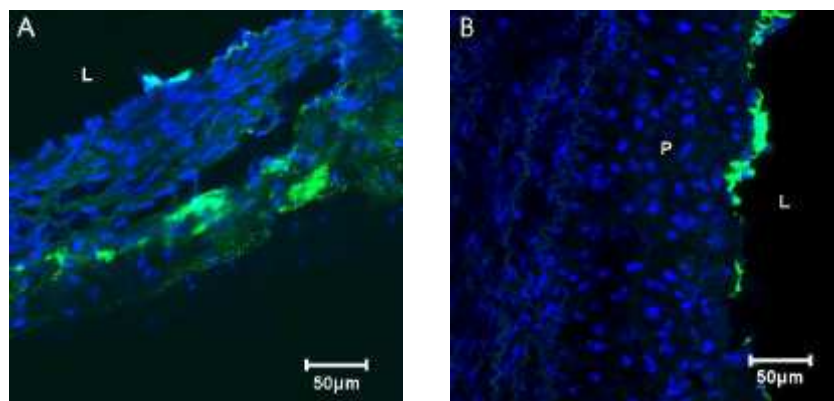


**Fig. 2:** *Confocal images: distribution of 110-nm particles in a non-atherosclerotic vessel segment (A) in comparison to an atherosclerotic segment (B).*

Observations of atherosclerotic arteries showed that plaques on the endothelial cell layer are able to inhibit even the penetration of the 110-nm nanoparticles (Fig. 2B). The plaque consists of collagen, fibrin, smooth muscle cells, foam cells, and macrophages, which form a rather solid layer on the inner vessel surface. Hence, they may act as a strong barrier to particle penetration. Preliminary experiments using nanoparticles as small as 57 nm in diameter have led to the same result (data not shown): hindrance of transportation into the vessel wall by a barrier of extended plaque formation.

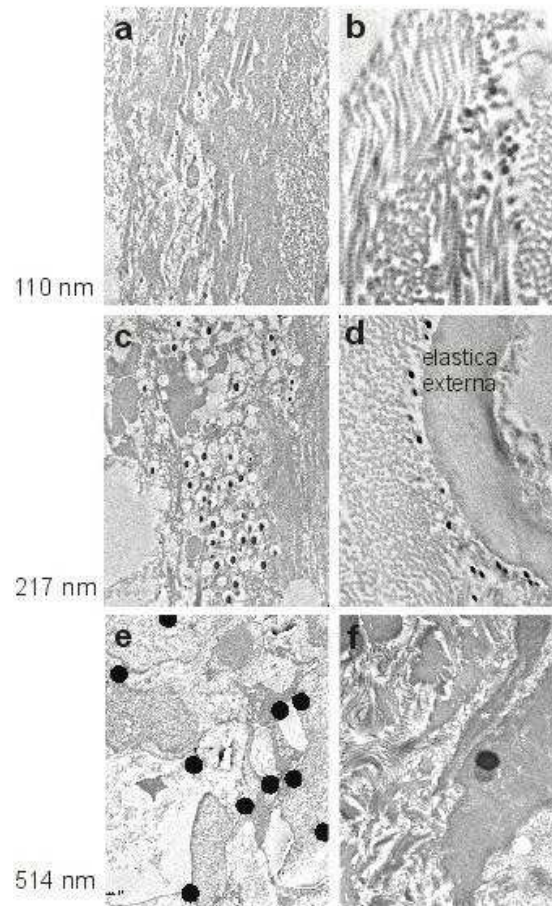


**Fig. 3:** Transmission electron micrographs of the accumulation of 110-, 217-, and 514-nm particles in the endothelial layer (A, B, E) and in the media (B, D, F) of the aorta abdominalis of New Zealand white rabbits (lumen left). Segment D provides clear proof of how the elastica tissue acts as a diffusion barrier.

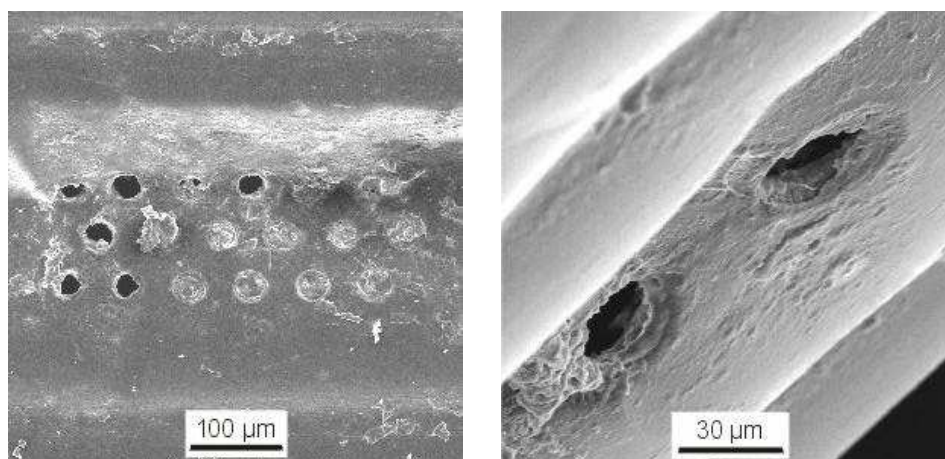


**Fig. 4:** Scanning electron micrographs of the infusion holes in a REMEDY balloon catheter showing one group comprising 18 channels (a) and 2 holes at higher magnification (b). Some holes remained filled with organic material after use.

The elastic connective tissue can also function as a strong transport barrier for the nanoparticles, as Fig. 3D illustrates. The 217-nm particles are strung like pearls alongside the interface to the *elastica externa*; the particles were neither able to penetrate nor to permeate the elastic tissue.

The CLSM image in Fig. 1C is part of a gallery of 7 optical sections (2.87  $\mu\text{m}$  each section). In one of the upper sections of this sequence, particle deposition in the endothelium and the adventitia was observed, as was particle deposition along a radial channel-like trace connecting the inner and outer regions of the vessel, as Fig. 1D shows. It is suggested that such traces originate from the directed stream of nanoparticles ejected under pressure through the holes of the perforated balloon catheter. The size and the configuration of the infusion holes in the catheter wall may, thus, influence the distribution characteristics of the nanoparticles in the blood vessel strongly. Fig. 4 shows the typical arrangement and shape of the holes in the REMEDY catheter used in this study. The 25- $\mu\text{m}$  holes are arranged in groups of 18, of which 6 such groups are distributed over the circumference in a repetitive manner at a distance along the catheter axis of approximately 5 mm. The hole diameter and the width of a diffusion channel in Fig. 1C are in the same order of magnification.

The feasibility of local drug delivery with a perforated balloon catheter for the prevention of restenosis was first demonstrated by Wolinski and Thung [10]. However, the intramural delivery efficiency and the retention time of liquid agents was low [10-13]. To overcome this drawback, microparticles have been evaluated as potential drug delivery vehicles [13-17]. The predominant sites of microparticle deposition were found to be the adventitial vasa vasorum, the periadventitial microvasculature, and along intimal disruptions [16,17] but usually not the target tissue, the media. One important aspect of these carrier systems is the effect of particle size on penetration behavior and cellular uptake by the vessel wall [18]. In addition to that, particle size is associated with biological response of the tissue to foreign biomaterials [19,20]. While

---

inflammatory reactions with subsequent fibrosis is a typical response of vascular tissue to particulate delivery systems ranging in size between 5 and 10  $\mu\text{m}$  [13,21], nanoparticles usually cause little or no focal inflammation.

Guzman et al. [22] found fluorescence-loaded PLGA particles of 90 to 250 nm predominantly at the lumen surface of the vessel wall and in the adventitial layer. Only a few particles were observed in the media [22]. Rome et al [18] suggested that particles smaller than 500 nm, which had mainly accumulated within the intimal and adventitial layers, reach the media via vasa vasora of the artery. Song et al [23] reported fluorescence activity of 100 to 200 nm rhodamin B-loaded PLGA nanoparticles in the media of a dog carotid artery, which was explained by the possible migration of particles from adsorption sites at the luminal surface.

Our study adds an additional aspect to the understanding of particle migration. The channel-like deposition patterns observed after application of 217-nm particles seem to be caused by the pressure-induced particle stream from the catheter pores through the intima and media into the adventitial layer. To achieve a similar effect using larger particles, the infusion pressure needs to be increased considerably. This could have detrimental consequences to the wound healing process of the injured vessel wall. When smaller nanoparticles ( $\leq 200$  nm) are applied, a lower infusion pressure is necessary; thus, the formation of extended vessel lesions is prevented. The most favorable pressure level should provide sufficient nanoparticle deposition in the vessel wall and, at the same time, avoid unrecoverable vessel irritations. According to our experience, pressure levels of about 2 to 4 atm are efficient and atraumatic in this model.

Possible anatomic barriers to any particle transportation through the wall tissue are the intact internal and external elastic laminae. Moreover, the presence of atherosclerotic plaques on the inner luminal surface strongly influences the particle penetration into the arterial wall, as our results have shown. Independent

---

of their size, nanoparticles are deterred at the surface of the dense plaque layer and are unable to penetrate the vessel wall. This observation points to additional complications of drug delivery strategies in restenosis.

## CONCLUSIONS

Because of their size, nanoparticles are suitable as drug carrier systems for localized application of therapeutic agents in restenosis therapy. In the present study, the local administration of polystyrene nanoparticles using a perforated balloon catheter could be successfully visualized by CLSM and transmission electron microscopy. It was demonstrated that nanoparticles can penetrate the non-atherosclerotic arterial vessel wall and that the penetration depth can be adjusted by varying the particle size. Direct evidence is provided for the existence of very local penetration paths of the nanoparticles as result of the pressure-directed particle stream during balloon infusion.

Apart from anatomic barriers — including the intact endothelial layer, as well as intact internal and external elastic laminae — atherosclerotic plaques seemed to prevent nanoparticulate drug carriers from penetrating the vessel wall in the absence of dissections. Further experiments on the effect of infusion pressure, suspension volume, and nanoparticle concentration are under way to clarify in detail the suitability of nanoparticles as effective intraluminal drug delivery systems for the prevention of restenosis after balloon angioplasty.

---

**REFERENCES**

- [1] A. Lafont, L.A. Guzman, P.L. Whitlow et al., Restenosis After Experimental Angioplasty : Intimal, Medial, and Adventitial Changes Associated With Constrictive Remodeling, *Circ Res* 76(6) (1995) 996-1002.
- [2] N.A. Scott, G.D. Cipolla, C.E. Ross et al., Identification of a Potential Role for the Adventitia in Vascular Lesion Formation After Balloon Overstretch Injury of Porcine Coronary Arteries, *Circulation* 93(12) (1996) 2178-2187.
- [3] G.S. Mintz, J.J. Popma, A.D. Pichard et al., Arterial Remodeling After Coronary Angioplasty : A Serial Intravascular Ultrasound Study, *Circulation* 94(1) (1996) 35-43.
- [4] T. Kimura, S. Kaburagi, T. Tamura et al., Remodeling of Human Coronary Arteries Undergoing Coronary Angioplasty or Atherectomy, *Circulation* 96(2) (1997) 475-483.
- [5] H. Hanke, T. Strohschneider, M. Oberhoff, E. Betz and K.R. Karsch, Time course of smooth muscle cell proliferation in the intima and media of arteries following experimental angioplasty, *Circ Res* 67(3) (1990) 651-659.
- [6] Y. Shi, J.E. O'brien, L. Ala-Kokko et al., Origin of Extracellular Matrix Synthesis During Coronary Repair, *Circulation* 95(4) (1997) 997-1006.
- [7] C. Hehrlein, C. Gollan, K. Donges et al., Low-Dose Radioactive Endovascular Stents Prevent Smooth Muscle Cell Proliferation and Neointimal Hyperplasia in Rabbits, *Circulation* 92(6) (1995) 1570-1575.

- 
- [8] K. Al-Lamee, Surface Modification of Stents for Improving Biocompatibility, *Medical Device Technology* (2000) 12-13.
- [9] E. Regar, G. Sianos and P.W. Serruys, Stent development and local drug delivery, *Br Med Bull* 59(1) (2001) 227-248.
- [10] H. Wolinsky and S.N. Thung, Use of a perforated balloon catheter to deliver concentrated heparin into the wall of the normal canine artery, *J Am Coll Cardiol* 15(2) (1990) 475-481.
- [11] D.W. Muller, E.J. Topol, G.D. Abrams, K.P. Gallagher and S.G. Ellis, Intramural methotrexate therapy for the prevention of neointimal thickening after balloon angioplasty, *J Am Coll Cardiol* 20(2) (1992) 460-466.
- [12] T.L. Lambert, V. Dev, E. Rechavia et al., Localized arterial wall drug delivery from a polymer-coated removable metallic stent. Kinetics, distribution, and bioactivity of forskolin, *Circulation* 90(2) (1994) 1003-1011.
- [13] I. Gradus-Pizlo, R.L. Wilensky, K.L. March et al., Local delivery of biodegradable microparticles containing colchicine or a colchicine analogue: effects on restenosis and implications for catheter-based drug delivery, *J Am Coll Cardiol* 26(6) (1995) 1549-1557.
- [14] R.L. Wilensky, K.L. March and D.R. Hathaway, Direct intraarterial wall injection of microparticles via a catheter: a potential drug delivery strategy following angioplasty, *Am Heart J* 122(4 Pt 1) (1991) 1136-1140.
- [15] R.L. Wilensky, K.L. March, I. Gradus-Pizlo et al., Regional and arterial localization of radioactive microparticles after local delivery by unsupported or supported porous balloon catheters, *Am Heart J* 129(5) (1995) 852-859.

- 
- [16] T.K. Nasser, R.L. Wilensky, K. Mehdi and K.L. March, Microparticle deposition in periarterial microvasculature and intramural dissections after porous balloon delivery into atherosclerotic vessels: quantitation and localization by confocal scanning laser microscopy, *Am Heart J* 131(5) (1996) 892-898.
- [17] F. Valero, M. Hamon, C. Fournier et al., Intramural injection of biodegradable microspheres as a local drug- delivery system to inhibit neointimal thickening in a rabbit model of balloon angioplasty, *J Cardiovasc Pharmacol* 31(4) (1997) 513-519.
- [18] J. Rome, V. Shayani, M. Flugelman et al., Anatomic barriers influence the distribution of in vivo gene transfer into the arterial wall. Modeling with microscopic tracer particles and verification with a recombinant adenoviral vector, *Arteriosclerosis and Thrombosis* 14(1) (1994) 148-161.
- [19] J.M. Anderson, Biodegradation and biocompatibility of PLA and PLGA microparticles, *Adv Drug Del Rev* 28 (1997) 5-24.
- [20] V. Labhasetwar, C. Song, W. Humphrey, R. Shebuski and J. Levy, Arterial Uptake of Biodegradable Nanoparticles: Effect of Surface Modifications, *J Pharm Sci* 87(10) (1998) 1229-1234.
- [21] V. Dev, N. Eigler, M.C. Fishbein et al., Sustained local drug delivery to the arterial wall via biodegradable microspheres, *Cathet Cardiovasc Diagn* 41(3) (1997) 324-332.
- [22] L.A. Guzman, V. Labhasetwar, C. Song et al., Local Intraluminal Infusion of Biodegradable Polymeric Nanoparticles. A novel Approach for Prolonged Drug Delivery After Balloon Angioplasty, *Circulation* 94 (1996) 1441-1448.

- 
- [23] C. Song, V. Labhasetwar, H. Murphy et al., Formulation and characterization of biodegradable nanoparticles for intravascular local drug delivery, *J Controlled Release* 43 (1997) 197-212.
- [24] C. Song, V. Labhasetwar, X. Cui, T. Underwood and R.J. Levy, Arterial uptake of biodegradable nanoparticles for intravascular local drug delivery: results with an acute dog model, *J Controlled Release* 54(2) (1998) 201-211.
- [25] M.K. Hong, S.C. Wong, A. Farb et al., Feasibility and drug delivery efficiency of a new balloon angioplasty catheter capable of performing simultaneous local drug delivery, *Coron Artery Dis* 4(11) (1993) 1023-1027.

## **CHAPTER 3**

---

### **EFFECTS OF DIFFERENT APPLICATION PARAMETERS ON PENETRATION CHARACTERISTICS AND ARTERIAL VESSEL WALL INTEGRITY AFTER LOCAL NANOPARTICLE DELIVERY USING A POROUS BALLOON CATHETER**

submitted to

European Journal of Pharmaceutics and Biopharmaceutics (2003)

---

## SUMMARY

Catheter-based local delivery of drug loaded nanoparticles agents offers a potential therapeutic approach to reducing restenosis. However, high delivery pressures and large volumes of infusates may cause severe vascular damage and increase intimal thickening. Therefore, we investigated the penetration pattern and vessel wall integrity of fluorescence-labelled nanoparticles (217 nm in diameter) into the non-atherosclerotic aorta abdominalis of New Zealand white rabbits in dependence of the volume (2.5 and 5 ml) and concentration (0.5 and 1 mg/ml) of the nanoparticle suspension, as well as the infusion pressure (2 and 4 atm) using a channelled balloon catheter (SCIMED REMEDY™ model RC 20/2.5). The location and penetration characteristics of nanoparticles in the arterial vessel wall were visualized using confocal laser scanning microscopy (CLSM) and transmission electron microscopy (TEM).

Catheter design and infusion pressure form a radial particle stream through intima and media into the adventitial layer of the aorta abdominalis. Infusion pressures of 4 atm in combination with high particle concentrations lead to effective nanoparticle delivery without severe vessel wall disruptions. Endothelium of the treated vessel segments was slightly affected during catheter insertion showing partly denudation of the innermost cell layer. TEM micrographs underlines transport functional properties of the vasa vasorum inside the vessel wall.

Consequently, local delivery efficiency of nanoparticulate carriers is critically affected by infusion pressure, and concentration of carrier suspensions. These factors need to be taken into consideration for the design of in vivo experiments.

---

## INTRODUCTION

Interventional procedures such as percutaneous transluminal balloon angioplasty (PTA) or stenting are most frequently accompanied by arterial vessel re-obstruction also known as restenosis. This process is characterized by intimal hyperplasia and vessel remodelling [1-3]. The neointimal formation results from vascular smooth muscle cell (VSMC) migration and proliferation into the media [4] followed by the formation of a new extra cellular matrix [5].

Apart from the application of drug eluting stents for local delivery [6,7], the development of balloon catheter delivery systems [8] allows the infusion of drug-loaded micro- [9-12] or nano-carriers [13-16] to provide a local and sustained drug release at the site of angioplasty. This technique ensures higher drug concentrations than systemic administration [17]. Although recent studies have demonstrated that particles < 300 nm easily penetrate the vessel wall and appear, therefore, to be promising carrier systems in restenosis therapy [15,18], their successful application strongly depends on the particular infusion conditions. For instance, the infusion pressure and the volume of the infusate are crucial parameters that may cause severe vascular damage and enhanced intimal thickening [19].

The present study describes the effects of particle suspension volume, particle concentration, and infusion pressure on the intramural distribution of fluorescence-labelled polystyrene nanoparticles into the non-atherosclerotic vessel wall of the aorta abdominalis in New Zealand white rabbits using a channelled balloon catheter. The aim of this study was to determine how to modulate the infusion parameters for an optimal nanoparticle delivery without severe intramural dissections. Our investigations have shown that the particle migration through the wall tissue is pressure dependent and is characterized by channel-like deposition patterns corresponding to the porous balloon catheter design. The increase of nanoparticle suspension volume could not improve the intramural particle concentration.

---

## **MATERIALS AND METHODS**

### **Local delivery catheter**

The delivery device, a channelled balloon catheter (SCIMED REMEDY™ model RC 20/2.5, lot 3377794, Boston Scientific, Natick, MA), has been described in detail by Hong [20]. Briefly, it is a 3-lumen over-the-wire catheter with separate ports for balloon dilation and local drug delivery, which allows separation of the high inflation pressure for angioplasty from the low pressure desirable for local nanoparticle delivery. The balloon carries 18 channels, with one group of 30- $\mu$ m diameter pores per channel in a spiral pattern for local delivery. In order to further reduce vessel wall injuries the particle suspension is allowed to leak through the micro pores rather than be propelled by jet streams. The catheter shaft is 3.4 French. Balloons used in this study were 20 mm in length and 2.5 mm in diameter.

### **In-situ catheterization and local delivery of fluorescence-labelled nanoparticles**

The investigation conformed to the guidelines for the care and use of laboratory animals published by the US National Institute of Health (“Principles of Laboratory Animal Care”, NIH publication No. 85-23, revised 1985) and were approved by an external review committee for laboratory animal care.

Four non-atherosclerotic male New Zealand white rabbits weighing 3.5 to 4 kg were sacrificed using a mixture of embutramide, mebenzonium iodide, and tetracaine hydrochloride. To perform angioplasty and local nanoparticle delivery, the aorta abdominalis was exposed in situ (averaging 20-30 mm in length) and cut longitudinally. The catheter was placed above the aortic bifurcation. The location, quantity, and penetration depth of 217 nm yellow-green labelled polystyrene nanoparticles were evaluated in relationship to particle concentration, injection pressure, and suspension volume of Fluoresbrite™ plain microspheres YG suspended in water (Polyscience Inc, Warrington,

PA). The use of fluorescence-labelled instead of fluorescence-loaded nanoparticles avoids any unintentional dye release that would prevent the exact determination of particle distribution by CLSM. The experimental set-up is described in Tab. 1.

Animal no.	Vessel segment	Infusion Pressure [atm]	Suspension Volume [ml]	Particle Concentration [mg/ml]
1	distal	2	2	0.25
1	proximal	4	2	0.25
2	distal	2	2.5	0.25
2	proximal	2	5	0.25
3	distal	2	2	0.5
3	proximal	2	2	1.0
4	proximal		no infusion	

**Tab. 1:** *Experimental setup for nanoparticle infusion at different settings (Particle size: 217 nm).*

In all experiments the angioplasty balloon was inflated and maintained at a dilating pressure of 8 atm until the entire nanoparticle suspension was infused. A non-treated vessel segment served as negative control. Immediately after the delivery procedure the treated and control vessel segments were excised and fixed in a formalin solution (4% v/v) for CLSM studies or glutaraldehyde (2.7% v/v) in phosphate buffered saline (PBS) 0.1M, pH 7 for electron microscopy.

---

### **Confocal laser scanning microscopy (CLSM)**

Arterial segments, frozen in cooled isopentane, were embedded in Tissue Freezing Medium (Jung, Germany). Cross-sections of 20- $\mu\text{m}$  thickness were cut using a Frigocut 2700 cryo-microtome (Reichert-Jung, Germany) and mounted on SuperFrost plus (Menzel-Glaeser, Germany) glass slides. They were counterstained with 4',6-diamidino-2-phenylindole (DAPI, 1  $\mu\text{g}/\text{mL}$ ) (Molecular Probes, Leiden, The Netherlands) solution in PBS for 30 minutes under light exclusion and embedded in PBS/glycerol (2:1 v/v). Localization of fluorescence-labelled nanoparticles was performed using a CLSM (Axiovert, Zeiss CLSM 501, Jena, Germany) equipped with a Zeiss Neofluor 40\*/1.3 objective. Excitation wavelengths were 364 nm (long-pass filter [LP] 385 nm) for DAPI and 488 nm (LP 505 nm) for the yellow-green labelled nanoparticles. All confocal images were acquired with the same settings with respect to laser intensity, filter block, and detector gain.

### **Transmission electron microscopy (TEM)**

The fixed blood vessels were rinsed 3 times with 0.15M PBS, pH 7, for 1 hour each and postfixed for 75 minutes using 2% osmium tetroxide solution. Small parts of the vessels were embedded for ultramicrotomy using Durcupan ACM (Fluka, Switzerland), a four component water-soluble embedding medium. After dehydration of the tissues in a water-soluble aliphatic polyepoxide as described elsewhere [18], the dehydrated tissue was placed in a polymerization mixture according to the manufacturer's protocol and left overnight at 4  $^{\circ}\text{C}$  for final mixing and embedding. Polymerization was performed in a freshly prepared mixture of the above composition for 4 days at 42 $^{\circ}\text{C}$ .

Ultrathin sections, approximately 50 nm thick, were obtained using a Leica Ultracut UCT microtome and a diamond knife (Leica Microsystems, Germany). The sections were collected on copper grids covered with a

---

supporting thin collodium/carbon film. Final staining of the sections included the treatment with uranyl acetate for 15 minutes and with lead citrate for 9 minutes. Microscopic examinations were carried out in a JEM 3010 transmission electron microscope (Jeol, Japan), equipped with a 2k x 2k Slow-scan CCD camera and a LaB6 cathode, operated at 300 kV.

### **Scanning electron microscopy (SEM)**

The inner surface morphology of the blood vessels after catheterization was controlled using both TEM, as well as SEM observations. The glutaraldehyde fixed specimens were dehydrated using a critical-point drying apparatus Polaron E3000 (Bio-Rad Microscience) after stepwise replacement of the water by acetone, which is then substituted by carbon dioxide. Finally, the dried specimens were coated with a thin gold evaporation layer to prevent charging. Sample characterization was performed by scanning electron microscopy using a CamScan Series 4 (CamScan, USA) at 20 kV acceleration voltage.

### **Semi-quantitative analyses of penetration depth and fluorescent intensity**

Selective particle distributions and tissue autofluorescence complicated the determination of a defined front line of fluorescent nanoparticles. Consequently, the penetration depth was measured semi-quantitatively and graded on a scale from 1 to 3 according to Fram [21]. Briefly, grade 1 described penetration into the inner one-third of the vessel wall, grade 2 into the inner two-third, and grade 3 into the outer one-third of the vessel wall of the aorta abdominalis. The fluorescence intensity was graded in the same manner on a scale from 1 to 3, corresponding to light, moderate, and intense fluorescence.

---

## RESULTS AND DISCUSSION

As a result of the catheter insertion into the aorta abdominalis and its removal, as well as catheter dilatation during ballooning, there is always the risk of mechanical injury to the endothelial layer. Generally, the affected vessel segments showed little or no damaging of the endothelium (Fig. 1a and 1c), although in some selected cases we observed some disturbances of the endothelial layer (Fig. 1b and 1d). The cross-sections of the treated arteries usually did not show any severe vessel wall disruptions. In CLSM images, the light green autofluorescence, at an excitation wavelength of 488 nm, as seen in cross-sections of control experiments without nanoparticle infusion was well distinguishable from the blue DAPI stained nuclei of smooth muscle, endothelial, and adventitial cells, as well as from the nanoparticles themselves (Fig. 2a).

One method to enhance drug delivery efficiency is the use of smaller drug-loaded nanoparticles. Further possibilities include the increase of nanoparticle suspension volume, particle concentration, or infusion pressure. Our results of semi-quantitative analyses of penetration depth and fluorescence intensity after delivery of 217 nm-sized fluorescence-labelled nanoparticles in dependence of the latter parameters are shown in Tab. 2.

The increase of suspension volume from 2.5 to 5 ml did not lead to a higher fluorescence activity in several analysed cross-sections from treated vessel segments as derived from a comparison of Fig. 2b and c. Only light fluorescence in the intimal and medial layer could be observed. The capacity of the vessel tissue appears to be low for large volumes of drug solutions or drug carrier suspensions.

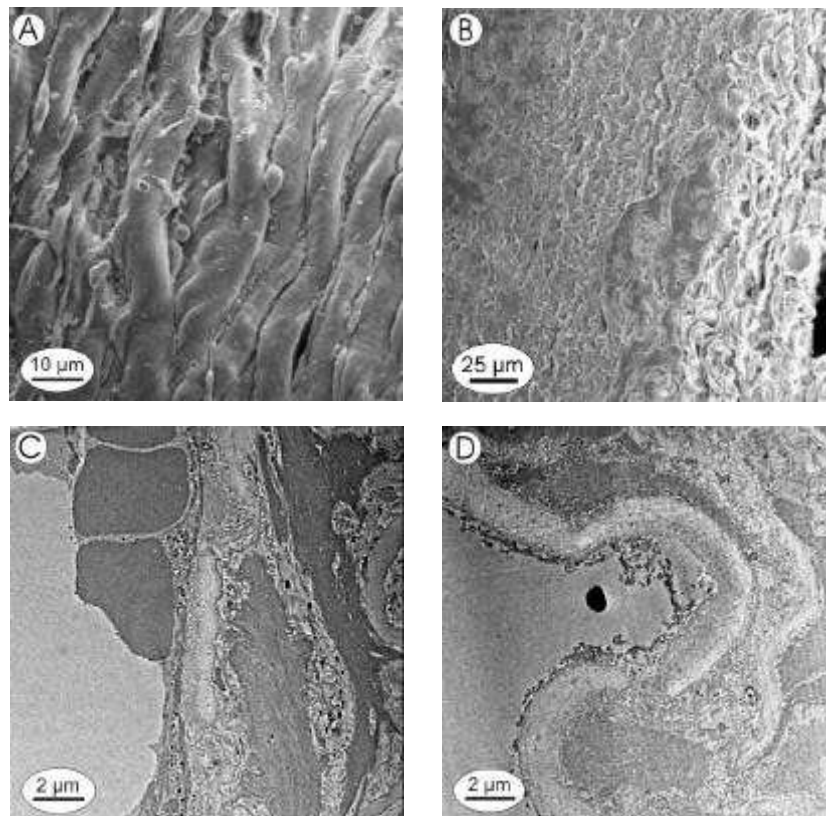


**Fig. 1:** SEM images (a, b) and TEM images (c, d) of the endothelial layer of the aorta abdominalis. After balloon dilatation and nanoparticle infusion the endothelium appears sporadically intact (a, c). In Figures b and d the endothelial layer appears to have been completely removed.

In contrast, a remarkable increase in nanoparticle uptake was observed as a consequence of an increased infusion pressure from 2 to 4 atm (Fig. 3a and b). In a number of cases, the nanoparticles poured in a funnel-shaped manner through the intimal layer into the medial tissue as shown by CLSM in Fig. 3b, as well as by the TEM images in Fig. 3c. Occasionally, the formation of a particle cloud with high fluorescence activity extending up to the adventitial region of the vessel wall could be observed (Fig. 3b). At the interface between the arterial tissue and the lumen, the particles seemed to stream back into the luminal area and build particle clusters. The channel-like particle streams at the infusion site have a diameter of about 25  $\mu\text{m}$  which correlates with the pore diameter of the balloon catheter.

Parameter	Value	Penetration depth	Fluorescence intensity
Infusion Pressure [atm]	2 / 4	2 / 3	2 / 3
Particle Concentration [mg/ml]	0.5 / 1	3 / 3	2 / 3
Suspension Volume [ml]	2.5 / 5	2 / 2	2 / 1

**Tab. 2:** *Infusion characteristics: Semi quantitative analysis of penetration depth and fluorescence intensity. Penetration depth is graded into 1 = inner one-third, 2 = inner two-thirds, 3 = outer one-third of the vessel wall. Intensity of fluorescence was graded into 1 = light, 2 = moderate, and 3 = intense fluorescence.*

Apart from the depicted penetration characteristics of the nanoparticles, which tend to cross the successive layers of the vessel wall preferably along infusion-induced diffusion channels, other possible transport pathways are revealed in Fig. 4. The TEM micrographs show cross-sections ( Fig. 4a and c) and longitudinal sections (Fig. 4b) of the vasa vasora with and without nanoparticle incorporations. These examples are evidence for the transport functional properties of the vasa vasorum.

Moreover, in Fig. 5 an extensive fluorescence signal over all vessel wall layers is shown with a substantially higher intensity at an increased particle concentration of 1 mg/ml (Fig. 5b) compared to concentrations of 0.5 mg/ml (Fig. 5a).

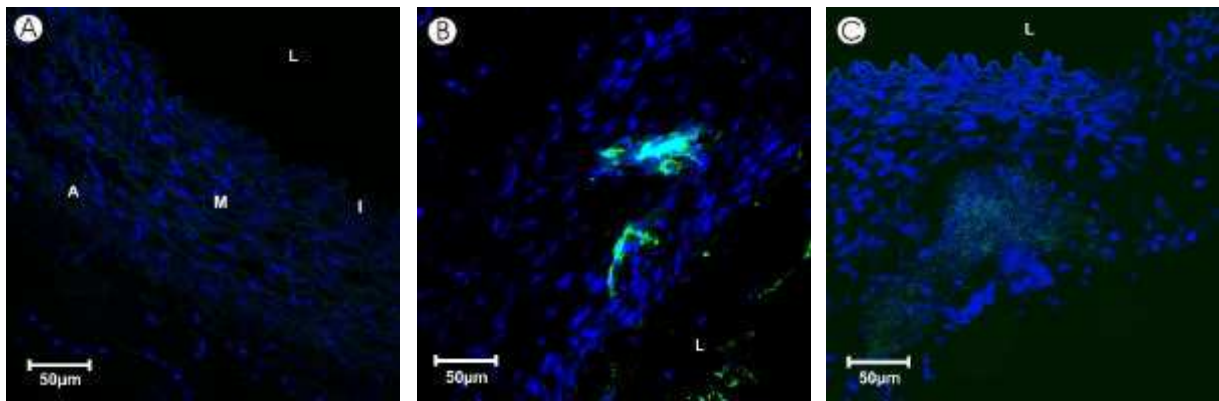


**Fig. 2:** CLSM analysis of the nanoparticle distribution in the vessel wall of the aorta abdominalis of New Zealand white rabbits: Nuclei (blue) stained with DAPI, catheter-delivered yellow-green labeled polystyrene nanoparticles (green). L, M, and A indicate the lumen, media, and adventitia. (a) Balloon-dilated segment of aorta abdominalis: Control experiment without nanoparticle infusion. (b) Infusion of 2.5 ml nanoparticle suspension (0.25 mg/ml, 2 atm) in comparison to (c) 5 ml suspension.

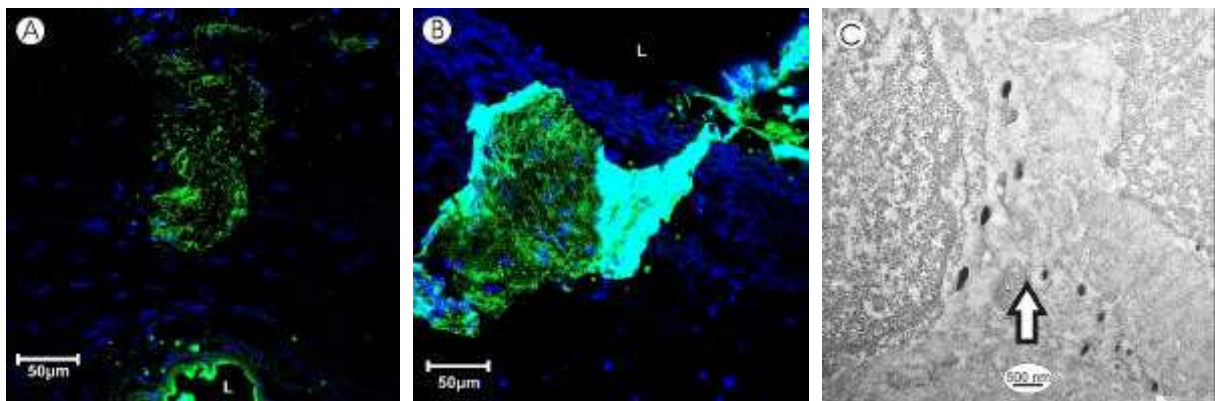


**Fig. 3:** CLSM images of the nanoparticle distribution in the vessel wall after infusion at (a) 2 atm and (b) 4 atm. (b) shows a radial channel-like particle influx into the vessel wall with a “cloudy” particle accumulation spreading over the intimal medial and adventitial layer. (c) transmission electron micrograph of funnel shaped particle deposition in the medial layer.

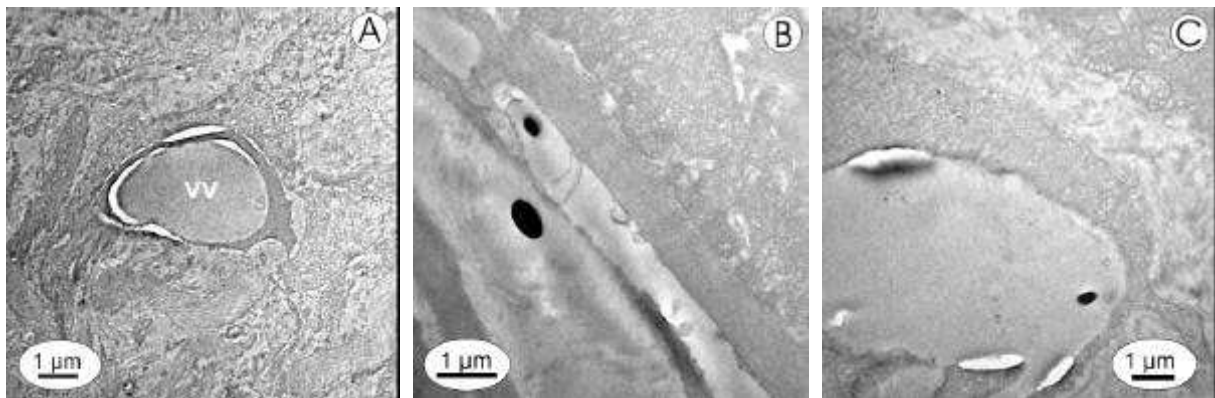


**Fig. 4:** Transmission electron micrographs of a vasa vasorum (a - c) with nanoparticle deposition displayed in (b) and (c).

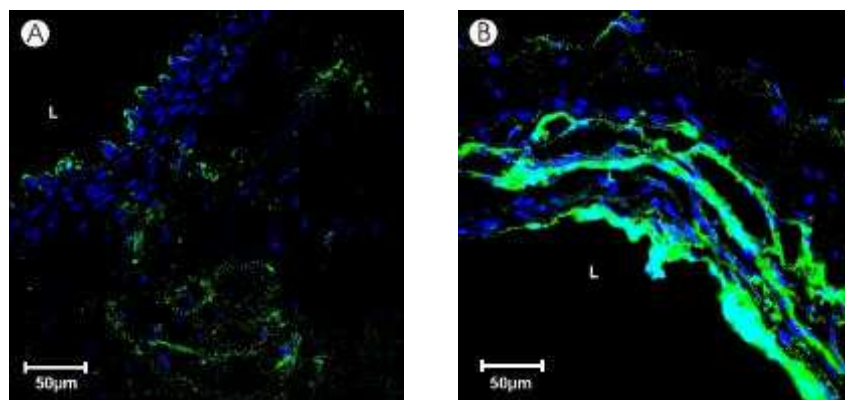


**Fig. 5:** CLSM images of arterial vessel segments infused with nanoparticle suspensions of (a) 0.5 mg particles per ml and (b) 1.0 mg particles per ml.

Although the microporous design of balloon catheters was effective for the local infusion of anti-restenotic drugs [19], the intramural drug delivery is considered to be associated with additional vessel trauma, such as endothelial abrasion, disruptions of intima or elastica lamina, and dissections of the arterial vessel wall. Recent studies have described a direct relationship between the damage of arterial vessels and infusion pressure of local delivery during percutaneous transluminal angioplasty [22,23]. Wolinsky et al. found that the infused dye entered such crevices and that the disruptions were indeed induced by the angioplasty procedure [24]. The injuries in the arterial vessel wall may

---

also have been caused by high pressure jet streams from the application pores of the perforated balloon catheter [25,26]. Furthermore, vessel wall disruptions and intimal hyperplasia were more prominent at higher inflation pressures during balloon angioplasty [27], as well as at higher infusion pressures during catheter-based nanoparticle application [28].

Despite some occasional endothelial abrasion caused by catheter intervention, the cross-sections of the present study did not reveal any noticeable dissections of the vessel wall at infusion pressures of 2 and 4 atm or at higher fluid volumes. These observations are in agreement with the findings of Gunn, who showed that local delivery of oligonucleotides for antisense therapy caused no evident vessel wall disruptions at infusion pressures between 1 and 6 atm [29].

Whereas some researchers did not observe any significant differences in the delivery efficiency of drug solutions [30] or fluorescent-labelled microparticles [11] at increasing infusion pressures, Fram and co-workers have shown that the penetration depth of horseradish peroxidase was directly related to the infusion pressure [21]. Our results also demonstrate an enhancement of particle deposition at the delivery site with increasing pressure. On the other hand, however, in the present study the evaluation of the depth of vessel wall penetration revealed no differences at infusion pressures of 2 or 4 atm. The fluorescence-labelled nanoparticles were visible in all vessel wall layers arranged in a funnel-like manner without vascular damage. Data from a non-atherosclerotic rabbit carotid artery model using a channelled balloon catheter indicated jet injuries which were detected in areas where the application pores directly contacted the vessel wall [26]. We suppose that the described deposition pattern is the result of the observed infusion-induced particle stream from the catheter pores.

It has become evident that fluid volumes of more than 2 ml do not effectively increase the drug delivery efficiency simply because of the low

---

capacity of the treated vessel wall segment. Instead, high fluid volumes may increase the traumatic side effects during local drug delivery with porous balloons considerably, as reported by Herdeg [26]. Consequently, it is reasonable to increase the drug delivery efficiency by using higher concentrated drug or drug-carrier solutions, rather than larger volumes.

Limitations of the present study are the lack of quantitative information about the absolute particle mass delivered to the vessel wall which is an important aspect in the validation of the biological effect of drug loaded particles. Also, when using non-atherosclerotic vessel segments one has to be aware that atherosclerotic plaques may reduce nanoparticle delivery. Finally, this study has not taken any delayed vascular damage, such as neointimal thickening and the associated increase in the SMC proliferation activity, into account.

## CONCLUSIONS

We observed a channel-like particle penetration into the vessel wall of the aorta abdominalis as a function of catheter design; however, we were able to determine that the leaking effect of the channelled balloon seemed to prevent traumatic jet streams to the greatest possible extent. Consequently, the increase of the infusion pressure from 2 or 4 atm promoted nanoparticle delivery without causing severe vessel wall ruptures. The local delivery efficiency of particulate drug carriers depended on different factors such as catheter design, particle size, infusion pressure, and concentration of drug carriers. Whereas an increased particle concentration consequently led to a higher suspension viscosity, increased infusion pressures were required for the delivery of the viscous suspensions, which may cause severe damages of the vessel wall architecture. Therefore, it is extremely important to define well-balanced parameters for particle size, infusion pressure, particle concentration and administrated volume specific to the catheter system used. Nevertheless, nanoparticulate drug and gene

---

carriers based on biodegradable polymers offer a promising approach for the treatment of restenosis after angioplasty.

## REFERENCES

- [1] A. Lafont, L.A. Guzman, P.L. Whitlow et al., Restenosis After Experimental Angioplasty : Intimal, Medial, and Adventitial Changes Associated With Constrictive Remodeling, *Circ Res* 76(6) (1995) 996-1002.
- [2] G.S. Mintz, J.J. Popma, A.D. Pichard et al., Arterial Remodeling After Coronary Angioplasty : A Serial Intravascular Ultrasound Study, *Circulation* 94(1) (1996) 35-43.
- [3] T. Kimura, S. Kaburagi, T. Tamura et al., Remodeling of Human Coronary Arteries Undergoing Coronary Angioplasty or Atherectomy, *Circulation* 96(2) (1997) 475-483.
- [4] H. Hanke, T. Strohschneider, M. Oberhoff, E. Betz and K.R. Karsch, Time course of smooth muscle cell proliferation in the intima and media of arteries following experimental angioplasty, *Circ Res* 67(3) (1990) 651-659.
- [5] Y. Shi, J.E. O'brien, L. Ala-Kokko et al., Origin of Extracellular Matrix Synthesis During Coronary Repair, *Circulation* 95(4) (1997) 997-1006.
- [6] E. Regar, G. Sianos and P.W. Serruys, Stent development and local drug delivery, *Br Med Bull* 59(1) (2001) 227-248.
- [7] J.E. Sousa, M.A. Costa, A.G. Sousa et al., Two-year angiographic and intravascular ultrasound follow-up after implantation of sirolimus-eluting stents in human coronary arteries, *Circulation* 107(3) (2003) 381-383.

- 
- [8] D. Brieger and E. Topol, Local drug delivery systems and prevention of restenosis, *Cardiovasc Res* 35(3) (1997) 405-413.
- [9] I. Gradus-Pizlo, R.L. Wilensky, K.L. March et al., Local delivery of biodegradable microparticles containing colchicine or a colchicine analogue: effects on restenosis and implications for catheter-based drug delivery, *J Am Coll Cardiol* 26(6) (1995) 1549-1557.
- [10] R.L. Wilensky, K.L. March, I. Gradus-Pizlo et al., Regional and arterial localization of radioactive microparticles after local delivery by unsupported or supported porous balloon catheters, *Am Heart J* 129(5) (1995) 852-859.
- [11] T.K. Nasser, R.L. Wilensky, K. Mehdi and K.L. March, Microparticle deposition in periarterial microvasculature and intramural dissections after porous balloon delivery into atherosclerotic vessels: quantitation and localization by confocal scanning laser microscopy, *Am Heart J* 131(5) (1996) 892-898.
- [12] F. Valero, M. Hamon, C. Fournier et al., Intramural injection of biodegradable microspheres as a local drug- delivery system to inhibit neointimal thickening in a rabbit model of balloon angioplasty, *J Cardiovasc Pharmacol* 31(4) (1997) 513-519.
- [13] V. Labhasetwar, C. Song and J. Levy, Nanoparticle drug delivery systems for restenosis, *Adv Drug Del Rev* 24 (1997) 63-85.
- [14] L.A. Orloff, A.J. Domb, D. Teomim, I. Fishbein and G. Golomb, Biodegradable implants strategies for inhibition of restenosis, *Adv Drug Del Rev* 24 (1997) 3-9.
- [15] C. Song, V. Labhasetwar, X. Cui, T. Underwood and R.J. Levy, Arterial uptake of biodegradable nanoparticles for intravascular local drug

- 
- delivery: results with an acute dog model, *J Controlled Release* 54(2) (1998) 201-211.
- [16] I. Fishbein, M. Chorny, S. Banai et al., Formulation and delivery mode affect disposition and activity of tyrphostin-loaded nanoparticles in the rat carotid model, *Arterioscler Thromb Vasc Biol* 21(9) (2001) 1434-1439.
- [17] S.M. Franklin and D.P. Faxon, Pharmacologic prevention of restenosis after coronary angioplasty: review of the randomized clinical trials, *Coron Artery Dis* 4(3) (1993) 232-242.
- [18] U. Westedt, L. Barbu-Tudoran, A.K. Schaper et al., Deposition of Nanoparticles in the Arterial Vessel by Porous Balloon Catheters: Localisation by Confocal Laser Scanning Microscopy and Transmission Electron Microscopy, *AAPS PharmSci* 4(4) (2002) article 41.
- [19] C.R. Lambert, J.E. Leone and S.M. Rowland, Local drug delivery catheters: functional comparison of porous and microporous designs, *Coron Artery Dis* 4(5) (1993) 469-475.
- [20] M.K. Hong, S.C. Wong, A. Farb et al., Feasibility and drug delivery efficiency of a new balloon angioplasty catheter capable of performing simultaneous local drug delivery, *Coron Artery Dis* 4(11) (1993) 1023-1027.
- [21] D.B. Fram, T. Aretz, M.A. Azrin et al., Localized intramural drug delivery during balloon angioplasty using hydrogel-coated balloons and pressure-augmented diffusion, *J Am Coll Cardiol* 23(7) (1994) 1570-1577.
- [22] B. Goldman, H. Blanke and H. Wolinsky, Influence of pressure on permeability of normal and diseased muscular arteries to horseradish

- 
- peroxidase. A new catheter approach, *Atherosclerosis* 65(3) (1987) 215-225.
- [23] E.C. Santoian, M.B. Gravanis, J.E. Schneider et al., Use of the porous balloon in porcine coronary arteries: rationale for low pressure and volume delivery, *Cathet Cardiovasc Diagn* 30(4) (1993) 348-354.
- [24] H. Wolinsky and C.S. Lin, Use of the perforated balloon catheter to infuse marker substances into diseased coronary artery walls after experimental postmortem angioplasty, *J Am Coll Cardiol* 17(6 Suppl B) (1991) 174B-178B.
- [25] D.W. Muller, E.J. Topol, G.D. Abrams, K.P. Gallagher and S.G. Ellis, Intramural methotrexate therapy for the prevention of neointimal thickening after balloon angioplasty, *J Am Coll Cardiol* 20(2) (1992) 460-466.
- [26] C. Herdeg, M. Oberhoff, A. Baumbach et al., Local drug delivery with porous balloons in the rabbit: assessment of vascular injury for an improvement of application parameters, *Cathet Cardiovasc Diagn* 41(3) (1997) 308-314.
- [27] Y. Asada, A. Kisanuki, A. Tsuneyoshi et al., Effects of inflation pressure of balloon catheter on vascular injuries and subsequent development of intimal hyperplasia in rabbit aorta, *Atherosclerosis* 121(1) (1996) 45-53.
- [28] T. Kimura, K. Miyauchi, S. Yamagami, H. Daida and H. Yamaguchi, Local delivery infusion pressure is a key determinant of vascular damage and intimal thickening, *Jpn Circ J* 62(4) (1998) 299-304.
- [29] J. Gunn, C. Holt, L. Shepherd et al., Intra-coronary drug delivery via porous balloon: Local or regional?, *Circulation* 92(Suppl I) (1995) I-671.

- 
- [30] A. Baumbach, C. Herdeg, M. Kluge et al., Local drug delivery: impact of pressure, substance characteristics, and stenting on drug transfer into the arterial wall, *Catheter Cardiovasc Interv* 47(1) (1999) 102-106.

## **CHAPTER 4**

---

### **PACLITAXEL LOADED NANOPARTICLES FROM BIODEGRADABLE POLY(VINYL ALCOHOL)-GRAFT- POLY(LACTIDE-CO-GLYCOLIDE) FOR CATHETER BASED LOCAL TREATMENT OF RESTENOSIS**

in preparation for publication:

Journal of Controlled Release

## SUMMARY

Restenosis artery after percutaneous transluminal angioplasty (PTA) and stenting remains a challenge for the treatment of patients with atherosclerotic diseases. Catheter-based local delivery of biodegradable nanoparticles (NP) with sustained release characteristics, potentially represents a therapeutic approach to reduce the restenosis. Paclitaxel loaded NP (0, 0.5, 1, 2 % (w/w)) consisting of poly(vinyl alcohol)-graft-poly(lactide-co-glycolide) (PVA-g-PLGA) with varying PLGA chain length as well as poly(lactide-co-glycolide) (PLGA), were prepared by a solvent evaporation technique. NP of < 180 nm in diameter characterised by photon correlation spectroscopy (PCS), scanning electron microscopy (SEM), and atomic force microscopy (AFM) are spherical and show smooth surfaces. Yields typically range from 80 to 95 % with encapsulation efficiencies between 77 and 87 % (theoretical loading 2%) The extent of initial in vitro paclitaxel release (drug burst) was affected by the PVA-g-PLGA composition. A decreased PLGA chain length increased drug release rates. Blank nanoparticles from PVA<sub>300</sub>-g-PLGA(30) and PVA<sub>300</sub>-g-PLGA(15) showed excellent biocompatibility in rabbit vascular smooth muscle cells (RbVSMC) at polymer concentrations of 0.37 mg/ml. Paclitaxel-loaded NP have decreased the cell viability more effectively than the free drug. Confocal laser scanning microscopy of RbVSMC confirmed the cellular uptake of nanoparticles composed of fluorescently labelled PVA<sub>300</sub>-g-PLGA(15) loaded with Oregon green labelled paclitaxel. Cells showed a clearly increased fluorescence activity with a co-localisation of paclitaxel and polymer nanoparticles after 6 hours. These results demonstrates that PVA<sub>300</sub>-g-PLGA comb polyesters are suitable for sustained paclitaxel release and may have potential for catheter based delivery to prevent restenosis after PTA.

## INTRODUCTION

The recurrent luminal narrowing of an artery (restenosis) as a consequence of excessive intimal hyperplasia limits the long-term success of arterial interventions such as percutaneous transluminal angioplasty (PTA) and stenting in the treatment of patients with atherosclerotic disease. Restenosis is characterised by vascular smooth muscle cell (VSMC) migration and proliferation into the media [1] followed by extracellular matrix formation [2]. To inhibit VSMC proliferation, drugs must be delivered at high concentrations for a prolonged period of time. Catheter-based local delivery of pharmacologic agents offers a potential approach to reduce restenosis, minimizing undesirable systemic side effects. However, recent studies demonstrated that the delivery efficiency and intramural retention of directly infused drug solutions remains rather low [3,4]. Thus, colloidal drug carriers based on biodegradable polymers have been developed to provide local drug release and sustained retention of drug in the arterial wall. Recent studies have demonstrated that nanoparticles can be delivered more efficiently to the arterial tissue than microparticles [5-7]. Numerous drugs were investigated for the inhibition of intimal thickening [8]. A promising approach to inhibit restenosis is the controlled release of paclitaxel [9,10]. Paclitaxel, a very potent anti proliferative drug which binds to the  $\beta$ -subunits of tubulin, promotes the formation of extremely stable and non-functional microtubule bundles. As a result, cell replication is blocked in late G<sub>2</sub> and M phase of the cell cycle [11]. Due to the poor solubility of paclitaxel in water, the solvent displacement technique [12], which is widely used for encapsulation of lipophilic drugs, is an attractive method to form nanoparticles. Several different types of biodegradable polymers such as polylactide (PLA) [13,14], poly (lactide-co-glycolide) (PLGA) [15,16], or polycaprolactone (PCL) [17] have been used to formulate sustained release nanoparticles. In the present study, nanoparticles from biodegradable comb polyesters [18,19] were prepared

using the solvent displacement method. These brush-like grafted polyesters consists of a hydrophilic polymer backbone, PVA, onto which hydrophobic PLGA is grafted. This polymer structure offers various possibilities to modify drug release kinetics. Firstly, the water uptake and swelling properties of the matrix can be varied by changing the hydrophilic part of the polymer. Or secondly, the degradation and release behavior can be modified by grafting PLGA with different chain length onto the backbone [20].

Our study was carried out to characterize nanoparticles from PVA-g-PLGA comb polyesters with regard to their applicability as vascular paclitaxel delivery system by investigating drug release, in vitro cytotoxicity, and cellular uptake behavior.

## **MATERIALS AND METHODS**

### **Materials**

Linear PLGA 50:50 (RG 503H, Mw 28, 000 g/mol was supplied by Boehringer Ingelheim (Germany). Paclitaxel (Genexol™) was kindly provided by Sam Yang Corp.(Seoul, Korea). Radio-labelled paclitaxel (paclitaxel-[2-benzoyl ring-UL- <sup>14</sup>C]) was obtained from Sigma (Sigma Chemicals, Germany). Oregon Green labelled Paclitaxel and 7-methoxy-coumarin-3-carbonyl azide for fluorescence labelling of PVA<sub>300</sub>-g-PLGA was purchased from Molecular Probes (Leiden, Netherlands). Poloxamer 188 (Pluronic F 68™) was supplied by BASF (Parsippany, NJ)). The liquid scintillation cocktail was obtained from Packard BioScience (Ultima Gold™ LS cocktail, Groningen, Netherlands). All other chemicals of analytical grade were purchased from Sigma (St. Louis, MO).

### **Poly((polyvinyl alcohol)-g-(D,L-lactide-co-glycolide))**

Synthesis and characterization were described by Breitenbach et al. [18]. Briefly, comb polyesters were synthesized by a stannous octoate catalyzed ring-

opening polymerization of lactide and glycolide (1:1) in the presence of the backbone poly(vinyl alcohol) (PVA;  $M_w$  15 kg/mol, polymerization degree 300, hydrolysis degree 88%) under anhydrous conditions. The polymers used for nanoparticle preparation were described in table 1. The following nomenclature will be used to specify the polymers: PVA<sub>300</sub>-g-PLGA(XX). The number in parenthesis refers to the mass ratio of branched PLGA, which is grafted (g) onto hydrophilic backbone, compared to the PVA.

For cellular nanoparticle uptake studies PVA<sub>300</sub>-g-PLGA(15) was fluorescently labelled as follows: 7-methoxy-coumarin-3-carbonyl azide was added to a solution of the polymer in N-methyl-pyrrolidone. The reaction mixture was stirred at 80 °C for 4 hours. After cooling to room temperature, the solution was poured into demineralized water and the precipitate was collected by filtration. The product was washed several times and dried in a vacuum chamber at room temperature for 6 days. The theoretical degree of substitution was 9.6 %. Infrared and <sup>1</sup>H-NMR spectroscopy confirmed the coupling of the fluorescent marker to the polymer with an excitation wavelength of 340 nm and an emission wavelength of 430 nm as determined by fluorescence spectroscopy.

### **Nanoparticle preparation**

Nanoparticles were formed by a modified solvent displacement technique, described in detail elsewhere [21]. Briefly, polymer (20 mg) and paclitaxel (0, 0.5, 1, 2 mg) were co-dissolved in 2 ml acetone. The resulting solution was added at constant flow rate of 10.0 ml/min to 10 ml of a stirred (500 rpm) aqueous phase of filtrated (0.2 µm, Schleicher & Schuel, Germany) and double-distilled water containing 0.1 % (m/m) poloxamer 188 (Pluronic™ F68) using a syringe with injection needle (Sterican™ 0.6 × 25 mm; B Braun, Melsungen, Germany). For the release study, nanoparticles were directly prepared in the release medium composed of a phosphate buffered (0.05M, I = 0.01, pH 7.4) poloxamer 188 solution. The resulting colloidal suspension was stirred for 2 h

under reduced pressure to remove residual organic solvent. The nanoparticle suspension was stored at 4 °C until use. For determination of drug loading efficiency and in vitro drug release, <sup>14</sup>C-labelled and unlabelled paclitaxel were mixed at a mass ratio of 1 / 250. The nanoparticle yield was determined gravimetrically after preparation, and additionally, after the passage through a channelled balloon delivery catheter (SCIMED REMEDY™ model RC 20/2.5, lot 3377794, Boston Scientific, Natick, MA). The catheter used carries 18 channels, with 1 group of 30-µm diameter pores per channel for infusion of drug solutions, or particle suspensions into the vessel wall [22]. All measurements were performed in triplicate.

Nanoparticles for cellular uptake studies consisted of a mixture fluorescently labelled PVA<sub>300</sub>-g-PLGA(15) (20%) and unlabelled PVA<sub>300</sub>-g-PLGA(15) (80%) loaded with 0.1 % Oregon green labelled paclitaxel.

## **Nanoparticle characterization**

### *Particle size measurement*

For measurement of average size and size distribution of the nanoparticle suspensions by photon correlation spectroscopy (PCS) (Zetasizer 4/AZ 110; Malvern Instruments, UK), each sample was diluted with filtrated and distilled water to a nanoparticle concentration of 0.5 mg/ml to avoid multiscattering events. The photon correlation spectroscopy software V 1.26 was used to calculate mean diameter and width of fitted gaussian distribution. Moreover, the NP size was determined after passage through the channelled balloon catheter. Each measurement was performed in triplicate.

### *Scanning electron microscopy (SEM)*

The morphology of nanoparticles was characterized by SEM using a Hitachi S-4100 microscope (Hitachi, Germany). A drop of the nanoparticle

suspension (2 mg/ml) was placed on a glass cover slide and dried under vacuum for 12 h. After that, the slides were mounted on aluminium pins using double-sided adhesive tape. Prior to microscopical examination the samples were coated with a gold layer under vacuum for 30 seconds (Edwards Auto 306, Edwards, Germany).

#### *Atomic force microscopy (AFM)*

A drop of the nanoparticle suspension was directly placed on a silicon chip. Atomic force microscopy was performed with a Digital Nanoscope IV Bioscope (Veeco Instruments, Santa Barbara, CA) as described elsewhere [23]. The vibration damped microscope was equipped with pyramidal Si<sub>3</sub>N<sub>4</sub> tips (NCH-W, Veeco Instruments, Santa Barbara, CA) on a cantilever with a length of 125 µm, a resonance frequency of about 220 kHz and a nominal force constant of 36N/m. To avoid damage of the sample surface all measurements were performed in the tapping mode. The scan speed was proportional to the scan size with a scan frequency from 0.5 to 1.5 Hz. Images were obtained by displaying amplitude, height and phase signal of the cantilever in the trace direction recorded simultaneously.

#### *Determination of encapsulation efficiency (EE)*

After centrifugation of 1 ml of the nanoparticle suspension (10 minutes at 10 000 rpm) the clear supernatants were removed and the sediments were dissolved in acetone before mixing with 5 ml of scintillation cocktail. The activity of radio labelled paclitaxel in supernatants and residues was quantified by liquid scintillation counting (LSC) (Tri-Carb 2100TR, Packard BioScience, Germany). The encapsulation efficiency was calculated by comparing the actual and theoretical loading in consideration of the <sup>14</sup>C-paclitaxel / paclitaxel ratio. Each sample was measured in quadruplicate.

---

*In vitro release of paclitaxel*

One ml of the nanoparticle suspension in 1.5 ml Eppendorf cups (Eppendorf, Germany) was placed in an incubator at 37°C. At predetermined time intervals, the buffer was withdrawn after centrifugation and replaced by fresh buffer. The amount of drug released and the encapsulation efficiency were determined in quadruplicate as described above.

**In-vitro cell culture studies***Rabbit vascular smooth muscle cell (RbVSMC) culture*

The cells were isolated from abdominal aortas of New Zealand white rabbits [24] and cultured in DMEM (Dulbecco's modified Eagle medium, Sigma-Aldrich, Germany) supplemented with 2 mM glutamine (Sigma-Aldrich, Germany) and 10% fetal calf serum (Gibco, Germany) at 37°C, 95% r.h. and 8.5% CO<sub>2</sub>. Vascular smooth muscle origin was confirmed by immunocytochemical staining with monoclonal antibodies against smooth muscle alpha actin (Progen Ind., Australia). Assays were always performed in the exponential growth phase of the cells. Absence of mycoplasmas was assured using the DAPI (4,6-diamidino-2-phenylindole) staining method (Molecular Probes, Leiden, The Netherlands).

*In-vitro cytotoxicity using MTT Assay*

In-vitro cytotoxicity of blank, paclitaxel loaded nanoparticles from PVA<sub>300</sub>-g-PLGA(15) and PVA<sub>300</sub>-g-PLGA(30), and free paclitaxel were investigated using the primary RbVSMC culture. Nanoparticles were prepared under aseptic conditions. Paclitaxel was dissolved in 96% ethanol. To obtain different test concentrations, several dilutions of paclitaxel stock solution and nanoparticle suspensions were prepared with DMEM culture medium. Ethanol amounts used for dilution showed no influence on the cell viability during the

experiments. RbVSMC were seeded into 96-well microtiter plates (Nunclon™, Nunc, Germany) at a density of 5000 cells/well. After 24 h the culture medium was replaced with different dilutions of the stock solutions. After an incubation period of 24 h the culture medium was replaced with fresh, drug-, and nanoparticles- free culture medium. After an additional incubation time of 48 h the viability of the cells was evaluated by the MTT assay (n = 7). MTT (3-(4,5-dimethylthiazol-2-yl)-2,5-diphenyl tetrazolium bromide) (Sigma-Aldrich, Germany) was dissolved in phosphate buffered saline at 5 mg/ml and 20 µl were added to each well reaching a final concentration of 0.5 mg MTT/ml. After an incubation time of 4 h unreacted dye was removed by aspiration, the purple formazan product was dissolved in 200 µl/well dimethyl sulfoxide and quantitated by a plate reader (Titertek Plus MS 212, ICN, Germany) at wavelengths of 570 and 690 nm. Poly(ethylene imine) 750 kDa (BASF, Germany) at 1 mg/ml in DMEM was used as a positive control and poly(ethylene) 600 (Merck, Germany) at 1mg/ml in DMEM as a negative control.

#### *Cellular nanoparticle uptake study using confocal laser scanning microscopy (CLSM)*

For CLSM experiments a Zeiss Axiovert 100 M microscope coupled to a Zeiss LSM 510 scan module was used. Cells were seeded at a density of 20,000 cells per well in 8 well chamber slides (Lab Tek, Nunc, Germany). After 24 h medium was removed and cells were incubated with 50 µl particle suspension (2mg/ml, theoretical paclitaxel loading: 0.1 % (w/w)). After 6 h NP containing medium was removed again and cells were washed three times with phosphorous buffered saline (PBS). Fixation of cells was performed by incubation with 400 µl paraformaldehyde solution 3 % in PBS for 20 minutes. For excitation of the coumarine derivative attached to the polymer PVA<sub>300</sub>-g-PLGA(15) an Enterprise UV laser with a wavelength of 364 nm was used.

Excitation of Oregon Green attached to paclitaxel was performed by using an argon laser with a wavelength of 488 nm. Images were recorded in multitracking mode using longpass filters of 385 nm and 505nm.

## RESULTS AND DISCUSSION

### NP characterization

The solvent evaporation method appears to be particularly suitable for the preparation of PVA-g-PLGA nanoparticles [21]. The mechanism of particle formation thought to occur according to “diffusion-stranding” process found in spontaneous emulsification also designated as Marangoni – effect [25]. The morphology of nanoparticles prepared by the solvent displacement technique is exemplarily shown for NP from PVA<sub>300</sub>-g-PLGA in Fig. 1 and 2. The surface of spherical NP appeared to be smooth and without pores, similar to NP from PLA, or PLGA [16,26]. The mean particle size ranged between 140 and 170 nm (Fig. 3) as confirmed by SEM. Apparently, the encapsulation of paclitaxel did not affect the nanoparticle size, or polydispersity indices (0.1 to 0.17) suggesting uniform, and monomodal size distributions. Particle yields were in the range of 80 to 94 % (Fig. 4), and were comparable to recently published results [27]. The passage of nanoparticles through the channelled balloon catheter did not influence the particle size or yield, as shown in Fig. 3 and Fig. 4. The encapsulation efficiency (EE) at a theoretical loading of 2 % ranged from 77 % for PVA-g-PLGA (10) NP to 87 % for PVA-g-PLGA(30) NP. In comparison PLGA NP showed a EE of 80% equal to NP from PVA-g-PLGA(15).

In contrast to other researchers who visualized cellular NP uptake with fluorescence loaded nanoparticles [28,29], we prepared NP using 7-methoxycoumarin-3-aminocarbonyl–conjugated PVA<sub>300</sub>-g-PLGA(15). The use of fluorescently labelled instead of fluorescence-loaded particles avoids any unintentional dye release that would prevent the exact determination of the particle distribution by confocal laser scanning microscopy (CLSM).

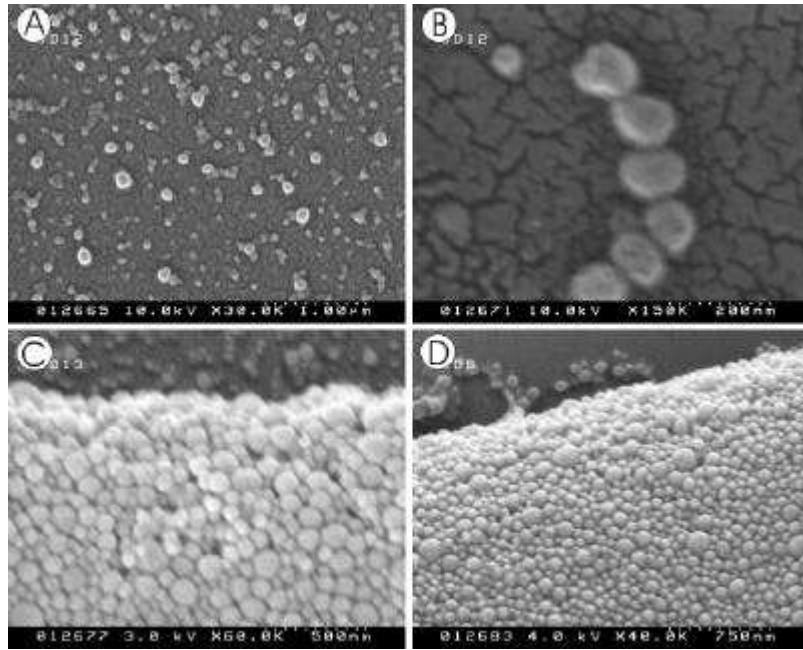


**Fig. 1:** Scanning electron micrographs of nanoparticles prepared from (A), (B)  $PVA_{300}$ -g-PLGA(30), (C)  $PVA_{300}$ -g-PLGA(15), and (D) fluorescence labelled  $PVA_{300}$ -g-PLGA(15) loaded with 0.5 % paclitaxel.

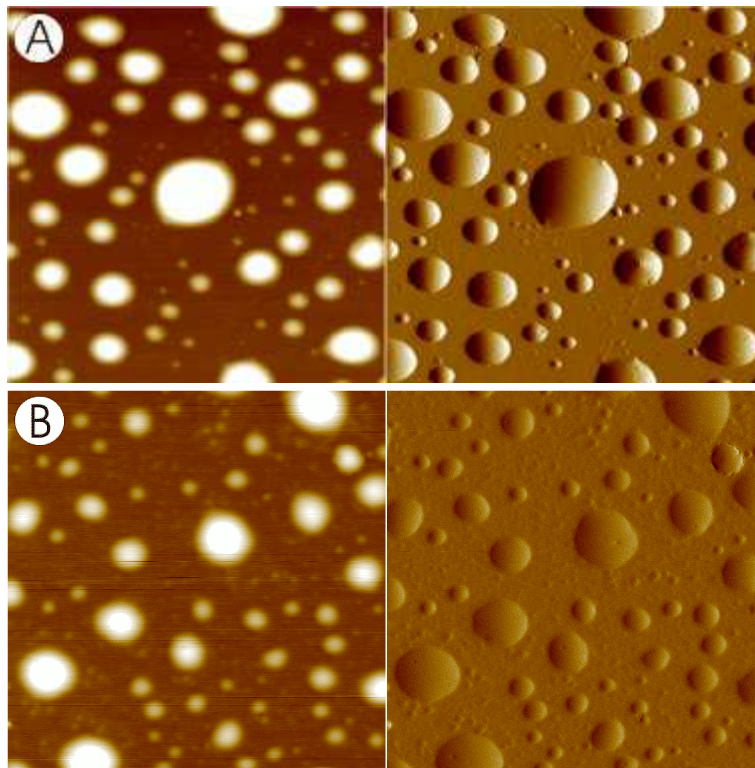


**Fig. 2:** Atomic force micrographs showing surface properties of polymer nanoparticles prepared from (A)  $PVA_{300}$ -g-PLGA(15), and (B) fluorescence labelled  $PVA_{300}$ -g-PLGA(15). Each single image has a edge length of 5  $\mu$ m.

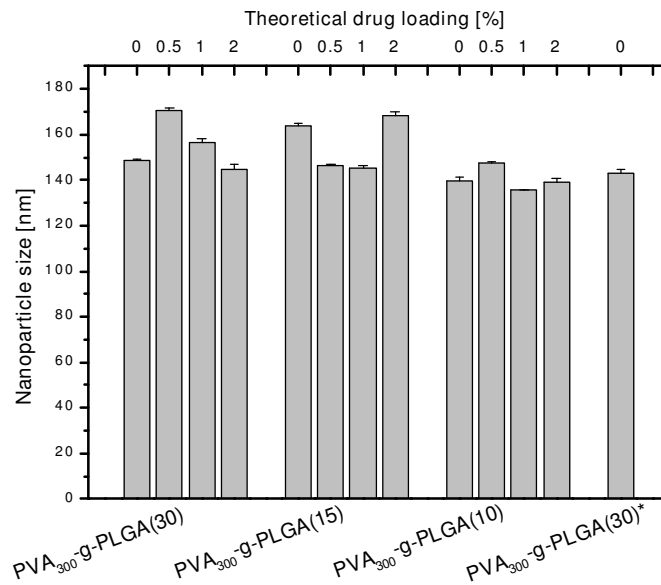


**Fig. 3:** Size of nanoparticles (NP) prepared from PVA<sub>300</sub>-g-PLGA determined by photon correlation spectroscopy. PVA<sub>300</sub>-g-PLGA(30)\* = NP batch for size determination after passage through a channelled balloon delivery catheter (SCIMED REMEDY™). All measurements were performed in triplicate.

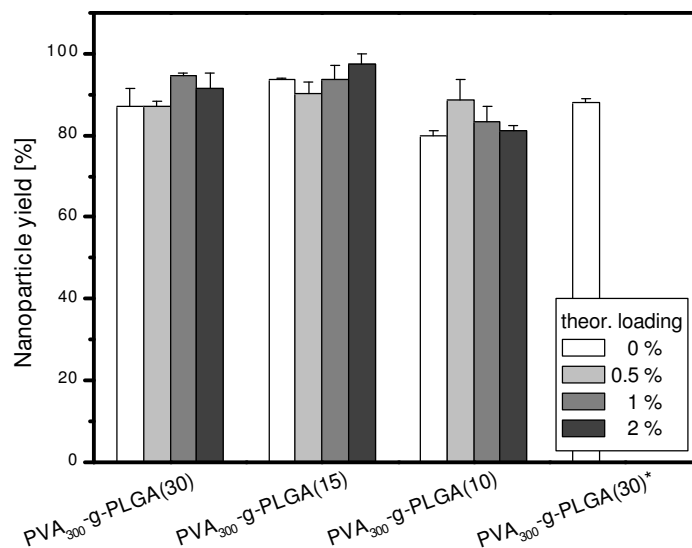


**Fig.4:** Yield of nanoparticles prepared from three different PVA<sub>300</sub>-g-PLGA comb polyesters. It is expressed as the ratio between the polymer mass in the suspension and the theoretical amount. PVA<sub>300</sub>-g-PLGA(30)\* = NP batch for yield determination after passage through a channelled balloon delivery catheter (SCIMED REMEDY™). All measurements were performed in triplicate.

Fluorescently labelled paclitaxel loaded nanoparticles thus obtained for cellular uptake studies have a particle size of  $118.4 \text{ nm} \pm 7.3 \text{ nm}$  with a polydispersity index of  $0.1 \pm 0.024$  (Fig. 3), and additionally, show the same shape and surface characteristics (Fig. 1 and 2) as unlabeled nanoparticles.

### **In vitro drug release**

The influence of polymer composition on the cumulative drug release of paclitaxel loaded NP is shown in Fig. 5. The early release phase is dominated by an initial drug burst. In the case of PVA<sub>300</sub>-g-PLGA(10) nearly 80 % of the encapsulated paclitaxel was released during the first day. An increased chain length resulted in a substantial decrease of burst rates as observed for PVA<sub>300</sub>-g-PLGA(15) (56 %) and PVA<sub>300</sub>-g-PLGA(30) NP (38%). PLGA NP exhibited the lowest burst release of ca. 35 %. The following release phase of all NP species was characterized by a slow but continuous profile over a time period of 22 days. Other authors observed comparable release behavior with regard to PLGA NP [26,27]. The paclitaxel release exhibited a biphasic release pattern which was characterized by an initial drug burst during the first 24 h, followed by a slower release phase.

The burst release of hydrophobic paclitaxel from the nanoparticles is possibly due to the influence of the hydrophilic backbone and the PLGA chain length of the polymers. The lower the PLGA chain length the lower the lipophilicity of the polymer, and furthermore, the lower the solubility of paclitaxel in the polymer, resulting in an increased amount of free paclitaxel and a decreased EE compared to the other comb polyesters, and especially to PLGA [19].

Another important aspect is the presence of surfactant acting as stabilizing agent for the NP suspension. While the hydrophobic drug containing organic solution was added to the surfactant containing water phase, the paclitaxel may

accumulate in the hydrophobic domains of the surfactant molecules. When the NP solidify in the aqueous phase and surfactant molecules attach to the hydrophobic NP surface, the drug is not able to diffuse back into the solid core of the nanoparticles [30]. Dissolution and diffusion procedures of the drug, which was adsorbed onto the NP surface, could lead to an initial drug burst, while the slower and continuous release phase may be attributed to the diffusion of the drug localized in the NP core [31].

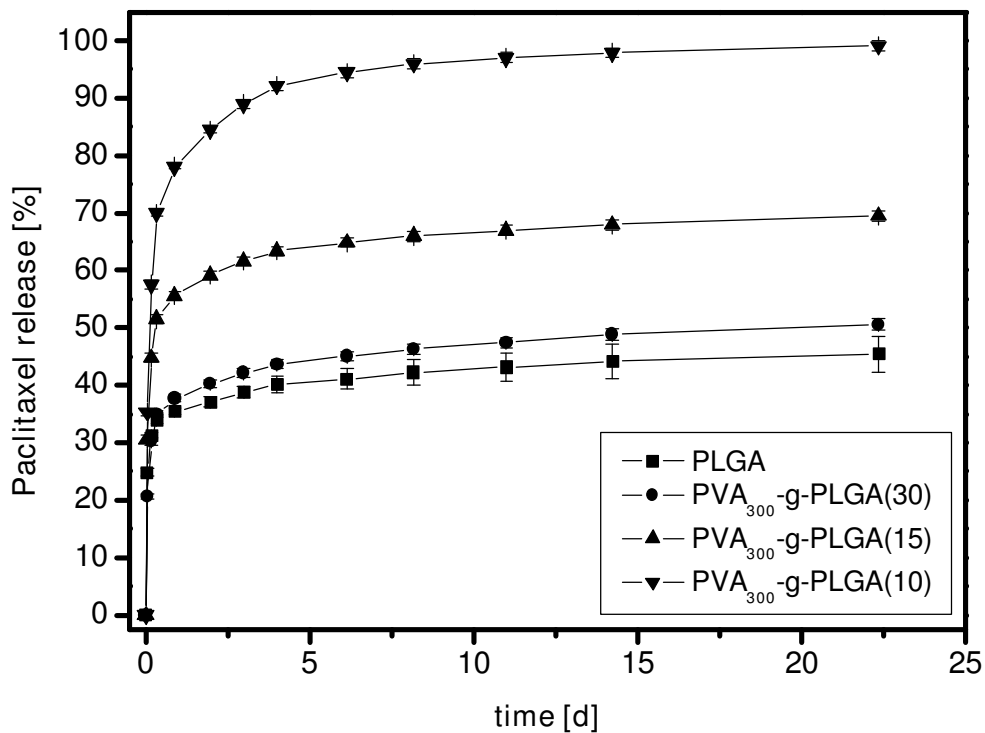


**Fig. 5:** Effect of the polymer composition on the *in vitro* paclitaxel release from nanoparticles loaded with 2 % paclitaxel / <sup>14</sup>C-paclitaxel (mass ratio 250:1). (Encapsulation efficiencies ranges from 77 to 87 %). The drug released was determined by liquid scintillation counting (LSC). Each sample was measured in quadruplicate.

Nevertheless, the burst release is clinically desirable to achieve initial high drug concentrations in the target tissue. After release of a loading dose, the

following, and substantial sustained drug release rate is to obtain a constant drug level to prevent excessive VSMC proliferation persistently. Previous results of in-vitro cell culture studies showed a paclitaxel induced decrease in cell viability of human VSMC at a drug concentration range of 0.1 to 10  $\mu\text{mol/L}$ , which is potentially favorable for local delivery. An increase in cell apoptosis was observed at higher drug levels (50 to 100  $\mu\text{mol/L}$ ) [32]. The intimal VSMC that follows vascular injury during angioplasty procedures reaches a maximum at 10 to 14 days and ends upon re-endothelization of the traumatized vessel segment. But due to a relatively short residence time of paclitaxel in VSMC, the application of free drug containing solutions could be less efficient to inhibit restenosis, as demonstrated for bovine VSMC [33], which underlines the need of sustained-release dosage forms of anti proliferative drugs. By specific variation of PVA-g-PLGA polymer composition we were able to adjust the initial drug dose, which is released immediately after the infusion of the nanoparticle suspension into the vessel wall, and subsequently, a delayed drug liberation provides a persistent effect on VSMC proliferation.

### **In vitro cytotoxicity**

The MTT test serves as an assay for proliferation and cell viability by measuring the metabolic activity of cells. Metabolically active cells are able to convert the yellow water-soluble tetrazolium salt (3-(4,5 dimethylthiazol-2-yl)-2,5-diphenyltetrazolium bromide) to a water-insoluble dark blue formazan by reductive cleavage of the tetrazolium ring. For in vitro cytotoxicity all components, which were used for nanoparticle preparation, were tested. The suspension stabilizer poloxamer 188 did not decrease the viability of RbVSMC up to concentrations of 10 mg/ml (data not shown). Pistel et al. (2001) have already demonstrated the good biocompatibility of PVA-g-PLGA polymer using the extraction method [19]. The non-toxic character of unloaded nanoparticles prepared from PVA<sub>300</sub>-g-PLGA(30) and PVA<sub>300</sub>-g-PLGA (15) was confirmed up

to NP concentration of ca. 370  $\mu\text{g/ml}$ , as shown in (Fig. 6). By contrast paclitaxel loaded PVA-g-PLGA nanoparticles showed a concentration dependent viability of RbVSMC. An increase of nanoparticle concentration from 3 to more than 300  $\mu\text{g/ml}$  was accompanied by a reduction in cell viability of about 30 %. Furthermore, and this effect highlights the rationale for the encapsulation of anti proliferative drugs for local vascular delivery, at higher drug levels free paclitaxel was less toxic compared to drug-loaded nanoparticles, probably due to a higher cellular uptake of nanoparticles (Fig. 6). Hence, nanoparticles formed a depot from which the paclitaxel is released continuously after the initial burst.

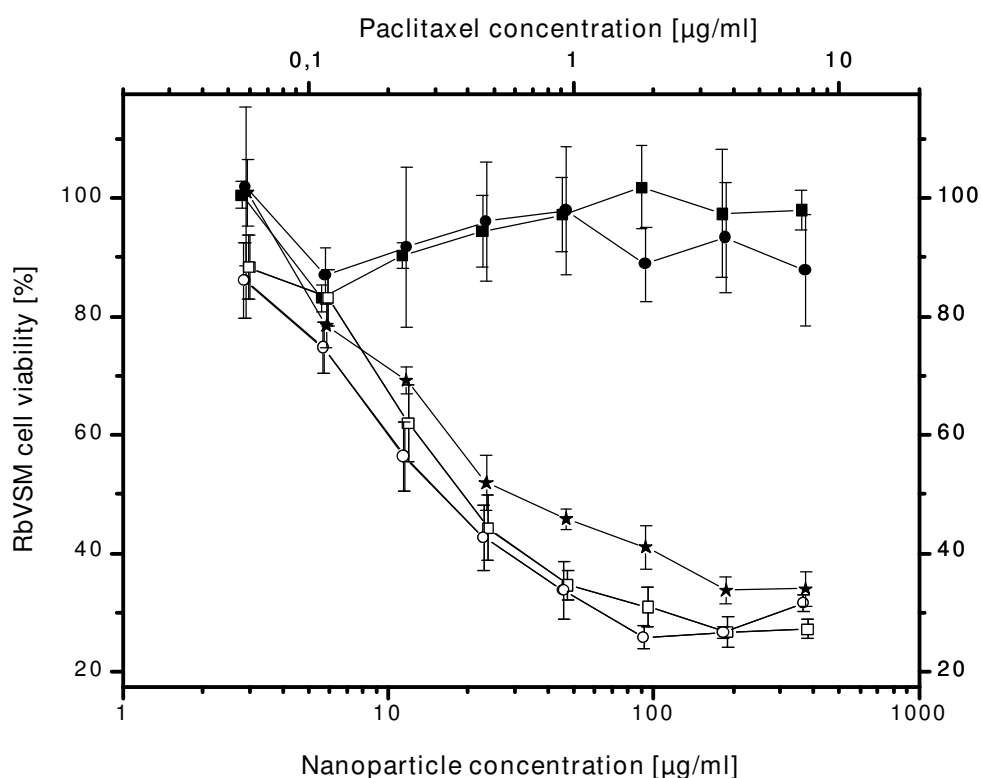


**Fig. 6:** Cytotoxicity of free paclitaxel (Ptx) (star symbol), blank nanoparticles (filled symbols) and Ptx-loaded nanoparticles (open symbols) (theoretical loading 2 %) from PVA<sub>300</sub>-g-PLGA(30) (open and filled squares) and PVA<sub>300</sub>-g-PLGA(15) (open and filled circles) by means of MTT assay.

### **Nanoparticle uptake into RbVSMC**

Confocal laser scanning microscopy of VSMC exposed to fluorescence labelled nanoparticles (blue fluorescence) loaded with 0.1 % of Oregon green labelled paclitaxel (green fluorescence) demonstrated an increased fluorescence activity in the cells after an incubation period of 6 h (Fig. 7). Based on results from the *in vitro* cytotoxicity test, fluorescently labelled paclitaxel in the chosen concentration did not affect cell viability of VSMC negatively during NP uptake experiments. The image shown is a z-section through the center of the cells and confirms that the fluorescence observed is the result of nanoparticle localization inside the cells and not on the membrane surface. The co-localization of NP and paclitaxel fluorescence appeared in yellow fluorescence as a consequence of NP internalization.

Various processes, such as phagocytosis [34], receptor mediated endocytosis, or fluid phase pinocytosis [33] are hypothesized for cellular uptake of particulate drug carriers in smooth muscle cells. In fact phagocytosis is generally associated with the uptake of large particles (> 500 nm) and not with NP of about 100 – 200 nm, which was confirmed by testing the phagocytic activity of human VSMC in the presence of NP *in vitro* [29].

As shown by Fig. 7, the size and localization the intracellular vesicles suggests the NP are probably located in the endosomal/lysosomal compartment surrounding the nucleus [33,35]. The appearance of diffuse green and blue fluorescence indicates a subsequent NP escape into the cytoplasm, as hypothesized by Panyam et al. (2002) [35]. As a result of uptake inhibition at low temperatures and saturation kinetics during incubation with poly(ethylene oxide)-poly(lactide-co-glycolide) NP, Suh et al. (1998) proposed that the uptake is through adsorptive pinocytosis [33]. In contrast it was also demonstrated that in parts PLGA NP without any specific ligands were internalized nonspecifically through clathrin vesicles which are known to be involved in active receptor mediated endocytosis [35].

However, further investigations with regard to the mechanism of nanoparticle uptake and the kinetics of drug uptake and retention in the VSMC will be helpful to establish the efficiency of PVA-g-PLGA nanoparticles for the prevention of excessive proliferation of VSMC after balloon angioplasty.

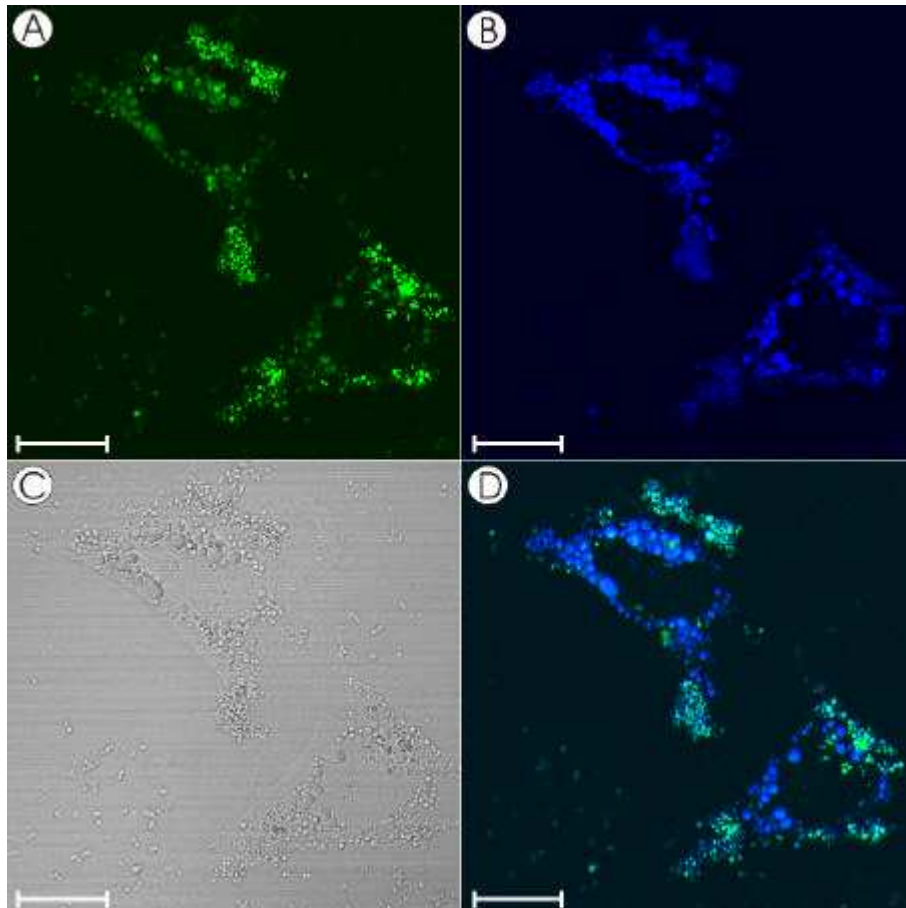


**Fig. 7:** CLSM images demonstrating intracellular nanoparticle ( $118.4 \text{ nm} \pm 7.3$ ;  $PI 0.1 \pm 0.024$ ) distribution in RbVSMC after 6 hours of incubation. (A) Distribution of Oregon Green labelled paclitaxel (green), and (B) of from 7-methoxy-coumarin-3-carbonyl azide labelled PVA<sub>300</sub>-g-PLGA(15) (blue) loaded with 0.1 % fluorescently labelled paclitaxel. (C) Differential interference contrast image showing the outline of the cells. (D) Overlay of (A) and (B) showing the co-localization of nanoparticles and paclitaxel. Each image shown is a z-section through the center of the cells supporting location of nanoparticles inside the cells. Scale bar represents  $20 \mu\text{m}$ .

---

## CONCLUSIONS

This study describes the formulation of biodegradable nanoparticles (<180 nm) using the solvent displacement technique for catheter-based local intraluminal drug delivery. PVA-g-PLGA comb polyesters are suitable biodegradable polymers for the nanoencapsulation of paclitaxel leading to encapsulation efficiencies of 87 %. By varying the composition of PVA-g-PLGA polymers the release kinetics can be adapted to the clinical requirements of drug delivery for prevention of restenosis. We have further demonstrated that unloaded PVA-g-PLGA nanoparticles are non toxic to RbVSMC and capable of sustained intracellular delivery of paclitaxel. Paclitaxel loaded nanoparticles decrease the cell viability of RbVSMC in-vitro more effectively than the free drug. Confocal laser scanning microscopy confirmed the uptake of paclitaxel-loaded nanoparticles. Because of their variability, PVA-g-PLGA polymers are well suitable candidates to encapsulate also hydrophilic agents, such as oligonucleotides, peptides or proteins [19].

These findings support the rationale for the design of colloidal drug delivery systems based on biodegradable nanoparticles from poly(vinyl alcohol)-g-lactide-co-glycolide), which offer attractive features for the prevention of restenosis after angioplasty.

## REFERENCES

- [1] H. Hanke, T. Strohschneider, M. Oberhoff, E. Betz and K.R. Karsch, Time course of smooth muscle cell proliferation in the intima and media of arteries following experimental angioplasty, *Circ Res* 67(3) (1990) 651-659.
- [2] Y. Shi, M. Pieniek, A. Fard et al., Adventitial Remodeling After Coronary Arterial Injury, *Circulation* 93(2) (1996) 340-348.

- 
- [3] D.W. Muller, E.J. Topol, G.D. Abrams, K.P. Gallagher and S.G. Ellis, Intramural methotrexate therapy for the prevention of neointimal thickening after balloon angioplasty, *J Am Coll Cardiol* 20(2) (1992) 460-466.
- [4] J.F. Mitchel, D.B. Fram, D.F. Palme et al., Enhanced intracoronary thrombolysis with urokinase using a novel, local drug delivery system. In vitro, in vivo, and clinical studies, *Circulation* 91(3) (1995) 785-793.
- [5] J. Rome, V. Shayani, M. Flugelman et al., Anatomic barriers influence the distribution of in vivo gene transfer into the arterial wall. Modeling with microscopic tracer particles and verification with a recombinant adenoviral vector, *Arteriosclerosis and Thrombosis* 14(1) (1994) 148-161.
- [6] I. Gradus-Pizlo, R.L. Wilensky, K.L. March et al., Local delivery of biodegradable microparticles containing colchicine or a colchicine analogue: effects on restenosis and implications for catheter-based drug delivery, *J Am Coll Cardiol* 26(6) (1995) 1549-1557.
- [7] T.K. Nasser, R.L. Wilensky, K. Mehdi and K.L. March, Microparticle deposition in periarterial microvasculature and intramural dissections after porous balloon delivery into atherosclerotic vessels: quantitation and localization by confocal scanning laser microscopy, *Am Heart J* 131(5) (1996) 892-898.
- [8] B. Bhargava, G. Karthikeyan, A.S. Abizaid and R. Mehran, New approaches to preventing restenosis, *Bmj* 327(7409) (2003) 274-279.
- [9] D.I. Axel, W. Kunert, C. Goggelmann et al., Paclitaxel Inhibits Arterial Smooth Muscle Cell Proliferation and Migration In Vitro and In Vivo Using Local Drug Delivery, *Circulation* 96(2) (1997) 636-645.

- 
- [10] C. Herdeg, M. Oberhoff, A. Baumbach et al., Local paclitaxel delivery for the prevention of restenosis: biological effects and efficacy in vivo, *J Am Coll Cardiol* 35(7) (2000) 1969-1976.
- [11] E.K. Rowinsky and R.C. Donehower, Paclitaxel (taxol), *N Engl J Med* 332(15) (1995) 1004-1014.
- [12] H. Fessi, J.P. Devissaguet, F. Puisieux and C. Thies, Process of the preparation of dispersable colloidal systems of a substance in the form of nanoparticles formation of colloidal nanoparticles, U.S. Patent 5,118,528, June 2, 1992.
- [13] M. Chorny, I. Fishbein and G. Golomb, Drug Delivery Systems for Treatment of Restenosis, *Crit Rev Ther Drug Carrier Syst* 17(3) (2000) 249-284.
- [14] I. Fishbein, M. Chorny, L. Rabinovich et al., Nanoparticulate delivery system of a tyrphostin for the treatment of restenosis, *J Controlled Release* 65(1-2) (2000) 221-229.
- [15] C. Song, V. Labhasetwar, X. Cui, T. Underwood and R.J. Levy, Arterial uptake of biodegradable nanoparticles for intravascular local drug delivery: results with an acute dog model, *J Controlled Release* 54(2) (1998) 201-211.
- [16] L. Mu and S.S. Feng, A novel controlled release formulation for the anticancer drug paclitaxel (Taxol): PLGA nanoparticles containing vitamin E TPGS, *J Control Release* 86(1) (2003) 33-48.
- [17] K.S. Soppimath, T.M. Aminabhavi, A.R. Kulkarni and W.E. Rudzinski, Biodegradable polymeric nanoparticles as drug delivery devices, *J Control Release* 70(1-2) (2001) 1-20.

- 
- [18] A. Breitenbach and T. Kissel, Biodegradable comb polyesters: Part 1 - Synthesis, characterisation and structural analysis of PLA and PLGA grafted onto water-soluble PVA as backbone, *Polymers* 39(14) (1998) 3261-3271.
- [19] K.F. Pistel, A. Breitenbach, R. Zange and T. Kissel, Brush-like biodegradable polyesters, part III, Protein release from microspheres of poly(vinyl alcohol)-graft-poly(D,L-lactic-co-glycolic acid), *J Control Release* 73(1) (2001) 7-20.
- [20] A. Breitenbach, K.F. Pistel and T. Kissel, Biodegradable comb polyesters Part II. Erosion and release properties of PVA-g-PLG, *Polymers* 41 (2000) 4781-4792.
- [21] T. Jung, A. Breitenbach and T. Kissel, Sulfobutylated poly(vinyl alcohol)-graft-poly(lactide-co-glycolide)s facilitate the preparation of small negatively charged biodegradable nanospheres [In Process Citation], *J Controlled Release* 67(2-3) (2000) 157-169.
- [22] S.M. Ropiak, Multiple hole drug delivery balloon, US 5,860,954, September 29, 1997.
- [23] V. Oberle, U. Bakowsky, I.S. Zuhorn and D. Hoekstra, Lipoplex formation under equilibrium conditions reveals a three-step mechanism, *Biophys J* 79(3) (2000) 1447-1454.
- [24] D.I. Axel, B.R. Brehm, K. Wolburg-Buchholz et al., Induction of cell-rich and lipid-rich plaques in a transfilter coculture system with human vascular cells, *J Vasc Res* 33(4) (1996) 327-339.

- 
- [25] D. Quintanar-Guerrero, E. Allémann, E. Doelker and H. Fessi, A mechanistic study of the formation of polymer nanoparticles by the emulsification-diffusion technique, *Colloid & Polymer Science* 275(7) (1997) 640-647.
- [26] S. Feng and G. Huang, Effects of emulsifiers on the controlled release of Paclitaxel (Taxol) from nanospheres of biodegradable polymers, *J Control Release* 71 (2001) 53-69.
- [27] C. Fonseca, S. Simoes and R. Gaspar, Paclitaxel-loaded PLGA nanoparticles: preparation, physicochemical characterization and in vitro anti-tumoral activity, *J Control Release* 83(2) (2002) 273-286.
- [28] J.S. Chawla and M.M. Amiji, Cellular uptake and concentrations of tamoxifen upon administration in poly(epsilon-caprolactone) nanoparticles, *AAPS PharmSci* 5(1) (2003) E3.
- [29] J. Panyam and V. Labhasetwar, Dynamics of Endocytosis and Exocytosis of Poly(D,L-Lactide-co-Glycolide) Nanoparticles in Vascular Smooth Muscle Cells, *Pharm Res* 20(2) (2003) 212-220.
- [30] R.H. Muller, K. Mader and S. Gohla, Solid lipid nanoparticles (SLN) for controlled drug delivery - a review of the state of the art, *Eur J Pharm Biopharm* 50(1) (2000) 161-177.
- [31] J.S. Chawla and M.M. Amiji, Biodegradable poly(epsilon -caprolactone) nanoparticles for tumor-targeted delivery of tamoxifen, *Int J Pharm* 249(1-2) (2002) 127-138.
- [32] D.I. Axel, W. Kunert, C. Goggelmann et al., Paclitaxel inhibits arterial smooth muscle cell proliferation and migration in vitro and in vivo using local drug delivery, *Circulation* 96(2) (1997) 636-645.

- 
- [33] H. Suh, B. Jeong, R. Rathi and S.W. Kim, Regulation of smooth muscle cell proliferation using paclitaxel-loaded poly(ethylene oxide)-poly(lactide/glycolide) nanospheres, *J Biomed Mater Res* 42(2) (1998) 331-338.
- [34] K.A. Foster, M. Yazdanian and K.L. Audus, Microparticulate uptake mechanisms of in-vitro cell culture models of the respiratory epithelium, *J Pharm Pharmacol* 53(1) (2001) 57-66.
- [35] J. Panyam, W.Z. Zhou, S. Prabha, S.K. Sahoo and V. Labhasetwar, Rapid endo-lysosomal escape of poly(DL-lactide-co-glycolide) nanoparticles: implications for drug and gene delivery, *Faseb J* 16(10) (2002) 1217-1226.

## CHAPTER 5

---

### **PACLITAXEL RELEASING STENTS FOR THE TREATMENT OF RESTENOSIS: BIODEGRADABLE COATINGS CONSISTING OF POLY(VINYL ALCOHOL)-GRAFT-POLY (LACTIDE-CO-GLYCOLIDE)**

in preparation for publication:

Journal of Controlled Release

## SUMMARY

Although substantial progress in catheter and stent design have improved success of percutaneous transluminal angioplasty (PTA) of atherosclerotic disease, the incidence of restenosis caused by in-stent neointimal hyperplasia remains a serious problem. Therefore, drug-eluting stents were developed for the site-specific delivery of anti-restenotic agents. We investigated biodegradable polyesters, namely poly(lactic-co-glycolic acid) (PLGA) and different poly(vinyl alcohol)-graft-poly(lactic-co-glycolic acid) (PVA-g-PLGA) as paclitaxel-eluting stent coating materials. In our studies PLGA showed sigmoid release behavior, paclitaxel release from PVA-g-PLGA films, in contrast, was continuous over 40 days without drug burst. Wide angle X-ray diffraction confirmed that paclitaxel is dissolved in the polymer matrix. Paclitaxel crystallisation becomes observable at drug loadings  $\geq 10\%$ . The effect of drug loading on polymer degradation was studied in films prepared from PVA<sub>300</sub>-g-PLGA(30) with paclitaxel loadings of 5 and 15% over a time period of 6 weeks. The results suggest a more heterogenous mechanism of degradation including surface and bulk erosion. Drug release rates from the PVA-g-PLGA films were improved resulting in more continuous release profiles. A model stent (Jostent peripheral) coated with Parylene N, a poly(p-xylylene) (PPX) derivate, was covered with a second layer of PVA<sub>300</sub>-g-PLGA(15), and PVA<sub>300</sub>-g-PLGA(30) by using air brush method. Morphology of coated stents, and film integrity after expansion from 3.12 mm to 5 mm was investigated by scanning electron microscopy (SEM). Except of some minor cracks, devices resisted mechanical stress during stent expansion.

## INTRODUCTION

All forms of percutaneous vascular interventions such as balloon angioplasty or stenting cause injury on the vessel leading to vessel recoil and neointima formation [1-4]. Stenting prevents vessel recoil and remodelling [5], but enhances intimal hyperplasia [6]. This neointima formation, which is responsible for in-stent restenosis, remains an important clinical problem in the treatment of vascular occlusions. Stent material and surface properties are key determinants in the formation of in-stent restenosis. Commonly used bare metal stents offer excellent mechanical stability, but often increase the incidence of thrombosis, fibromuscular proliferation and formation of restenosis. Polymer coatings have been suggested to improve stent biocompatibility. However, several biodegradable and non-biodegradable polymers have shown conflicting results provoking a severe tissue response [7]. Therefore, the formulation of stents which are loaded with anti-proliferative drugs, such as paclitaxel [8;9], or sirolimus [10] is an attractive approach for inhibition of neointimal hyperplasia.

Currently available drug-eluting stents systems (DESS) base on surfaces coated with drug containing polymer matrices, ceramic, or carbon coatings, as well as drugs directly applied to the stent surface. Randomised clinical trials [11], e.g. SIRIUS, RAVEL (Sirolimus-eluting Cypher™-stent) [12], or TAXUS I-VI (Paclitaxel-eluting stent) [13] have demonstrated their ability to reduce the incidence of restenosis following stenting.

Besides controlled and site-specific drug elution, the polymer matrix should have good mechanical properties in terms of flexibility and long lasting adherence to the stent surface at the required size when the device is deployed. Due to its elasticity, biostability and biocompatibility, poly(p-xylylene) (PPX) [14;15] ensures stent endothelization, and prevents acute vessel thrombosis, as well as foreign-body reactions after stent implantation. PPX derivatives, such as Parylene C and Parylene N are already recognized as Class VI polymers by the FDA.

Here we study paclitaxel-loaded polymeric film coatings based on poly (vinyl alcohol)-graft-poly(lactide-co-glycolide) (PVA-g-PLGA) comb polyesters. PVA-g-PLGA consist of a hydrophilic backbone, polyvinyl alcohol (PVA), which was grafted with PLGA chains. This non-toxic polymer structure offers various possibilities to modify drug release kinetics. Firstly, the water uptake and swelling properties of the matrix could be varied by changing the hydrophilic part of the polymer. Or, secondly, the degradation and release behavior may be assessable by grafting PLGA with different chain lengths onto the backbone [16;17]. Paclitaxel loaded films were studied with respect on polymer degradation and drug release behavior. To prove the mechanical integrity of the PVA-g-PLGA matrix, Jostent peripheral (JOMED, Germany) stents were coated twice, as illustrated schematically in Fig. 1. Firstly, stents were completely covered with Parylene N, using the chemical vapour deposition method (CVD) [18]. In a second step a solution of PVA-g-PLGA in chloroform is sprayed onto the stent struts by using air brush method forming a polymer matrix which covers only the outer, vessel wall directed surface. This prevents undesirable drug release into the blood stream, that may lead to systemic side effects in contrast to coatings formed by device dipping, which covers the total device surface.

## **MATERIALS AND METHODS**

### **Materials**

Linear PLGA 50:50 (RG 503H, Mw 28, 000 g/mol) was purchased from Boehringer Ingelheim (Germany). Paclitaxel (Genexol™) has been kindly provided by Sam Yang Corp.(Seoul, Korea). Radio labelled paclitaxel (paclitaxel-[2-benzoyl ring-UL- <sup>14</sup>C]) was obtained from Sigma (Sigma Chemicals, Germany). Dimethylacetamide (DMAc) was supplied from Fluka (Germany). Liquid scintillation cocktail was obtained from Packard BioScience

(Ultima Gold™ LS cocktail, Groningen, Netherlands). All other chemicals of analytical grade were purchased from Sigma (St. Louis, MO).

### **Poly((polyvinyl alcohol)-g-(D,L-lactide-co-glycolide))**

Synthesis and characterisation were carried out as described earlier [16,19]. Briefly, comb polyesters were synthesised by a stannous octoate catalysed ring-opening polymerisation of lactide and glycolide (1:1) in the presence of the backbone poly(vinyl alcohol) (PVA; MW 15 kg/mol, degree of polymerisation 300, degree of hydrolysis 88%) under anhydrous conditions. The polymers used for film preparation are described in Tab. 1. The following nomenclature will be used to specify the polymers: PVA<sub>300</sub>-g-PLGA(XX). The number in parenthesis refers to the mass ratio of branched PLGA, which is grafted (g) onto the hydrophilic backbone, compared to the PVA.

### **Preparation of polymer films**

Films were cast from an acetone solution of the polymers (5% w/v) on teflon plates containing paclitaxel in specified concentrations. After 72 h of solvent evaporation films were cut into discs using a punch cutter. The films were dried for three days in a drying chamber under reduced pressure at room temperature until constant weight was obtained.

### **Differential scanning calorimetry (DSC)**

Glass transition temperatures (T<sub>g</sub>) were measured using a differential scanning calorimeter (DSC7, Perkin Elmer, Germany). Film samples (5 mg) were sealed in aluminium pans and heated twice in a nitrogen atmosphere. Thermograms covering a range of (-)10°C to 220°C were recorded at a heating and a cooling rate of 10 °C per minute. The second run was used for T<sub>g</sub>

calculation (Pyris Software, Perkin Elmer, Germany). Calibration of the system was performed using gallium and indium standards.

### **Wide angle X-ray diffraction (WAXD)**

X-ray diffraction pattern of paclitaxel powder and paclitaxel-loaded films were recorded on a D-5000 diffractometer (Siemens, Germany) equipped with DiffracPlus 3.0 software (Bruker Rheinstetten) at room temperature. The scan range of  $2\theta$  was 2 to  $30^\circ$  at a rate of  $1^\circ 2\theta / \text{min}$ . The X-ray source was nickel filtered  $\text{CuK}\alpha$  radiation ( $\lambda = 1.54 \text{ \AA}$ ).

### **Size exclusion chromatography (SEC)**

Polymer solutions were injected into a thermostatted ( $60^\circ\text{C}$ ) Merck-Hitachi system (column: SDV linear M  $8 \times 300$  mm with a pre-column  $8 \times 50$ ,  $5 \mu\text{m}$ , Polymer Standard Service, Germany) equipped with a differential refractometer (RI 71) and a light scattering detector (MiniDawn,  $100 \mu\text{l}$  K5 cell, GaAs laser  $690 \text{ nm}$ , laser power  $30 \text{ mV}$ ). Chromatograms were obtained with N,N-dimethylacetamide containing lithium bromide ( $2.5 \text{ g/l}$ ) at a flow rate of  $0.5 \text{ ml/min}$ . Molecular weights were calculated using ASTRA V4.73 software (Wyatt, Technology Corp., CA).

### **Scanning electron microscopy (SEM)**

The morphology of prepared films and coated stents was characterised by SEM using a Hitachi S-4100 microscope (Hitachi, Germany). Dried specimens were mounted on aluminium pins using double-sided adhesive tape. Prior to microscopic examination samples were sputter coated with a gold layer under vacuum for 30 seconds (Edwards Auto 306, Edwards, Germany).

No.	Polymer	Polymer properties					Tg <sup>c</sup> (°C)
		M <sub>w</sub> PVA (kg/mol)	M <sub>w</sub> <sup>a</sup> (kg/mol)	M <sub>n</sub> <sup>a</sup> (kg/mol)	side chain length <sup>b</sup>	ratio lactide:glycolide	
1	PVA <sub>300</sub> -g-PLGA (15)	15	249.9	178.7	17.8	1:1	27.0
2	PVA <sub>300</sub> -g-PLGA (30)	15	438.1	319.1	31.7	1:1	28.8
3	Linear PLGA <sup>d</sup>	-	28.4	-	-	-	37.96

<sup>a</sup> determined by SEC (size exclusion chromatography) combined with MALLS (multi angle laser light scattering) using N,N dimethylacetamide containing 2.5 g/l LiBr as eluent.

<sup>b</sup> PLGA side chain length determined from <sup>1</sup>H-NMR.

<sup>c</sup> Tg (glass transition temperature) determined using differential scanning calorimetry (temperature range (-)10 – 220 °C; heating/cooling rate 10 °C/min)

<sup>d</sup> RG503H, supplied by Boehringer Ingelheim, Germany

**Tab. 1:** Characteristics of biodegradable polymers based on PVA<sub>300</sub>-g-PLGA comb polyesters and PLGA.

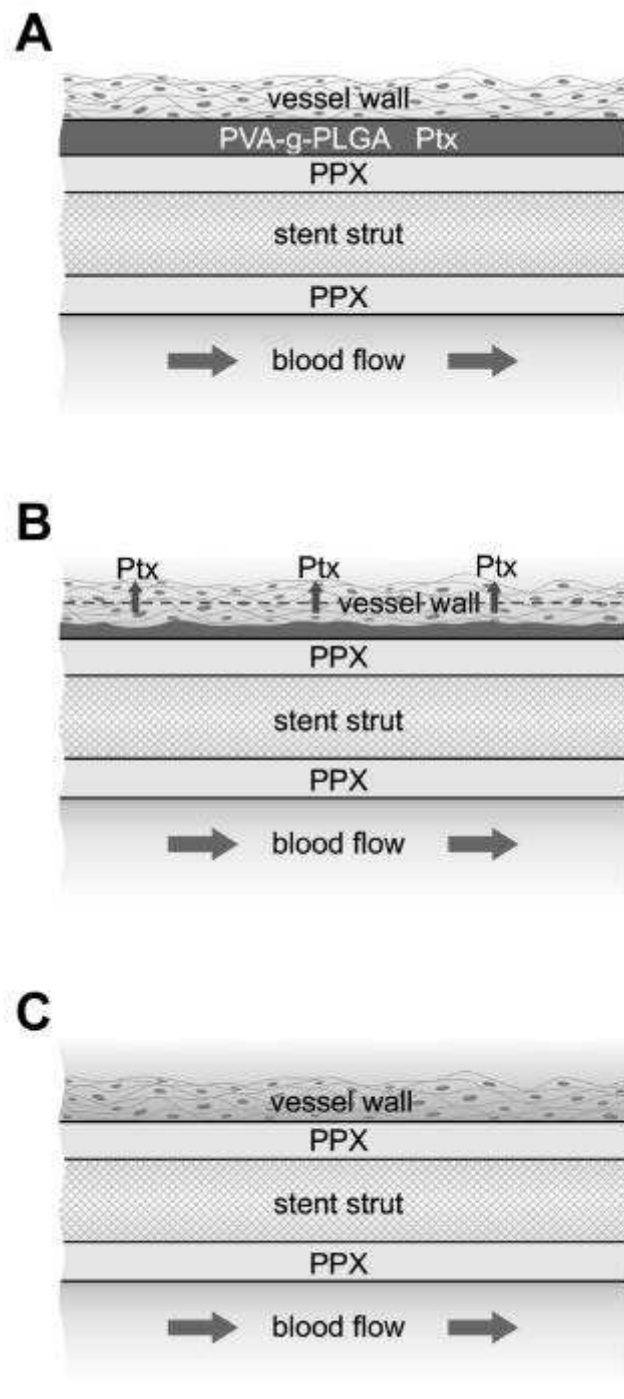


**Fig. 1:** Schematic illustration of functional and morphological changes of the double coated stent surface after stent implantation (A). Primary coating of PPX (Parylene N), covering the total stent surface, is generated using chemical vapour deposition (CVD). The outer, lesion site directed stent surface is coated with a paclitaxel (Ptx) containing and biodegradable layer based on PVA-g-PLGA using air brush method. PVA-g-PLGA coating degrades, the Ptx is released towards the vessel wall, and prevents excessive proliferation of smooth muscle cells, while the vascular lesion is able to heal (B). After degradation of the drug eluting layer, the PPX coating remains on the stent surface and ensures stent endothelization and long lasting stent compatibility to the surrounding vascular tissue.

### **In vitro degradation of polymer films**

Polymer films from PVA<sub>300</sub>-g-PLGA(30) ( $18.00 \pm 1.65$   $\mu\text{m}$  thickness) with paclitaxel loadings of 5 and 15 % were prepared as described above. Samples of known weight ( $39.66 \pm 2.41$  mg) were immersed in 5 ml phosphate buffered saline solution (PBS, 0.05M, pH 7.4) in glass vials and stored at 37°C. The buffer medium was periodically replaced during incubation experiments. At defined time intervals samples were recovered, washed with demineralised water, and subsequently lyophilised for 48 h followed by secondary drying at room temperature in vacuum for 7 days. To characterise the degree of degradation molecular weights (SEC), mass loss (gravimetrically) and film morphology (SEM) were investigated. Water uptake was determined gravimetrically after the water on the surface was removed by blotting. It was calculated as follows: Water uptake (%) =  $100 - (\text{Mass}(t)_{\text{wet}}/\text{Mass}(t)_{\text{dry}} \times 100)$ . Each sample was determined in triplicate.

### **In vitro paclitaxel release**

For in vitro release of drug loaded films <sup>14</sup>C-labelled and non-labelled paclitaxel were mixed in a mass ratio of 1 to 250 to a final theoretical loading of 5%. Films from PVA<sub>300</sub>-g-PLGA(15), PVA<sub>300</sub>-g-PLGA(30), and PLGA were cut into discs of 6 mm in diameter, which were incubated in 2 ml of different buffer solutions in glass vials at 37°C. At defined time intervals the buffer was withdrawn and 2 ml of fresh medium was added to the films. One milliliter of the supernatant was mixed with 5 ml of scintillation cocktail (Ultima Gold™). The activity of radio labelled paclitaxel for calculation of total drug release was quantified by liquid scintillation counting (LSC) (Tri-Carb 2900TR, Packard BioScience, Germany) at a counting time of 5 minutes for each sample. All measurements were performed in triplicate.

### Stent coating

Stents consisting of stainless steel (length 48 mm, diameter of 3.12 mm) (JOSTENT® peripheral, JOMED Implantate GmbH, Germany) were coated with poly (para-xylylene) (PPX) by using chemical vapor deposition (CVD) method [18]. In a next step the PPX layer was swollen in chloroform and covered by a second polymer layer consisting of PVA<sub>300</sub>-g-PLGA(15) or PVA<sub>300</sub>-g-PLGA(30) by using the spray coating method. For this purpose a polymer solution of 1 % (w/w) in chloroform was sprayed onto the stent surface at a distance of 5 cm using an air brush (Model Aero-pro Classic 10, Hansa, Germany) and dried under vacuum for 2 days at room temperature prepared for scanning electron microscopy analysis as described above. Stents were examined in the non-expanded state and after dilatation of tempered devices (37°C) from 3.12 to 5 mm by crimping on a thorn of stainless steel.

## RESULTS AND DISCUSSION

The aim of this study was the evaluation of PVA-g-PLGA comb polyesters for the preparation of paclitaxel eluting stent coatings. The insertion of a hydrophilic backbone PVA into hydrophobic PLGA chains led to a more continuous drug release profiles [16]. The modification of PLGA chain length allowed the adjustment of the drug release from coated stents to the clinical requirements of drug delivery. Factors contributing to paclitaxel release from polymer films are most notably balance of hydrophobic and hydrophilic components, glass transition temperature (T<sub>g</sub>), as well as degradation (loss of molecular weight) and erosion (mass loss) kinetics.

The glass transition temperature (T<sub>g</sub>) of polymers has an important effect on the drug release [20], and above all, on the flexibility of the stent coating, which is important for the film integrity during stent crimping and implantation using balloon catheters. Tab. 2 displays the T<sub>g</sub> of two different PVA-g-PLGAs and linear PLGA. The T<sub>g</sub> of pure linear PLGA is 9 °C higher compared to T<sub>g</sub> of

PVA-g-PLGA(30) (28.8 °C). By decreasing the PLGA chain length the T<sub>g</sub> decreases, as seen for PVA-g-PLGA(15) (27.0 °C). Thus, flexibility of polymer film increases, which is important for the matrix integrity after stent expansion inside the treated vessel segment. The incorporation of paclitaxel reinforces the decrease of glass transition temperature by increasing the drug loading. The shift of the T<sub>g</sub> of polymers to lower temperatures is due to the drug, which is at least partly molecularly dispersed in the polymer matrix. The drug acts as a plastiziser that influences flexibility of films at body temperature.

Polymer	Glass transition temperature [°C]				
	Loading [%]	0	5	10	15
PVA <sub>300</sub> -g-PLGA(15)		27.0	25.4	21.9	21.3
PVA <sub>300</sub> -g-PLGA(30)		28.8	26.8	22.7	21.6
Linear PLGA		37.96	27.3	25.6	24.5

**Tab. 2:** Glass transition temperature of paclitaxel loaded films determined using differential scanning calorimetry (scanning range – 10 to 220 °C, heating/cooling rate 10 °C/min).

Moreover, by using SEM morphological changes of films were observed by increasing the drug loading (Fig. 2). Paclitaxel-free films exhibited a smooth surface without pores and corrugations. Although thermograms obtained using DSC did not show any melting point for paclitaxel, films became partly rough and round, and furthermore, rosette-like structures were observable on the surface by increasing the paclitaxel content up to 15%. This phenomenon could be explained by the slight paclitaxel mass in the samples which was possibly under the detection limit of DSC. For this reason we used WAXD to

characterise the dispersion state of paclitaxel at different loadings more detailed (Fig. 3).

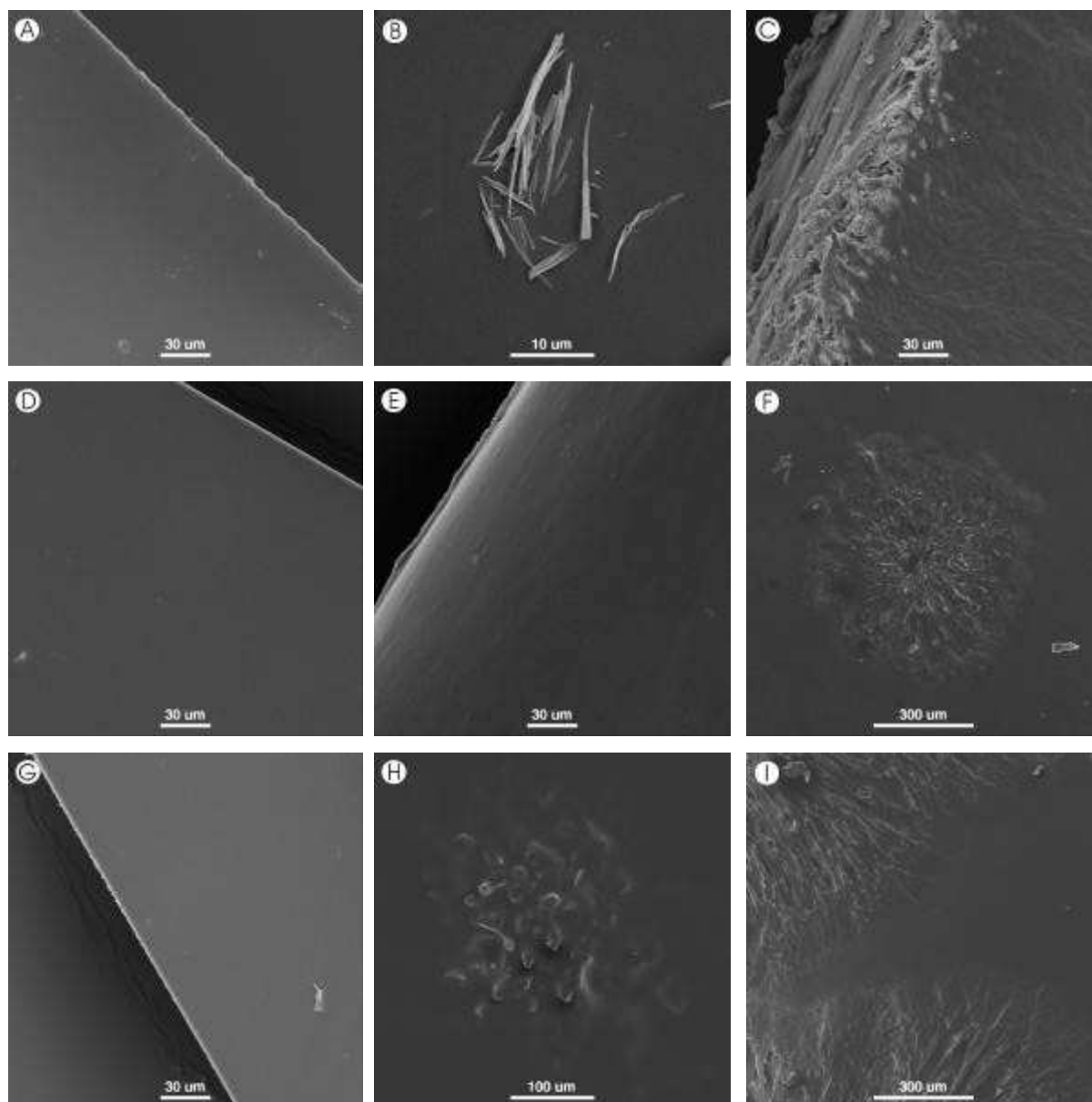


**Fig. 2:** Scanning electron microscopy (SEM) images of paclitaxel (Ptx)-loaded films prepared from (a - c) PLGA, (d - f) PVA<sub>300</sub>-g-PLGA(30), and (g - i) PVA<sub>300</sub>-g-PLGA(15) with drug loadings of 5 % (a, d, g), 10 % (b, e, h) and 15 % (c, f, i).

At drug loadings of less than 10 % WAXD profiles did not show any peaks of crystallised drug similar to those of unloaded polymer films (not shown) suggesting that the paclitaxel is soluble in the polymer matrix. Contrastingly, at a drug content of  $\geq 10\%$  WAXD patterns of films became more irregular, and crystallisation peaks were slightly increased. Similar results were reported by Jeon et al. (2000) who observed a concentration dependent norfloxacin crystallisation in PLGA nanoparticles using WAXD [21]. Several diffraction maxima are present at the same  $2\Theta$  as observed in the diffractogram of paclitaxel. There is evidence that drug and polymer formed a solid dispersion. Due to the high drug levels lipophilicity of polymer matrix increases and may decelerate polymer degradation.

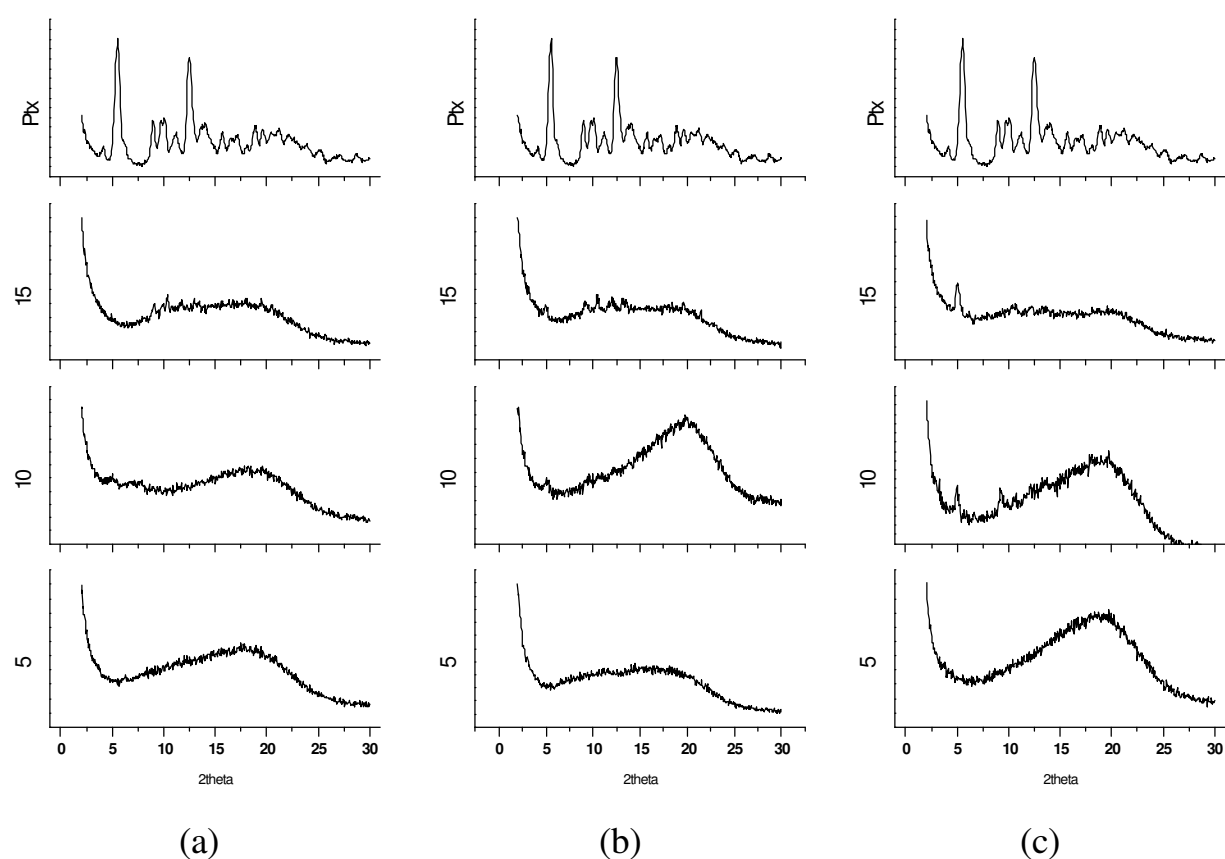


**Fig. 3:** Wide angle X-ray diffraction pattern of paclitaxel and paclitaxel (Ptx)-loaded films prepared from (a) PLGA, (b) PVA<sub>300</sub>-g-PLGA(30), and (c) PVA<sub>300</sub>-g-PLGA(15) with drug loadings of 5, 10, and 15%.

The polymer composition dependent paclitaxel release is described in Fig. 4. Drug liberation was performed in normal phosphate buffered saline (PBS) (Fig. 4a), and in PBS containing human serum albumin (HSA, 1%) (Fig. 4b). Protein carriers, e.g. serum albumin (SA) or  $\alpha$ 1-acid glycoprotein ( $\alpha$ GP) tend to bind to polymer surfaces and other hydrophobic compounds. Association of drugs with tissue fixed proteins have a retaining effect within the treated vessel segment, limiting their distribution from the target tissue [22-24]. For this reason we also examined the influence of HSA on the paclitaxel release behavior. In case of PLGA, an initial lag phase is followed by a more rapid release as a consequence of polymer erosion leading to a sigmoidal liberation profile of paclitaxel in both, HSA containing and HSA free medium. Similar release kinetics were reported for a paclitaxel-eluting stent system (Conor Medstent, MedSystems) which contains strut elements with stacked layers of drug and PLGA. Initial and late release rates were controlled by adding top and bottom polymer layers [25]. Biphasic release profiles were described for the TAXUS NIRx paclitaxel-eluting stent with an initial burst within the first 24 h followed by a slow release over a 10 days period. The drug was incorporated in a copolymer system. Release rates were altered via the drug/polymer ratio and coating thickness [26]. The stent used in the RAVEL study is coated with a nonerodable mixture of poly(ethyl methacrylate) and n-butylmethacrylate blended with sirolimus, a immunosuppressive agent with anti-proliferative properties [27,28]. To regulate drug release an inert coating is applied as diffusion barrier that provides a controlled release rate of 80 % within a time period of 30 days. In contrast to PLGA coatings, PVA-g-PLGA films did not reveal any burst release. Furthermore, release rates from PVA-g-PLGA devices were clearly improved resulting in more continuous and linear release profiles, particularly in the albumin containing phosphate buffer system (Fig. 4b).

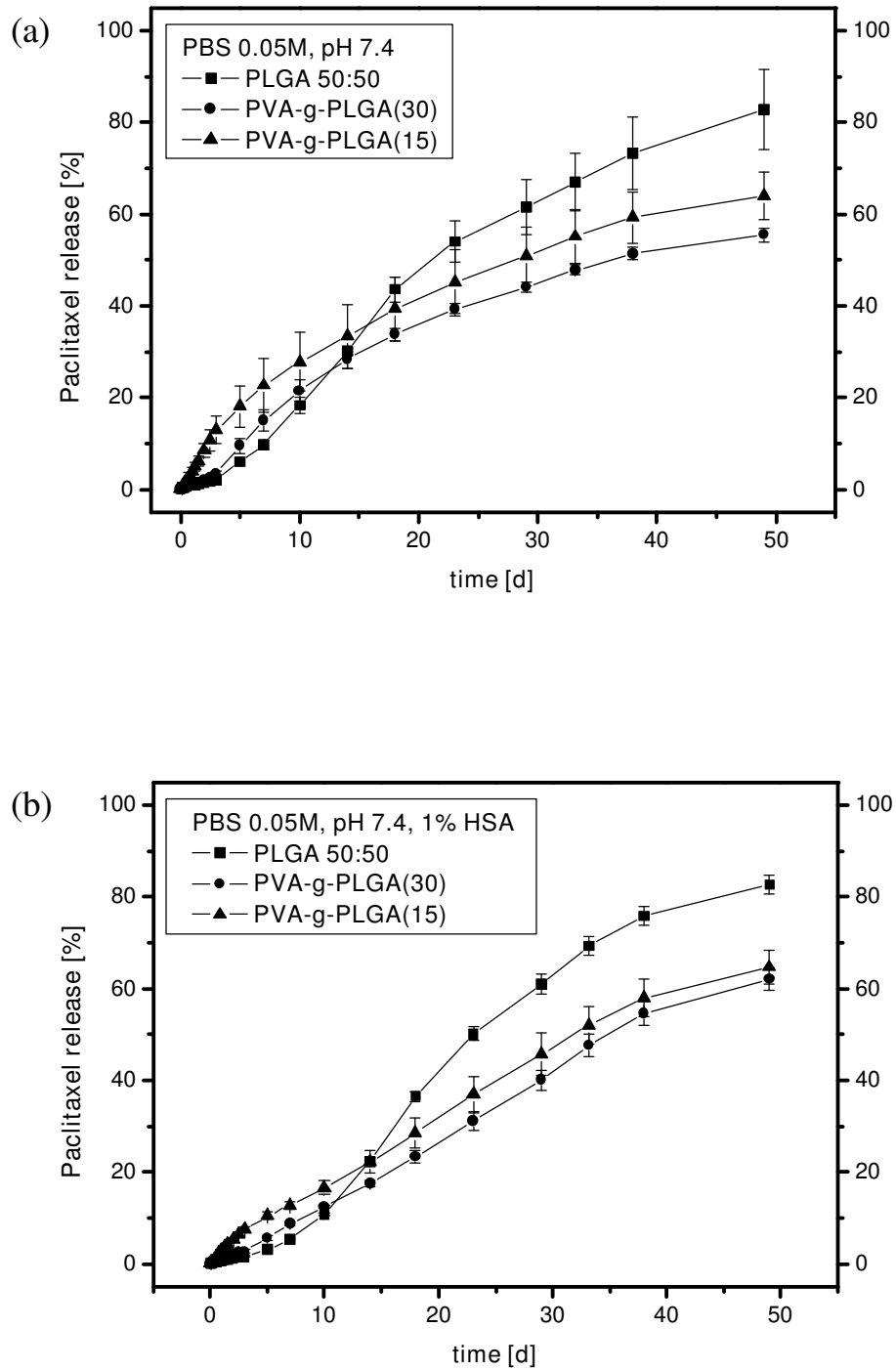
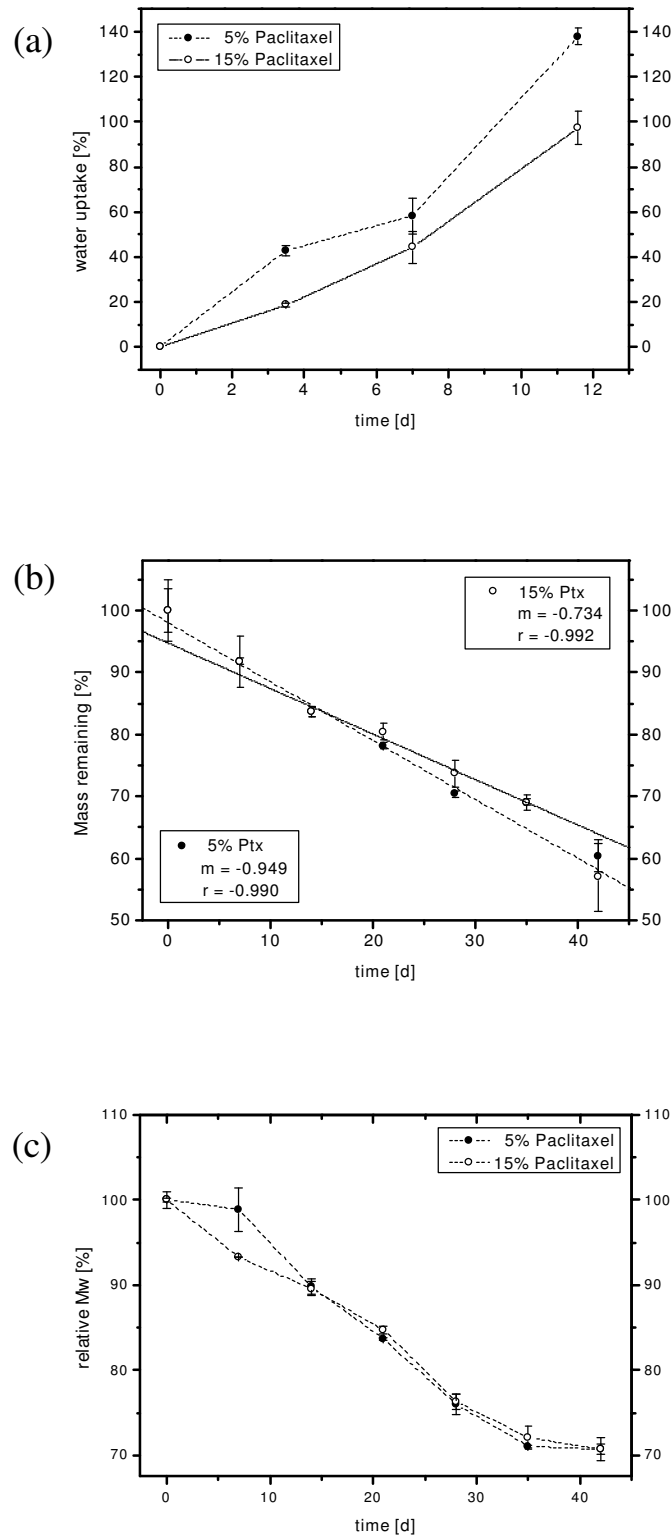


Fig. 4: In vitro release of paclitaxel from polymer films of PVA<sub>300</sub>-g-PLGA and linear PLGA in (a) PBS (0.05M, pH 7.4), and (b) in PBS containing 1% human serum albumin (HSA).



**Fig. 5:** (a) Water uptake, (b) mass loss ( $M_w$ ) and (c) molecular weight of PVA<sub>300</sub>-g-PLGA(30) loaded with 5 (full circles) and 15% (open circles) paclitaxel in 0.05M PBS, pH 7.4, 37°C.

After 48 days 83 % of the incorporated paclitaxel was released from the PLGA matrices, whereas 56 to 64 % of the drug was liberated from the PVA-g-PLGA films at the same time. Only small differences in release rates of branched polyesters could be observed. Nevertheless, the paclitaxel release tends towards a slightly faster paclitaxel release from PVA-g-PLGA(15) films in contrast to those of PVA-g-PLGA(30). To achieve faster release rates, it would be useful to study PVA-g-PLGA films with a lower PLGA substitution.

Breitenbach et al. (2000) previously proposed a bulk erosion mechanism for PVA-g-PLGA with a high PLGA content, whereas polymers with a lower PLGA rate erodes in a more surface front-like manner [16]. But the question is in which way paclitaxel was released, and how the drug-loading influences the degradation and erosion properties of PVA-g-PLGA? For this reason we investigated mass and molecular weight loss as well as water uptake of PVA-g-PLGA(30) films with paclitaxel loadings of 5 and 15%, exemplarily. As depicted in Fig. 5a the amount of incorporated lipophilic drug influenced the water uptake within the first 12 days of incubation with PBS, which is increased for the films with 5% paclitaxel. Due to the mass and molecular weight loss rate of films with 5% and 15% paclitaxel were found to be constant and almost equal. Without an initial lag phase the film mass decreased at a constant rate during 42 days of incubation (Fig. 5a), which is in agreement with the surface erosion mechanism for low molecular weight PVA-g-PLGA. The profile for molecular weight loss (Fig. 5b) is comparable to those, observed for bulk erosion of linear PLGA [16]. In addition, the examination of morphological changes of incubated films by scanning electron microscopy could not clarify the degradation mechanism considerably and revealed indications for both surface front-like and bulk erosion mechanism. Fig. 6 shows a time-series of SEM images after incubation with PBS. The initially smooth surface was found to be porous after 7 days. Further on, pore development in the inner phase was observed. The pore density and size increased with time up to 35 days of

incubation. Film surface became irregular, rough and porous progressively. Nevertheless, the release behaviour of lipophilic paclitaxel from PVA-g-PLGA films is well controllable by using PVA-g-PLGA polyesters, exhibiting sustained, and clearly improved release profiles in contrast to PLGA.

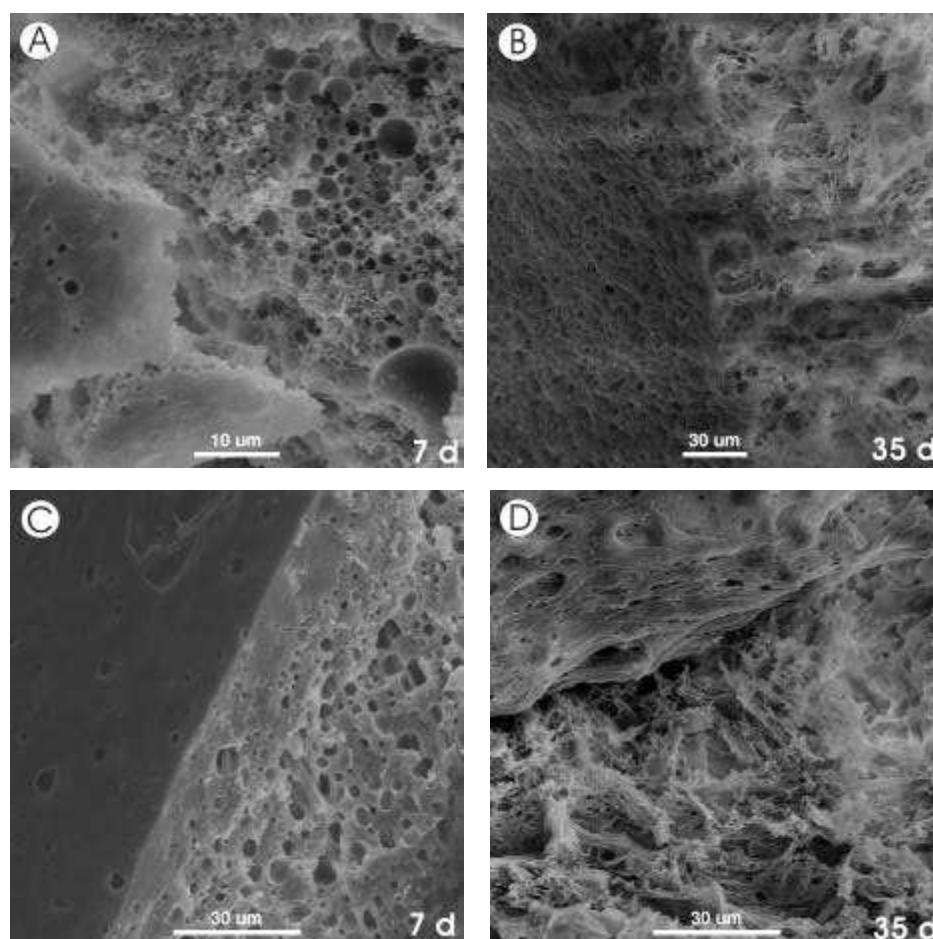


**Fig. 6:** Typical scanning electron micrographs of eroding PVA<sub>300</sub>-g-PLGA(30) films after 7 and 35 days of incubation: (A) and (B) 5% paclitaxel, (C) and (D) 15% paclitaxel.

Besides pharmacokinetic requirements of drug delivery vehicles, polymeric coatings have to be resistant during stent implantation and expansion. Therefore, we investigated the morphology of PVA-g-PLGA coated stents before and after stent expansion from 3.12 mm to 5 mm by scanning electron microscopy (Fig. 7). It turned out that a brand new stent showed deposition of impurities on the metal surface, which may be deposited during manufacturing

process (Fig. 7a and 7b). The polymeric layers were able to mask these impurities and to smooth the surface. Partly, the coated stent showed small pits indicating that the PVA-g-PLGA layer is very thin or incomplete at these sites. Nevertheless, after stent dilatation the polymer films exhibited adherence to the greatest possible extent (Fig. 7c and 7e). Except for some cracks at the mechanical stressed sites of the stent struts, the integrity of the coating was not affected, as displayed in Figure 7d and 7f.

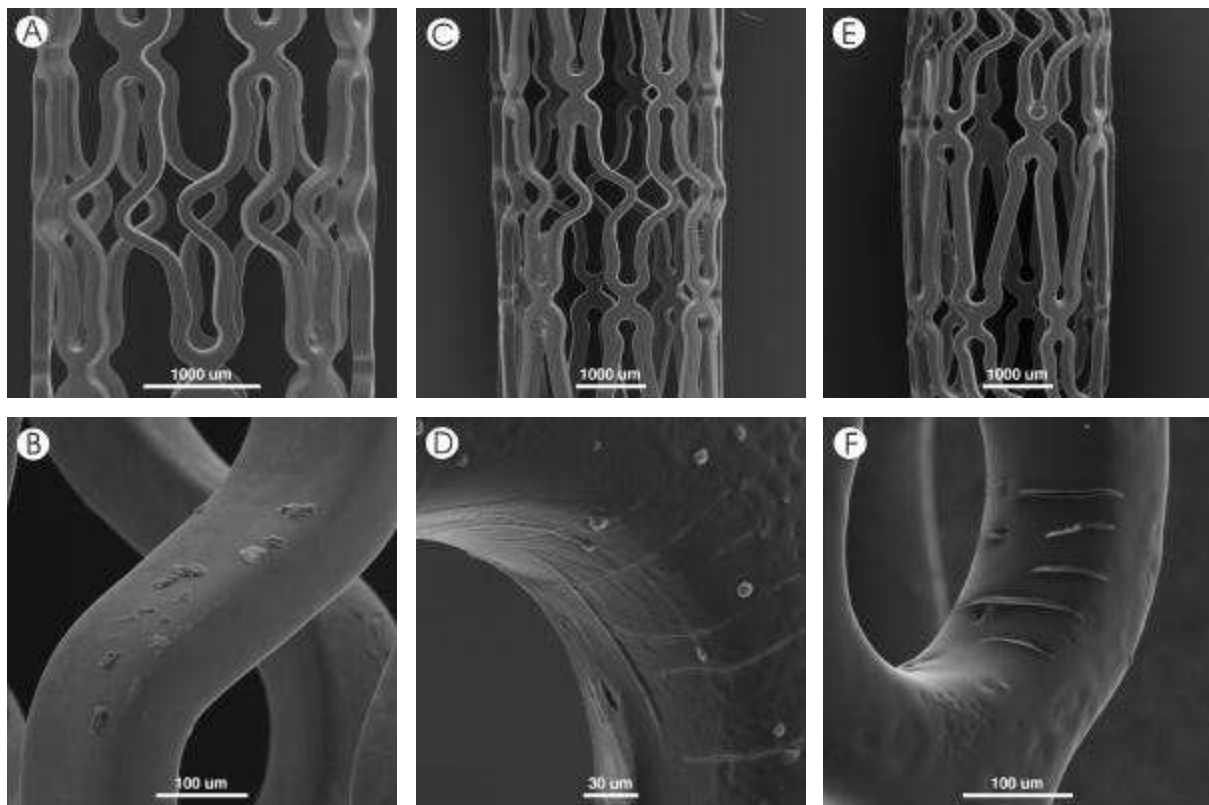


**Fig. 7:** Scanning electron microscopy images of Jostent® peripheral stent implants: bare metal stent (a), (b). Stent coated with Parylene N and PVA<sub>300</sub>-g-PLGA(30) (c), (d), and with Parylene N and PVA<sub>300</sub>-g-PLGA(15) (e), (f) in different magnifications.

---

## CONCLUSIONS

Drug eluting stents represent an interesting field in interventional vascular surgery. Several drug delivery devices have shown tremendous promise in the long –term prevention of restenosis. We were able to synthesize biocompatible and biodegradable polyesters by grafting PLGA chains onto a PVA backbone, which showed good mechanical stability and adherence on Parylene N coated stent surfaces after stent expansion. Physico-chemical properties of paclitaxel-loaded films were studied using differential scanning calorimetry (DSC) and wide angle X-ray diffraction (WAXD). By increasing drug loading the film matrices turned from a solid solution into a solid dispersion at higher paclitaxel amounts. Furthermore, PVA-g-PLGA polymers provide a controlled and continuous paclitaxel release. With respect on the variability and proved biocompatibility, PVA-g-PLGA comb polyesters seem to be promising candidates for sustained release of lipophilic drugs like paclitaxel, and, based on recently published data [17], additionally for the release of hydrophilic, macromolecular drugs, such as peptides, proteins, or DNA, which are of note in the treatment of restenosis as well. However, further studies are necessary to optimize the coating method, and prove possible deleterious effects on the coating integrity during incubation with buffer solution in-vitro, and after sterilisation.

## REFERENCES

- [1] G.S. Mintz, J.J. Popma, A.D. Pichard et al., Arterial Remodeling After Coronary Angioplasty : A Serial Intravascular Ultrasound Study, *Circulation* 94(1) (1996) 35-43.

- 
- [2] A. Lafont, L.A. Guzman, P.L. Whitlow et al., Restenosis After Experimental Angioplasty : Intimal, Medial, and Adventitial Changes Associated With Constrictive Remodeling, *Circ Res* 76(6) (1995) 996-1002.
- [3] N.A. Scott, G.D. Cipolla, C.E. Ross et al., Identification of a Potential Role for the Adventitia in Vascular Lesion Formation After Balloon Overstretch Injury of Porcine Coronary Arteries, *Circulation* 93(12) (1996) 2178-2187.
- [4] T. Kimura, K. Miyauchi, S. Yamagami, H. Daida and H. Yamaguchi, Local delivery infusion pressure is a key determinant of vascular damage and intimal thickening, *Jpn Circ J* 62(4) (1998) 299-304.
- [5] H. Mudra, C. Di Mario, P. De Jaegere et al., Randomized comparison of coronary stent implantation under ultrasound or angiographic guidance to reduce stent restenosis (OPTICUS Study), *Circulation* 104(12) (2001) 1343-1349.
- [6] H. Hanke, T. Strohschneider, M. Oberhoff, E. Betz and K.R. Karsch, Time course of smooth muscle cell proliferation in the intima and media of arteries following experimental angioplasty, *Circ Res* 67(3) (1990) 651-659.
- [7] W.J. Van Der Giessen, A.M. Lincoff, R.S. Schwartz et al., Marked Inflammatory Sequelae to Implantation of Biodegradable and Nonbiodegradable Polymers in Porcine Coronary Arteries, *Circulation* 94(7) (1996) 1690-1697.
- [8] D.I. Axel, W. Kunert, C. Goggelmann et al., Paclitaxel inhibits arterial smooth muscle cell proliferation and migration in vitro and in vivo using local drug delivery, *Circulation* 96(2) (1997) 636-645.

- 
- [9] C. Herdeg, M. Oberhoff, A. Baumbach et al., Local paclitaxel delivery for the prevention of restenosis: biological effects and efficacy in vivo, *J Am Coll Cardiol* 35(7) (2000) 1969-1976.
- [10] M. Hilker, M. Buerke, M. Guckenbiehl et al., Rapamycin reduces neointima formation during vascular injury, *Vasa* 32(1) (2003) 10-13.
- [11] E. Grube, U. Gerckens, R. Muller and L. Bullesfeld, Drug eluting stents: initial experiences, *Z Kardiol* 91 Suppl 3 (2002) 44-48.
- [12] K. Toutouzas, C. Di Mario, R. Falotico et al., Sirolimus-eluting stents: a review of experimental and clinical findings, *Z Kardiol* 91 Suppl 3 (2002) 49-57.
- [13] S. Silber, Paclitaxel-Eluting Stents: Are They All Equal? An Analysis of Six Randomized Controlled Trials in De Novo Lesions of 3,319 Patients, *J Interv Cardiol* 16(6) (2003) 485-490.
- [14] A. Greiner. Poly(p-xylylene)s (Structure, Properties, and Applications), in *The Polymeric Materials Encyclopedia*, Vol. 9, (J.C. Salamone, ed.), CRC Press, 1996, pp. 7171.
- [15] O. Schäfer, F. Brink-Spalink, C. Schmidt et al., Synthesis and properties of -phenylalkyl-substituted poly(p-xylylene)s prepared by base-induced 1,6-dehydrohalogenation, *Macromolecular Chemistry and Physics* 200(8) (1999) 1942-1949.
- [16] A. Breitenbach, K.F. Pistel and T. Kissel, Biodegradable comb polyesters Part II. Erosion and release properties of PVA-g-PLG, *Polymers* 41 (2000) 4781-4792.

- 
- [17] K.F. Pistel, A. Breitenbach, R. Zange and T. Kissel, Brush-like biodegradable polyesters, part III, Protein release from microspheres of poly(vinyl alcohol)-graft-poly(D,L-lactic-co-glycolic acid), *J Control Release* 73(1) (2001) 7-20.
- [18] C. Schmidt, V. Stümpflen, J.H. Wendorff et al., Structural analysis of PPX prepared by vapor phase pyrolysis of [2.2]paracyclophane, *Acta Polymer* 49 (1998) 232-235.
- [19] A. Breitenbach and T. Kissel, Biodegradable comb polyesters: Part 1 - Synthesis, characterisation and structural analysis of PLA and PLGA grafted onto water-soluble PVA as backbone, *Polymers* 39(14) (1998) 3261-3271.
- [20] R. Jalil and J.R. Nixon, Microencapsulation using poly (L-lactic acid) III: Effect of polymer molecular weight on the microcapsule properties, *J Microencapsul* 7(1) (1990) 41-52.
- [21] H. Jeon, Y. Jeong, M. Jang, Y. Park and J. Nah, Effect of solvent on the preparation of surfactant-free poly(DL-lactide- co-glycolide) nanoparticles and norfloxacin release characteristics [In Process Citation], *Int J Pharm* 207(1-2) (2000) 99-108.
- [22] M. Lemaire, W.M. Pardridge and G. Chaudhuri, Influence of blood components on the tissue uptake indices of cyclosporin in rats, *J Pharmacol Exp Ther* 244(2) (1988) 740-743.
- [23] J.P. Tillement, S. Urien, P. Chaumet-Riffaud et al., Blood binding and tissue uptake of drugs. Recent advances and perspectives, *Fundam Clin Pharmacol* 2(3) (1988) 223-238.

- 
- [24] M.A. Lovich, C. Creel, K. Hong, C.W. Hwang and E.R. Edelman, Carrier proteins determine local pharmacokinetics and arterial distribution of paclitaxel, *J Pharm Sci* 90(9) (2001) 1324-1335.
- [25] A. Finkelstein, D. Mcclean, S. Kar et al., Local drug delivery via a coronary stent with programmable release pharmacokinetics, *Circulation* 107(5) (2003) 777-784.
- [26] A. Colombo, J. Drzewiecki, A. Banning et al., Randomized study to assess the effectiveness of slow- and moderate-release polymer-based paclitaxel-eluting stents for coronary artery lesions, *Circulation* 108(7) (2003) 788-794.
- [27] J.E. Sousa, M.A. Costa, A. Abizaid et al., Lack of Neointimal Proliferation After Implantation of Sirolimus-Coated Stents in Human Coronary Arteries : A Quantitative Coronary Angiography and Three-Dimensional Intravascular Ultrasound Study, *Circulation* 103(2) (2001) 192-195.
- [28] H. Wieneke, T. Sawitowski, S. Wnendt et al., Stent coating: a new approach in interventional cardiology, *Herz* 27(6) (2002) 518-526.

## **CHAPTER 6**

---

### **SUMMARY AND OUTLOOK FOR FURTHER STUDIES**

## SUMMARY

Despite improved technologies restenosis remains the main problem of catheter-based interventions after a percutaneous transluminal angioplasty in artery disease. Local and sustained application of antiproliferative agents is a promising approach to solve the problem of intimal hyperplasia. In recent years, two different concepts for local drug delivery have attained increased importance: On the one hand, colloidal drug carriers, which can be infused directly into the vessel wall during the angioplasty procedure using special delivery catheters and on the other hand, the development of drug eluting stents. Biocompatible, biodegradable polymers are one of the most important instruments used to control the release of pharmacological active substances. A new type of branched, biodegradable polyesters, poly(vinyl alcohol)-graft-poly(lactide-co-glycolide) (PVA-g-PLGA), possesses very interesting features for the local and sustained release of paclitaxel. Therefore, the objective of this work was to investigate these polymers with regard to the preparation of paclitaxel loaded nanoparticles and stent coatings, and to evaluate their applicability as drug carriers to prevent intimal hyperplasia.

As a result of a poor delivery efficiency and intramural retention of infused agents, researchers have developed colloidal drug carrier systems from biodegradable polymers, which can be administered to the arterial vessel wall using porous balloon catheters. Several studies have demonstrated that particle size plays an important role in the penetration and cellular uptake, as described in **Chapter 2**. In this study the size dependent penetration and distribution of fluorescently labelled polystyrene nanoparticles (110, 217, and 514 nm in diameter) was investigated after local delivery into the vessel wall of the aorta abdominalis of New Zealand white rabbits using confocal laser scanning microscopy (CLSM). In contrast to recently reported observations, the examined

cross-sections did not show severe disruptions of the vessel wall. While nanoparticles of  $\leq 217$  nm deposited predominantly in the medial layer, 514 nm nanoparticles accumulated at the luminal surface. Furthermore, formation of pressure induced infusion channels was observed. When using transmission electron microscopy (TEM) to evaluate deposition, nanoparticles of 110 and 217 nm in size were found within the media and along the elastica lamina externa. Atherosclerotic plaques and elastic connective tissue were shown to act as strong anatomical barriers influencing penetration and permeation behavior of nanoparticles.

In addition to particle size other parameters, such as infusion pressure, particle suspension volume, as well as particle concentration, play an important role in catheter-based delivery. The effects of these factors on intraluminal particle distribution were investigated by CLSM, SEM, and TEM after infusion of fluorescently labelled polystyrene nanoparticles of 217 nm, as described in **Chapter 3**. Our results demonstrated pressure dependent particle migration through the vessel wall tissue, as characterized by channel-like deposition patterns corresponding to the porous balloon catheter design. Nanoparticles were localized in the intima, media, and adventitia. The infusion of 2 ml of a particle suspension (1 mg/ml) at an infusion pressure of 4 bar promoted delivery efficiency without causing severe vessel wall ruptures. In contrast, an increase in the suspension volume to 5 ml could not improve the delivery efficiency. The capacity of the vascular tissue at the delivery site appears to be small resulting in an escape of the solution or suspension into the blood stream. Possibly, large volumes may cause additional vessel ruptures. As a result of the interventional procedure the treated vessel segments showed partial damage and denudation of the endothelial layer. In spite of improved techniques, these injuries were difficult to avoid. Apart from the penetration characteristics observed, TEM images from cross and longitudinal sections of the vessel displayed vasa vasora

with nanoparticle incorporations, thus confirming results in recent studies, which described the transport properties of these small vessels. The vasa vasora is a network of small vessels spread throughout the adventitia and in the larger vessels can penetrate the media to supply the vessel wall.

The next step of this work included the preparation of paclitaxel loaded nanoparticles using the solvent evaporation technique and subsequent characterization of nanoparticle size, shape, yield, and encapsulation efficiency. Further experiments, detailed in **Chapter 4**, provided information about the drug release, the cytotoxicity of loaded and non-loaded nanoparticles, as well as their uptake into rabbit vascular smooth muscle cells (RbVSMC) in-vitro. PVA-g-PLGA nanoparticles were characterized by photon correlation spectroscopy (PCS), scanning electron microscopy (SEM), and atomic force microscopy (AFM). It was shown that NP formulations consist of round spheres with smooth surfaces and had a mean particle diameter of 140 to 180 nm in size. Particle yields typically ranged from 80 to 95 % with encapsulation efficiencies between 77 and 87 %. A decrease in the PLGA fraction of the polymer resulted in an increase in drug release rates. After an initial burst release, a slow, but continuous release for about 22 days was observed. The burst effect could be desirable to achieve high initial drug concentrations in the target tissue. After release of the loading dose, the subsequent sustained drug release rate should be substantial enough to obtain a constant drug level in the tissue and prevent excessive VSMC proliferation. Blank nanoparticles from PVA<sub>300</sub>-g-PLGA(30) and PVA<sub>300</sub>-g-PLGA(15) showed a high biocompatibility to RbVSMC at particle concentrations of 370 µg per ml. Paclitaxel-loaded NP possess an increased anti proliferative effect in comparison to the free drug. This indicated an improved cellular uptake of nanoparticles. CLSM of RbVSMC confirmed uptake of nanoparticles composed of 7-methoxycoumarine labelled PVA<sub>300</sub>-g-PLGA(15) (blue fluorescence) loaded with Oregon Green labelled paclitaxel

(green fluorescence) after a 6 hour incubation period. Based on previous observations, the mechanism for NP uptake and intracellular distribution could be characterized as pinocytosis or/and endocytosis, followed by transportation to endosomes.

In **Chapter 5** the focus was shifted from NP to polymeric stent coatings consisting of PVA-g-PLGA, which were designed to provide a controlled and sustained release of paclitaxel. Drug release rate were influenced by the polymer structure. In contrast to release from NP, film matrices prepared from PVA-g-PLGA(30) and PVA-g-PLGA(15) showed a more continuous release. In contrast, linear PLGA exhibited a sigmoid, non linear paclitaxel release. A decrease of PLGA side chain length, as well as an increase of drug loading leads to lower glass transition temperatures ( $T_g$ ) influencing the flexibility of the films which is an important aspect due to the coating integrity during stent crimping and implantation. At drug loadings of more than 10 %, wide angle X-ray diffraction (WAXD) patterns of films confirmed paclitaxel crystallization within the films, which influenced water uptake obviously due to the lipophilicity of the substance. As a result, the influence of drug loading on the mass loss and molecular weight ( $M_w$ ) loss was investigated by incubation of film devices made from PVA-g-PLGA(30) with 5 and 15% paclitaxel. Matrices with 5% paclitaxel exhibited increased water uptake within 12 days. Film mass and  $M_w$  of the polymer decreased in a linear manner within 42 days independent of the degree of loading. The results suggest a more heterogenous mechanism of degradation including surface and bulk erosion. Scanning electron micrographs gave the impression of time-dependent changes in device morphology during the incubation period. Metallic stent implants were coated with PVA-g-PLGA(30) and PVA-g-PLGA(15) using an air brush technique, to examine film integrity after stent expansion from 3.12 to 5 mm. With except of minor crack formation at the mechanically stressed sites of the stent SEM analyses demonstrated total

film adhesion. Furthermore, impurities on the surface and a partly non-uniform thickness of the coating was observed. To conclude, comb polyesters are potential candidates for controlled release matrices coated on stent implants, although findings reinforce the fact that further work is necessary to optimize the coating procedure.

## **OUTLOOK FOR FURTHER STUDIES**

Based on the results from in-vitro characterization of paclitaxel-loaded nanoparticles, animal studies may be useful to elucidate the efficiency of colloidal drug carriers in vivo [1]. The infusion of fluorescently- or radio-labelled substances encapsulated into nanoparticles could help to further characterize the diffusion pathways and deposition patterns within the arterial vessel wall using CLSM or autoradiography.

As already mentioned, the air brush technique for stent coating needs further optimization. Direct modification of parameters, such as spraying distance, duration, polymer concentration, or viscosity of the polymer solutions, may be useful to control film thickness according to the desired clinical requirements. Another important aspect of stent-based drug delivery technology is the investigation of mechanical properties of the polymers. The polymer coating must be durable enough to withstand handling during crimping onto the balloon catheter yet elastic enough to endure the expansion of the stent. The coating must also adhere to the surface under in vitro and in vivo conditions and remain stable during the sterilization process, which includes alterations in molecular weight, polydispersity, and release behavior [12].

The potential of comb polyesters (PVA-g-PLGA) has already been demonstrated in recent studies [13,14]. The variability of the polymer composition and the possibility of grafting positively [15] or negatively charged

structures [16,17] to the polymer backbone offers great flexibility for the incorporation of both hydrophilic and hydrophobic substances, i.e. polymer properties can be adjusted to suit those of the drug molecules. Therefore, another impulse for further investigations may be the use of other, potentially antirestenotic drugs. Some promising candidates are summarized in Tab. 1.

<b>Substance</b>	<b>Mechanism of action</b>	<b>Lit.</b>
<b>Antiproliferative agents</b>		
Sirolimus	inhibits production of proteins essential for cell division, immunosuppressive and antiproliferative properties	[2]
Tacrolimus	see Sirolimus	[3]
Angiopeptin	Somatostatin analogue; inhibits many cytokines and growth factors; potentially antiproliferative effects	[4]
Tyrosin kinase inhibitor	interfere with intracellular cell signalling that regulate cell proliferation and differentiation	[5]
<b>Antisense oligonucleotides against</b>		
NF $\kappa$ B	inhibition of activation of many cytokines, growth factors; anti-inflammatory, antiproliferative effect	[6]
E2F decoy	transcription factor; blocking the activation of genes mediating the cell cycle; antiproliferative effect	[7]
c-myc	inhibition of the cell cycle; antiproliferative effect	[8]
<b>Others</b>		
VEGF	stimulate endothelial proliferation; avoiding intimal hyperplasia	[9]
Saratin	inhibit von Willebrand factor-dependent platelet adhesion; decrease platelet aggregation; potentially avoiding intimal hyperplasia	[10]
Iloprost	prostacyclin analogue; antithrombotic potentially antiproliferative	[11]

**Tab. 1:** Potential candidates for incorporation into colloidal or film matrices composed of PVA-g-PLGA comb polyesters.

## ZUSAMMENFASSUNG

Trotz verbesserter Techniken ist die Entwicklung einer Restenose nach einer perkutanen transluminalen Angioplastie (PTA) atherosklerotischer Gefäße weiterhin eines der zentralen Probleme katheterinterventioneller Therapien. Daher könnte die lokale und anhaltende Applikation antiproliferativ wirkender Substanzen einen wesentlichen Beitrag zur Vermeidung einer Restenose leisten. In den letzten Jahren kristallisierten sich zwei verschiedene Applikationssysteme heraus. Zum einen Wirkstoff-beladene Nanopartikel, die während der Gefäßdilataion durch spezielle Ballonkatheter direkt in die Gefäßwand injiziert werden. Zum anderen erfahren Wirkstoff-beschichtete Stents eine immer größer werdende Aufmerksamkeit in Forschung und Klinik. Biokompatible und bioabbaubare Polymere werden hierbei zu einem wichtigen Instrument. Sie sollen ein kontrolliertes Freisetzen definierter Mengen eines Wirkstoffes gewährleisten. Eine neue Klasse bioabbaubarer Polymere, die sogenannten Kammpolymere (PVA-g-PLGA), scheinen für die lokale und anhaltende Applikation von Paclitaxel sehr geeignet zu sein. Aus diesem Grund war es Ziel der vorliegenden Arbeit, diese Polymere zur Herstellung von Paclitaxel-beladenen Nanopartikeln sowie Stentbeschichtungen zu verwenden, und deren Eignung als Trägersysteme zur Therapie einer Restenose zu überprüfen.

Aufgrund einer zu geringen Verweildauer und damit auch geringen Wirksamkeit lokal applizierter Wirkstofflösungen, wurden kolloidale, bioabbaubare Trägersysteme entwickelt, die mit Hilfe von perforierten Ballonkathetern während einer PTA in die Gefäßwand eingebracht werden. Dabei spielt die Partikelgröße eine wichtige Rolle für die Applikationseffizienz, die in **Kapitel 2** genauer untersucht wurde. Hierfür wurden Fluoreszenz-markierte Polystyrolnanopartikel mit einem Durchmesser von 110, 217 und 514 nm in die Gefäßwand der Aorta abdominalis von weißen Neuseeland Kaninchen appliziert, und die Partikelverteilung mit Hilfe der konfokalen Laser Scanning

Mikroskopie (CLSM) untersucht. Während der Applikation in unserem Modell entstanden im Gegensatz zu einigen früheren Studien keine Gefäßrupturen. Während Nanopartikel  $\leq 217$  nm vor allem im Zielgewebe, der Media, detektiert wurden, zeigte sich, dass sich die 514 nm Nanopartikel vor allem auf der luminalen Oberfläche abschieden. Im weiteren konnten kleinere, druckinduzierte Infusionskanäle beobachtet werden. Zur präziseren Lokalisierung der Nanopartikel in den einzelnen Geweben diente die Transmissionselektronenmikroskopie (TEM). So wurden Partikel von 110 und 217 nm zwischen den glatten Muskelzellen der Media und perlenkettenartig entlang der *Elastica lamina externa* gefunden, während sich 514 nm große Partikel vor allem in der Endothelschicht befanden. Anatomische Barrieren, wie das dichte Bindegewebe der *Elastica lamina interna* und *externa*, können hierbei eine Verteilung der Partikel im Gewebe beeinflussen.

Neben der Partikelgröße spielen auch andere Applikationsparameter eine wichtige Rolle. So wurden in **Kapitel 3** Infusionsdruck, Volumen und Konzentration der Partikelsuspension untersucht. Lokalisierung und Penetrationscharakteristika Fluoreszenz-markierter Polystyrolnanopartikel (217 nm) in der Arterienwand wurden mit Hilfe von CLSM, TEM und Rasterelektronenmikroskopie (REM) analysiert. Dabei bildeten sich an einigen Stellen in der Gefäßwand Infusionskanäle aus, deren Durchmesser an der lumenseitigen Infusionsstelle dem der Katheterporen entsprach. Die Partikel waren in Intima, Media und Adventitia zu finden. Die Verwendung von großen Partikelkonzentrationen (1 mg/ml), einem Suspensionsvolumen von 2 ml und Infusionsdrücken von 4 bar war hierbei am effektivsten bei gleichzeitiger Vermeidung zusätzlicher Gefäßtraumata. Das arterielle Gewebe scheint nicht in der Lage zu sein, sehr große Suspensionsvolumina aufzunehmen. Zum einen würde ein Großteil durch das Lumen und den Blutkreislauf abfließen. Zum anderen könnten wiederum Gefäßrupturen entstehen. Die Katheterintervention

hatte sichtbaren Einfluss auf die Integrität der Endothelschicht, wie elektromikroskopische Aufnahmen verdeutlichten. Das Endothel wurde partiell durch den Katheter verletzt und sogar abgetragen. Diese Verletzungen sind trotz verbesserter Techniken bis jetzt kaum zu vermeiden. Im Weiteren bestätigten transmissionselektronenmikroskopische Untersuchungen der infundierten Arterienabschnitte, dass auch die Vasa vasora für einen Nanopartikeltransport innerhalb der Arterienwand verantwortlich sind.

Die wichtigen Erkenntnisse zur Charakteristik der Partikelpenetration durch Variation verschiedener Parameter, ließ nun eine gezielte Herstellung Paclitaxel-beladener Nanopartikel entsprechender Größe zu, um diese dann später auch in einen in-vivo Tiermodell testen zu können. Doch zunächst mussten PVA-g-PLGA Nanopartikel, hergestellt mittels „Solvent – Displacement“- Technik, bezüglich Größe, Aussehen und Beladungsgrad genauer charakterisiert werden. Desweiteren sollten Versuche zur Paclitaxelfreisetzung, sowie Zytotoxizität und Partikelaufnahme an glatten Muskelzellen der Aorta abdominalis aus weißen Neuseeland Kaninchen, die Eignung der Partikel in vitro unter Beweis stellen, wie in **Kapitel 4** beschrieben wurde. Die zwischen 140 und 180 nm großen, monodispers verteilten NP hatten eine kugelige Form und eine glatte Oberfläche, wie Untersuchungen mit Rasterelektronen- und Rasterkraftmikroskopie zeigen konnten. Die Partikelausbeute lag zwischen 85 und 90%, während Verkapselungsausbeuten von 77 - 87% erzielt wurden. Mit zunehmendem PLGA-Anteil im Polymer, konnte auch die Freisetzungsgeschwindigkeit erhöht werden. Nach einem großen Wirkstoffburst während der ersten 24 Stunden der in vitro Freisetzung, flachten die Freisetzungsprofile der untersuchten Partikelchargen stark ab, und das Paclitaxel wurde langsam aber kontinuierlich über einen Zeitraum von 22 Tagen freigesetzt. Ein initialer Burst muss aber zwangsläufig keinen Nachteil darstellen. So kann dadurch zu Beginn eine hohe Wirkstoffkonzentration

(Initialdosis) im Zielgewebe erreicht werden, um diese im Weiteren mit einer langsamen, aber konstanten Freisetzung zu stabilisieren (Erhaltungsdosis). Während nicht beladene NP aus PVA<sub>300</sub>-g-PLGA(30) und PVA<sub>300</sub>-g-PLGA(15) in Konzentrationen bis etwa 370 µg/ml im Wesentlichen untoxisch waren, zeigten beladene PVA-g-PLGA NP gegenüber unverkapseltem Wirkstoff eine gesteigerte Hemmung der metabolischen Aktivität des glatten Muskelzellen. Dies könnte auf eine verbesserte Aufnahme der NP in die glatten Muskelzellen zurückzuführen sein, wie mit Hilfe der CLSM beobachtet werden konnte. Hierzu wurde 7-Methoxycoumarin markiertes PVA-g-PLGA(15) (blaue Fluoreszenz) zur Verkapselung von Oregon Green markiertem Paclitaxel (grüne Fluoreszenz) verwendet. Sowohl die Polymerpartikel als auch das verkapselte Paclitaxel waren nach einer Inkubationszeit von 6 h deutlich in der Zelle zu sehen. Mögliche Aufnahmemechanismen wurden bereits vielfach in der Literatur diskutiert. Demnach wäre eine Aufnahme der Nanopartikel durch Pino- und/oder Endocytose mit anschließendem Transport zu Endosomen.

Abschließend wurden, wie in **Kapitel 5** beschrieben, die Eigenschaften von Polymerfilmen aus PVA-g-PLGA untersucht. Aufgetragen auf eine metallische Gefäßprothese (Stent) sollen sie eine kontrollierte und anhaltende Paclitaxelfreisetzung gewährleisten. Wie schon bei den Nanopartikeln beobachtet, so war auch bei den Filmen die Freisetzungsgeschwindigkeit von der Polymerzusammensetzung abhängig. Allerdings zeigten die Filme ein fast lineares Freisetzungsprofil. Die Erniedrigung der PLGA-Kettenlänge, wie auch die Erhöhung der Wirkstoffbeladung führen zu einer Erniedrigung der Glasübergangstemperatur (T<sub>g</sub>) der Polymere. Die Polymerfilme werden dadurch weicher und flexibler, was wiederum ein wichtiger Aspekt bezüglich der Filmintegrität während der Fixierung auf dem Ballonkatheter und nach der Implantation in das Gefäß ist. Bei Beladungen der Filmmatrix mit mehr als 10% Wirkstoff konnte mittels Weitwinkelröntgendiffraktometrie (WWRD)

festgestellt werden, dass sich zunehmend Kristallnester des Wirkstoffs bildeten. Die Veränderungen der Matrix konnten auch durch rasterelektronenmikroskopische Aufnahmen gezeigt werden. Da Paclitaxel in wässrigen Medien nur sehr schwer löslich ist, kann die Kristallbildung die Wasseraufnahme und damit den Polymerabbau maßgeblich beeinflussen. Dazu wurden Filme aus PVA-g-PLGA(30) mit einer 5 und 15%igen Paclitaxelbeladung hergestellt, und Wasseraufnahme, Massenverlust, sowie mögliche Veränderungen des Molekulargewichtes der Filme untersucht. Tatsächlich zeigten Filme mit geringerer Beladung eine gesteigerte Wasseraufnahme über einen Zeitraum von 12 Tagen. Der Massenabbau verlief unabhängig vom Beladungsgrad über 42 Tage linear. Bei 15%iger Beladung konnte ein verlangsamter Abbau beobachtet werden. Die Ergebnisse der Analyse des Massen- und Molekulargewichtsverlust zeigten, dass der Abbau sowohl Merkmale der Oberflächen- als auch der Bulk-Erosion zeigt. Elektronenmikroskopische Aufnahmen lieferten einen Eindruck von den Veränderungen der Filmmorphologie in Abhängigkeit der Zeit. Zuletzt wurden durch ein Air brush-Verfahren die Polymere auf Stents aufgebracht, um mittels REM zu untersuchen, ob die Filme nach der Expansion noch intakt blieben. Bis auf einige Risse an den mechanisch besonders beanspruchten Stellen der Metallglieder, blieb die Matrix unversehrt und haftete weiterhin auf der Stentoberfläche. Neben einigen Verunreinigungen konnte auch eine, an manchen Stellen ungleichmäßige Beschichtungsdicke beobachtet werden. Obwohl die Methode sicherlich noch einiger Optimierungsarbeit bedarf, scheinen die verwendeten Polymere zur Herstellung Paclitaxel beladener und freisetzender Stents durchaus geeignet zu sein.

## AUSBLICK

Nach einer umfangreichen in vitro Charakterisierung Paclitaxel-beladener Nanopartikel sind nun weiterführende Studien hinsichtlich ihrer Wirksamkeit in einem in-vivo Tiermodell [1] von großem Interesse. Gleichzeitig könnte durch die Applikation von Fluoreszenz- (Konfokale Laserscanning Mikroskopie) oder radioaktiv-markierten (Autoradiographie) Wirkstoff, die Verteilung im arteriellen Gewebe detaillierter analysiert werden.

Bezüglich der Paclitaxel freisetzenden Stents sind zunächst Untersuchungen zur Optimierung der Airbrush-Technik notwendig, so dass durch gezielte Veränderung von Parametern, wie z.B. Sprühabstand, Sprühdauer, Konzentration oder Viskosität der Polymerlösung, die Filmdicke auf dem Implantat gesteuert und entsprechend den klinischen Anforderungen angepasst werden kann. Die weiterführende Charakterisierung der mechanischen Stabilität direkt nach der Stentbeschichtung, aber auch nach der Inkubation mit Puffermedien ist genauso unumgänglich, wie die Untersuchung der Frage, ob die beschichteten Gefäßprothesen auch sterilisierbar sind, und welche Auswirkungen die Sterilisationsmethode auf die Eigenschaften des Polymers bezüglich Molekulargewicht, Polydispersität und Freisetzungseigenschaften hat [2].

Das Potential der Kammpolymere (PVA-g-PLGA) konnte schon in früheren Studien verdeutlicht werden [13,14]. Die Variabilität der Zusammensetzung, die Möglichkeit positive [15] oder negative [16,17] Ladungen einzufügen, machen sie auch für die lokale Applikation anderer Substanzen interessant, da die Eigenschaften der Polymere an die der Wirkstoffe angeglichen werden können. Neben der Anwendung von Paclitaxel, bieten auch andere Wirkstoffklassen vielversprechende Ansätze für die Restenoseprophylaxe, wie in Tab. 1 zusammengefasst ist.

<b>Substanz</b>	<b>Wirkmechanismus</b>	<b>Lit.</b>
<b>Antiproliferative Substanzen</b>		
Sirolimus	inhibiert Produktion von zur Zellteilung wichtige Proteine, immunsuppressive and antiproliferative Eigenschaften	[3]
Tacrolimus	vgl. Sirolimus	[4]
Angiopeptin	Somatostasin Analogon; inhibiert viele Zytokine und Wachstumsfaktoren; potentiell antiproliferative Eigenschaften	[5]
Tyrosin kinase Inhibitor	Greift in intrazelluläre Zellsignalkaskade ein und reguliert so Zellproliferation und -differenzierung	[6]
<b>Antisense Oligonukleotide gegen</b>		
NFκB	Hemmung der Aktivierung vieler Cytokine, Wachstumsfaktoren; anti-inflammatorische, antiproliferative Eigenschaften	[7]
E2F decoy	Transkriptionsfaktor; blockiert Aktivierung von Genen, die den Zellzyklus vermitteln; antiproliferative Wirkung	[8]
c-myc	Inhibierung des Zellzyklus; antiproliferative Wirkung	[9]
<b>Andere</b>		
VEGF	stimuliert die Proliferation der Endothelzellen; verhindert eine verstärkte Neointimabildung	[10]
Saratin	inhibiert die vom von-WF-abhängige Thrombozytenadhäsion; verhindert Thrombozytenaggregation, Intimahyperplasie	[11]
Iloprost	Prostazyklin Analogon; antithrombotische und potentiell antiproliferative Eigenschaften	[12]

**Tab. 1:** Mögliche Substanzen in der Restenoseprophylaxe zur Einbettung in kolloidale Wirkstoffträger oder Stentbeschichtungen aus PVA-g-PLGA Kammpolyestern.

---

**REFERENCES / LITERATURSTELLEN**

- [1] H. Alfke, H.J. Wagner, C. Calmer and K.J. Klose, Local intravascular drug delivery: in vitro comparison of three catheter systems, *Cardiovasc Intervent Radiol* 21(1) (1998) 50-56.
- [2] M. Hilker, M. Buerke, M. Guckenbiehl et al., Rapamycin reduces neointima formation during vascular injury, *Vasa* 32(1) (2003) 10-13.
- [3] E. Grube, U. Gerckens, R. Muller and L. Bullesfeld, Drug eluting stents: initial experiences, *Z Kardiol* 91 Suppl 3 (2002) 44-48.
- [4] M.K. Hong, K.M. Kent, R. Mehran et al., Continuous subcutaneous angiopeptin treatment significantly reduces neointimal hyperplasia in a porcine coronary in-stent restenosis model, *Circulation* 95(2) (1997) 449-454.
- [5] I. Fishbein, J. Waltenberger, S. Banai et al., Local Delivery of Platelet-Derived Growth Factor Receptor-Specific Tyrphostin Inhibits Neointimal Formation in Rats, 20(3) (2000) 667-676.
- [6] S. Yoshimura, R. Morishita, K. Hayashi et al., Inhibition of intimal hyperplasia after balloon injury in rat carotid artery model using cis-element 'decoy' of nuclear factor-kappaB binding site as a novel molecular strategy, *Gene Ther* 8(21) (2001) 1635-1642.
- [7] T. Nakamura, R. Morishita, T. Asai et al., Molecular strategy using cis-element 'decoy' of E2F binding site inhibits neointimal formation in porcine balloon-injured coronary artery model, *Gene Ther* 9(8) (2002) 488-494.

- 
- [8] N. Kipshidze, E. Keane, D. Stein et al., Local delivery of c-myc neutrally charged antisense oligonucleotides with transport catheter inhibits myointimal hyperplasia and positively affects vascular remodeling in the rabbit balloon injury model, *Catheter Cardiovasc Interv* 54(2) (2001) 247-256.
- [9] S. Rafii, B. Heissig and K. Hattori, Efficient mobilization and recruitment of marrow-derived endothelial and hematopoietic stem cells by adenoviral vectors expressing angiogenic factors, *Gene Ther* 9(10) (2002) 631-641.
- [10] C.P. Cruz, J. Eidt, J. Drouilhet et al., Saratin, an inhibitor of von Willebrand factor-dependent platelet adhesion, decreases platelet aggregation and intimal hyperplasia in a rat carotid endarterectomy model, *J Vasc Surg* 34(4) (2001) 724-729.
- [11] E. Alt, I. Haehnel, C. Beilharz et al., Inhibition of neointima formation after experimental coronary artery stenting: a new biodegradable stent coating releasing hirudin and the prostacyclin analogue iloprost, *Circulation* 101(12) (2000) 1453-1458.
- [12] L. Montanari, M. Costantini, E.C. Signoretti et al., Gamma irradiation effects on poly(DL-lactide-co-glycolide) microspheres, *J Control Release* 56(1-3) (1998) 219-229.
- [13] A. Breitenbach, K.F. Pistel and T. Kissel, Biodegradable comb polyesters Part II. Erosion and release properties of PVA-g-PLG, *Polymers* 41 (2000) 4781-4792.

- 
- [14] K.F. Pistel, A. Breitenbach, R. Zange and T. Kissel, Brush-like biodegradable polyesters, part III, Protein release from microspheres of poly(vinyl alcohol)-graft-poly(D,L-lactic-co-glycolic acid), *J Control Release* 73(1) (2001) 7-20.
- [15] L. Dailey, T. Schmehl, G. T. et al., Nebulization of biodegradable nanoparticles: impact of nebulizer technology and nanoparticle characteristics on aerosol features, *J Control Release* 86(1) (2003) 131-144.
- [16] T. Jung, A. Breitenbach and T. Kissel, Sulfobutylated poly(vinyl alcohol)-graft-poly(lactide-co-glycolide)s facilitate the preparation of small negatively charged biodegradable nanospheres [In Process Citation], *J Controlled Release* 67(2-3) (2000) 157-169.
- [17] T. Jung, W. Kamm, A. Breitenbach, G. Klebe and T. Kissel, Loading of tetanus toxoid to biodegradable nanoparticles from branched poly(sulfobutyl-polyvinyl alcohol)-g-(lactide-co-glycolide) nanoparticles by protein adsorption: a mechanistic study, *Pharm Res* 19(8) (2002) 1105-1113.

## **APPENDICES**

---

**LIST OF PUBLICATIONS**

**CURRICULUM VITAE**

---

## LIST OF PUBLICATIONS

### Research Articles

U. Westedt, L. Barbu-Tudoran, A.K. Schaper, M. Kalinowski, H. Alfke, T. Kissel, Deposition of nanoparticles in the arterial vessel by porous balloon catheters: localization by confocal laser scanning microscopy and transmission electron microscopy. AAPS PharmSci. 2002; 4(4): 41

U. Westedt, L. Barbu-Tudoran, A.K. Schaper, M. Kalinowski, H. Alfke, T. Kissel, Catheter-based nanoparticle delivery into the arterial vessel wall. Europ J Pharm Biopharm 2003, submitted

### Abstracts / Poster Presentations

U. Westedt, G. Schmittmann, A. Papadimitriou, T. Kissel, Stabilisation of rh-NGF against denaturation at the w/o-interface in the primary emulsion for microencapsulation. 46<sup>th</sup> Annual Congress of the International Association for Pharmaceutical Technology, Berlin, Germany, April 3 – 6 2000

U. Westedt, G. Schmittmann, A. Papadimitriou, T. Kissel, Adsorption on zinc carbonate stabilizes rhNGF against aggregation during w/o/w-microencapsulation. 27<sup>th</sup> Annual Meeting of the Controlled Release Society Paris, France, July 7 – 13 2002

---

U. Westedt, L. Barbu-Tudoran, A.K. Schaper, M. Kalinowski, H. Alfke, T. Kissel, Nanoparticle Localization after Porous Balloon Delivery into Arterial Vessels: Confocal Laser Scanning Microscopy and Transmission Electron Microscopy. 29<sup>th</sup> Annual Meeting of the Controlled Release Society, Seoul, Korea, July 20 – 25 2002

L. Barbu-Tudoran, U. Westedt, M. Kalinowski, H. Alfke, A.K. Schaper, T. Kissel, Microscopic Localisation of Nanoparticle Deposition in the Arterial Wall after Catheter-Based Intraluminal Infusion. 15<sup>th</sup> International Congress on Electron Microscopy, Durban, South Afrika, September 1 – 6 2002

### **Diploma thesis**

rh-NGF Mikropartikel: Eine Untersuchung zur Stabilisierung von Proteinen bei der Mikroverkapselung. Diplomarbeit, Philipps-Universität Marburg, Martin-Luther-Universität Halle-Wittenberg, July 07 1999

---

**CURRICULUM VITAE****Zur Person**

Ulrich Westedt  
Apotheker und Diplompharmazeut  
geboren am 04. April 1974 in Wolfsburg  
Staatsangehörigkeit: deutsch  
ledig

**Schulbildung**

1980 - 1984 | Grundschule Brome  
1984 - 1986 | Orientierungsstufe Rühren  
1986 - 1993 | Gymnasium Hankensbüttel  
Allgemeine Hochschulreife

**Wehrdienst**

07/1993 - 07/1994 | 3./ Panzergrenadierlehrbatallion 332 in Wesendorf

**Hochschulstudium**

10/1994 - 10/1998 | Pharmaziestudium, Philipps-Universität Marburg  
09/1996 | Erstes Staatsexamen  
10/1998 | Zweites Staatsexamen  
11/1999 | Drittes Staatsexamen; Approbation als Apotheker

**Praktische Ausbildung**

11/1998 - 04/1999 | Diplomarbeit, Philipps-Universität Marburg.  
„rh-NGF Mikropartikel: Eine Untersuchung zur  
Stabilisierung von Proteinen bei der  
Mikroverkapselung“. (Prof. Dr. T. Kissel und Prof.  
Dr. R. Neubert)

05/1999 – 11/1999 | Widukind Apotheke Wolfsburg (Gunter Nabel)

seit 12/1999 | Wissenschaftlicher Angestellter am Institut für  
Pharmazeutische Technologie und Biopharmazie,  
Philipps-Universität Marburg. Anfertigung der  
vorliegenden Dissertation unter der Leitung von  
Prof. Dr. T. Kissel